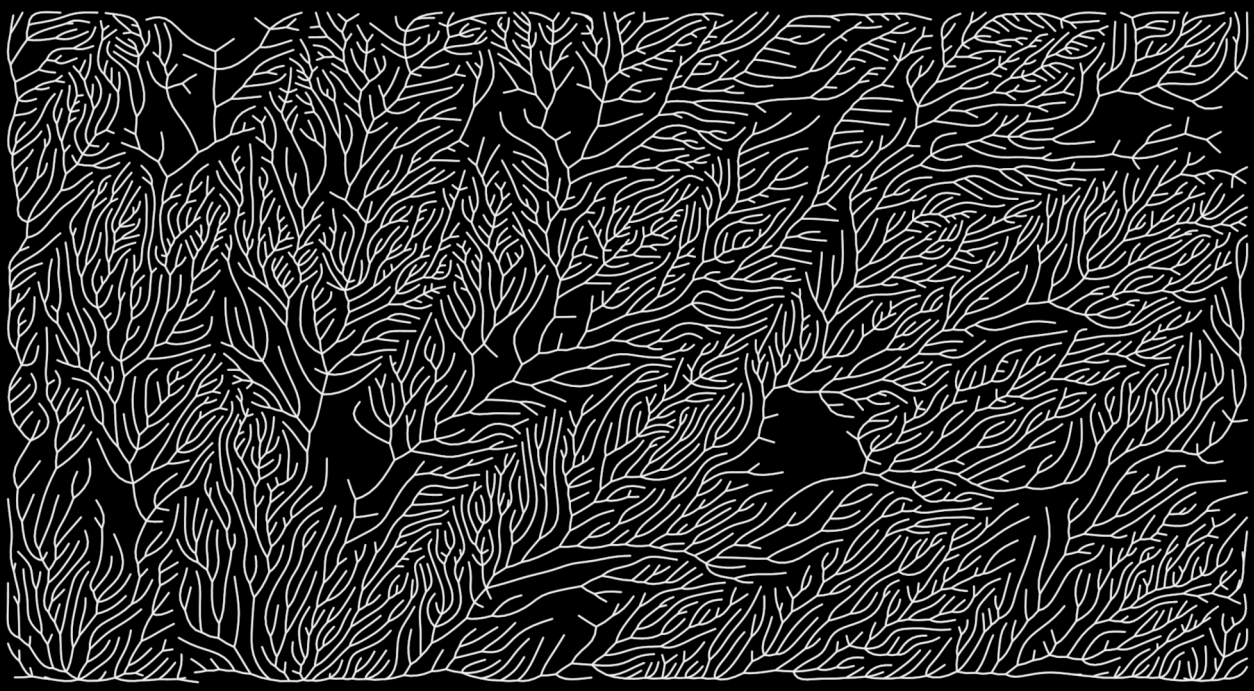

Diversity-dependence and the role of competition in clade diversification

Théo Pannetier

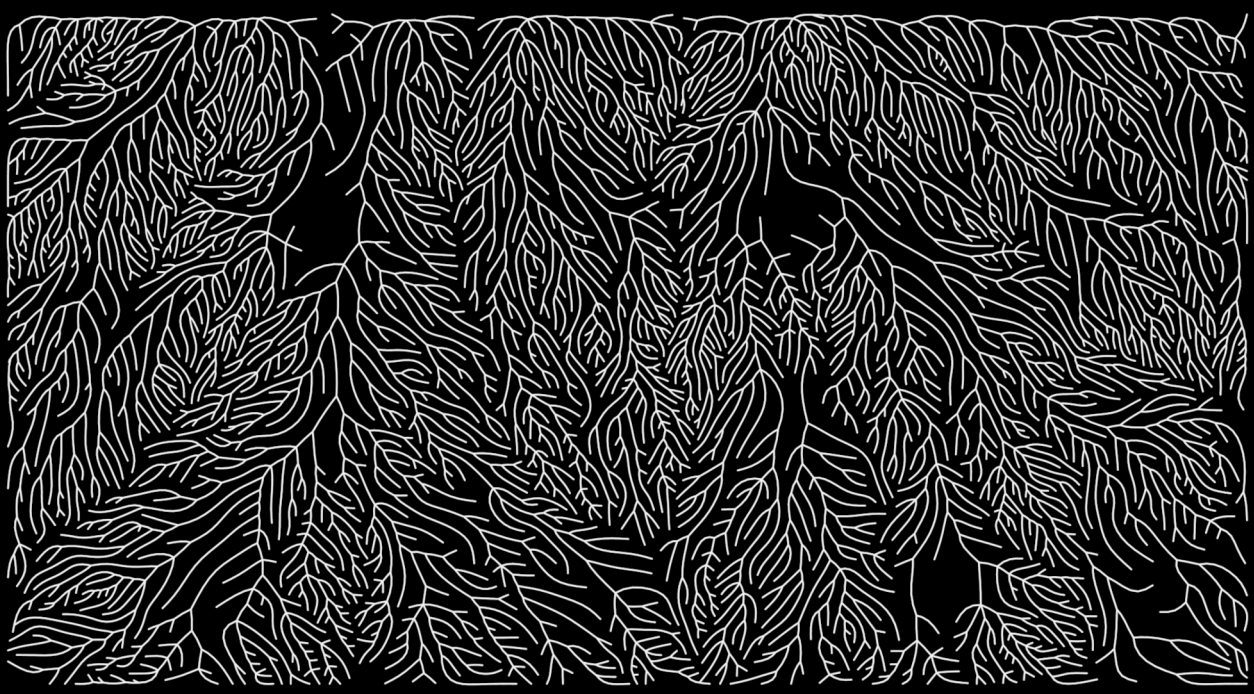

university of groningen

UNIVERSITY of STIRLING

Diversity-dependence and the role of competition in clade diversification

PhD thesis

to obtain the degree of PhD of the
University of Groningen
on the authority of the
Rector Magnificus Prof. C. Wijmenga
and in accordance with
the decision by the College of Deans

and

to obtain the degree of PhD of
University of Stirling
on the authority of the
Principal Prof. G. McCormac
and in accordance with
the decision by the College of Deans.

Double PhD degree

This thesis will be defended in public on

Tuesday 10 January 2023 at 12:45 hours

by

Théo Samuel Clément Pannetier

born on 18 April 1995
in Pithiviers, France

Supervisor
Prof. R.S. Etienne

Co-supervisors
Dr. A. B. Duthie
Dr L. Bunnefeld

Assessment Committee
Prof. D. Copplestone
Prof. A. Hurlbert
Prof. F. Hartig
Prof. G. S. van Doorn

The work described in this thesis was performed in the research group Theoretical & Evolutionary Community Ecology at the University of Groningen, the Netherlands; and in the Evolving Organisms research group in the Biological and Environmental Sciences department of the University of Stirling, Scotland, United Kingdom.

Cover Design: Growth Covers #2, copyright GarryKillian via Creative Market, with modifications by Théo Pannetier for the back cover | https://creativemarket.com/garrykillian

Cover Editing: Théo Pannetier

CONTENTS

1

INTRODUCTION

1

1.1. MACROEVOLUTION AND SPECIES DIVERSITY ON EARTH

THE number of species living today has proven hard to estimate [1], and is certainly not static. As new species are discovered, some are also undergoing speciation themselves, while others go extinct without even being surveyed. As a result, species diversity change over time due to both speciation and extinction. The distribution of species is also heterogeneous across geography, best illustrated by the correlation of species richness with latitude [2], and across taxonomy, with a high imbalance between sister taxa being a common feature of phylogenetic trees [3, 4]. For example, the two orders of Lepidosauria, Squamata and Rynchocephalia (tuataras), currently include more than 9,000 species for the former, against a single, or possibly two species for the latter [5]. Such imbalances, and more generally the distribution of biodiversity today on Earth, is the present outcome of evolutionary processes that have taken place in the past. Understanding past evolution is hence key to understand how ecosystems have been assembled.

Explaining the distribution and origins of the diversity of living organisms has been the central questions of natural history during the past two centuries, and its legacy can be found in modern macroevolution. Where early naturalists were interested in finding explanations for current diversity, macroevolution has focused on the formulation of general rules on how evolutionary processes take place at the multi-million-year timescale. Gould [6] famously coined the metaphor of the tape of life, emphasizing the importance of randomness in evolution, and how the face of diversity at a given time is contingent on past events. In spite of this, macroevolution is likely to have a deterministic component, as long-term trends in evolutionary changes emerge from regulated, ecological processes taking place over smaller timescales. The field of macroevolution aims at establishing how these processes extrapolate over millions of years, and if new patterns and mechanisms emerge when observing evolution at this coarser level. The study of diversification, in particular, focuses on observing the dynamics of diversity, observing the trends of change in multi-million-year diversity levels (patterns) and inferring what mechanisms control them (processes).

The pace and distribution of speciation and extinction events have shaped diversity in the past [7, 8], and revealing what ecological mechanisms drive them across taxa will help to inform how modern ecosystems have emerged and how they are likely to change in future times. Many insights have been obtained from the study of fossil faunas and floras and how they changed in composition through geological times. A major step forward has been the assembly of a continuous diversity reconstruction across diverse, well-conserved clades and the subsequent study of the patterns they exhibited. Most famously, Sepkoski's global reconstruction of marine taxa diversity spanning the entire Phanerozoic has provided important insights [9–11], along with the emergence of simulations as a tool for research in evolution. For example, Raup [12] has been able to estimate average, global extinction rates, while Walker and Valentine [13] used the fossil record along with simulations to test predictions from ecological niche theory. The main drawback of fossil studies has been the relative paucity of occurrences [14] – we only observe a fraction of the taxa that lived at a given time – and the many biases associated with this – the rate of preservation being highly heterogeneous across time and scale.

This issue has been addressed by using a different source of information – molecular

phylogenies. Molecular clock models have made it possible to date branching events in phylogenies reconstructed from extant taxa, making it possible to infer the pace at which the group diversified in the clade. Much progress has been made following the derivation of a likelihood expression for birth-death phylogenetic models [15], effectively making it possible to disentangle rates of speciation and extinction from a phylogeny [16] and to test for the factors that have driven them. Such inference methods have been extensively used to study models of range evolution [17, 18], modes of speciation [19, 20], or the influence of some traits in accelerating the diversification [21, 22].

The dialogue between molecular phylogenies and the fossil record has shown hard to establish [23, 24], as a result of correspondences between paleontological or morphological, and phylogenetic definitions of a species being unclear, although efforts are being made to reconcile both [25]. Nevertheless, the availability of two sources of information has helped shaping current knowledge on macroevolutionary trends.

Global trends in diversification have initially been inferred from the observation of the fossil record. Diversity might be richer today than it ever was before (Benton & Emerson 2007), however it seems evident that diversification is limited by controlling factors. Sepkoski [9] has noted that, similar to modes of population growth, taxonomic units are expected to accumulate exponentially under a positive, net rate of diversification. This prediction is incongruent with the 'low' levels of diversity observed today when compared to the length of the Phanerozoic and the rates estimated from the Cambrian explosion. In fact, diversity in the fossil record seems to build up following logistic growth, with taxonomic units accumulating over time until reaching a plateau. Such plateaus of diversity have been reported for the accumulation of marine orders over the entirety of the Phanerozoic [9], and marine families during Paleozoic times [10]. Equivalent observations have been made from molecular reconstructed phylogenies, at lower taxonomic scales, typically for genera and families [20, 26, 27]. Clades often exhibit logistic-like patterns of lineage accumulation through time, with bursts of branching early in the phylogeny, followed by a later slowdown toward the present. This, and the second observation that diversity rebounds rapidly after episodes of mass extinction [28–30], suggest that diversity levels impose a negative feedback on diversification, and that diversity is capped at an equilibrium level where the net diversification rate lies close to zero.

Such patterns of growth suggest a clear parallel with ecological processes observed at lower scales. In particular, the apparent limit to diversity presents analogies with environmental carrying capacities from island biogeography theory [31], and has been interpreted as the result of resource limitations and negative, competitive interactions between species inside a clade [8, 13, 23]. Due to competitive exclusion, species must occupy different ecological niches to coexist. The carrying capacity of the diversity-dependent model can be thought of as the number of niches available to species at a given time. As the number of occupied niches increase diversification is curbed due to strengthened competitive interactions. Competition has been proposed to affect either speciation rates, extinction rates, or both. Speciation can be hampered by the lack of free niches or ecological opportunities, preventing the survival of incipient species through increased competition, while increased competition and species packing should also result in reduced population sizes, making extinction more likely to happen from external, stochastic events. A simple way to illustrate this process is a logistic growth model, analogous to the

one used in population growth modelling and island biogeography. A carrying capacity is set to represent the maximum number of individuals (or, at the macroevolutionary scale, species) that can coexist at a given time, typically because of limited resources. As species accumulate, diversity growth rate (diversification rate) is hampered as diversity level approaches the carrying capacity. While this phenomenological model has been shown to provide a good fit to the dynamics of diversification followed by many clades [9, 32, 33], confirmation of the mechanism behind this pattern is more difficult to infer due to the paucity of information regarding the evolution of living groups in the past.

In fact, although the most emphasized hypotheses behind diversity-dependence revolve around niche dynamics, other mechanisms can produce similar dynamics (reviewed in Moen and Morlon [34]). For example, Pigot *et al.* [35] showed that diversity-dependent diversification slowdowns can also arise solely from allopatric speciation and range dynamics. In their model of geographic speciation, speciation probability diminishes as species pack in a finite area and their range is reduced, leading to lower probabilities of speciation by vicariance. Levinton [36] has noted that increased extinction through species packing can also happen in a neutral setting, in the absence of niche dynamics, as long as the number of organisms a given area can sustain is limited by the biomass of resources.

Diversity-dependence has become one of the major models of diversification, as it has a good heuristic value at explaining the diversification slowdowns that seem to be widespread in both the fossil record and in molecular phylogenies. Since it emphasizes the importance of resource limitations and competition in controlling species diversity, it is consistent with major macroevolutionary hypotheses. Early bursts of speciation for example, are the main feature of adaptive radiations [37], and more generally, the role of competition as the main driver of evolution at the macro-scale has been formulated in the Red Queen hypothesis [38], but originates from Darwin [39].

While the prevalence of the general pattern in both molecular phylogenies and fossil series has been well recognized, its interpretation is still the subject of debate [8]. The model is, in its inception, phenomenological, meant to provide a coherent ecological interpretation for the plateaus observed in multi-million years diversity curves. The breadth of its applicability across the tree of life, how ecological-scale processes combine and connect to evolutionary rates, and whether the observed patterns are indeed caused by the hypothesized mechanisms, all remain unclear.

1.2. THESIS OUTLINE

Through the scope of this dissertation, I discuss the implications of diversity-dependent diversification, both as a phenomenological and a mechanistic model. Each of the following research chapters address an aspect of diversity-dependent diversification, in turn tackling its detectability in molecular phylogenies (Chapter 2), modelling the ecological processes that are hypothesized to lead to it (Chapter 3), and challenging a central assumption of the model and exploring how it impacts inference (Chapter 4). Finally, I summarise the findings of these three chapters and discuss their implications for the field of macroevolution (Chapter 5), particularly in regard to recent developments that arose during the course of the PhD.

While the diversity-dependent model of diversification has been formulated to explain the apparent decline of the net diversification rate over the history of a clade, other types of processes are also relevant to explain this pattern. Namely, the time-dependent category of diversification models [40] represents processes where the net diversification rate can be any arbitrary function of time, for example a logistic decline. Given the similarity of diversity trajectories produced by both types of models, it is unclear which mode of diversification is driving the patterns observed in molecular phylogenies. This is important, since only diversity-dependence calls for a control of diversity on diversification rates. In **Chapter 2**, I focus on characterizing differences between diversity-dependence and time-dependence and develop a method to reliably infer which better explains the distribution of branches in molecular phylogenies.

Diversity-dependence is widely accepted as a macroevolutionary consequence of individuals, and eventually species competing for limited resources. While such an ecological scenario intuitively leads to diversity-dependent diversification, whether the simple exponential or linear forms of diversity-dependence considered in phenomenological models are consistent with it has seldom been investigated. In **Chapter 3**, I depart from the phenomenological view and study an individual-based model, where trait-mediated interactions between organisms and their environment drive an adaptive radiation in a finite ecological niche space. As the radiation proceeds, niche space fills up and speciation becomes much more complicated and infrequent, a process that is in line with the ecological interpretation of diversity-dependence. I measure the evolutionary rates, and the resulting form of diversity-dependence, that emerge in communities simulated under this model. I then use model selection and the likelihood of the phenomenological models to assess how the two main forms (linear and exponential) of diversity-dependence considered in the literature approximate the measured rates when complete fossil information is available, and what rates can be recovered in an empirical situation where only the reconstructed phylogeny is available.

As discussed above, an expected feature of ecological settings hypothesized to lead to diversity-dependence in evolutionary rates is the presence of a limited amount of resources, or equivalently a finite niche space. The vast majority of studies that consider diversity-dependence either implicitly or explicitly assume that all species in a clade compete among one another in an exclusive niche space, but there is *a priori* no reason to expect that the limits of such niche spaces match taxonomy. In **Chapter 4**, I extend the individual-based model used through Chapter 2 to consider the case of multiple clades evolving in a common niche space. The ecological scenario then approximates diversification on islands. I simulate diversification in this model with increasing immigration intensity and decreasing intensity of competition. I then assess whether ignoring competing clades impedes the detection of diversity-dependence in the resulting phylogenies, and whether the shared nature of diversity-dependence can be identified when complete communities are acknowledged as resulting from a single evolutionary process.

Through these approaches, I hope to bring a better understanding of this major diversification process and more generally, how ecological dynamics influence macroevolution.

1 REFERENCES

[1] M. J. Caley, R. Fisher, and K. Mengersen, *Global species richness estimates have not converged,* Trends in Ecology & Evolution **29**, 187 (2014).

[2] J. Rolland, F. L. Condamine, F. Jiguet, and H. Morlon, *Faster Speciation and Reduced Extinction in the Tropics Contribute to the Mammalian Latitudinal Diversity Gradient,* PLOS Biology **12**, e1001775 (2014).

[3] M. G. B. Blum and O. François, *On statistical tests of phylogenetic tree imbalance: The Sackin and other indices revisited,* Mathematical Biosciences **195**, 141 (2005).

[4] A. Mir, F. Rosselló, and L. Rotger, *A new balance index for phylogenetic trees,* Mathematical Biosciences **241**, 125 (2013).

[5] P. Uetz and A. Stylianou, *The original descriptions of reptiles and their subspecies,* Zootaxa **4375**, 257 (2018).

[6] S. J. Gould, *Wonderful Life: The Burgess Shale and the Nature of History* (WW Norton & Company, 1990).

[7] R. E. Ricklefs, *Estimating diversification rates from phylogenetic information,* Trends in Ecology & Evolution **22**, 601 (2007).

[8] D. L. Rabosky, *Diversity-Dependence, Ecological Speciation, and the Role of Competition in Macroevolution,* Annual Review of Ecology, Evolution, and Systematics **44**, 481 (2013).

[9] J. J. Sepkoski, *A kinetic model of Phanerozoic taxonomic diversity I. Analysis of marine orders,* Paleobiology **4**, 223 (1978).

[10] J. J. Sepkoski, *A kinetic model of Phanerozoic taxonomic diversity. III. Post-Paleozoic families and mass extinctions,* Paleobiology **10**, 246 (1984).

[11] J. J. Sepkoski, *Ten years in the library: New data confirm paleontological patterns,* Paleobiology **19**, 43 (1993).

[12] D. M. Raup, *A kill curve for Phanerozoic marine species,* Paleobiology **17**, 37 (1991).

[13] T. D. Walker and J. W. Valentine, *Equilibrium Models of Evolutionary Species Diversity and the Number of Empty Niches,* The American Naturalist **124**, 887 (1984).

[14] H. Morlon, *Phylogenetic approaches for studying diversification,* Ecology Letters **17**, 508 (2014).

[15] S. Nee, R. M. May, and P. H. Harvey, *The reconstructed evolutionary process,* Phil. Trans. R. Soc. Lond. B **344**, 305 (1994).

[16] S. Nee, E. C. Holmes, R. M. May, and P. H. Harvey, *Extinction Rates can be Estimated from Molecular Phylogenies,* Philosophical Transactions: Biological Sciences **344**, 77 (1994).

[17] A. L. Pigot and J. A. Tobias, *Species interactions constrain geographic range expansion over evolutionary time,* Ecology Letters **16**, 330 (2012).

[18] A. Castro-Insua, C. Gómez-Rodríguez, J.-C. Svenning, and A. Baselga, *A new macroecological pattern: The latitudinal gradient in species range shape,* Global Ecology and Biogeography **27**, 357 (2018).

[19] T. G. Barraclough and A. P. Vogler, *Detecting the Geographical Pattern of Speciation from Species-Level Phylogenies,* The American Naturalist **155**, 419 (2000).

[20] L. J. Harmon, J. A. Schulte, A. Larson, and J. B. Losos, *Tempo and Mode of Evolutionary Radiation in Iguanian Lizards,* Science **301**, 961 (2003).

[21] D. Pincheira-Donoso, T. Tregenza, M. J. Witt, and D. J. Hodgson, *The evolution of viviparity opens opportunities for lizard radiation but drives it into a climatic cul-de-sac: Viviparity and climate change,* Global Ecology and Biogeography **22**, 857 (2013).

[22] T. Jezkova and J. J. Wiens, *What Explains Patterns of Diversification and Richness among Animal Phyla?* The American Naturalist **189**, 201 (2017).

[23] R. S. Etienne, B. Haegeman, T. Stadler, T. Aze, P. N. Pearson, A. Purvis, and A. B. Phillimore, *Diversity-dependence brings molecular phylogenies closer to agreement with the fossil record,* Proceedings of the Royal Society B: Biological Sciences **279**, 1300 (2012).

[24] G. Hunt and G. Slater, *Integrating Paleontological and Phylogenetic Approaches to Macroevolution,* Annual Review of Ecology, Evolution, and Systematics **47**, 189 (2016).

[25] D. Silvestro, A. Antonelli, N. Salamin, and T. B. Quental, *The role of clade competition in the diversification of North American canids,* Proceedings of the National Academy of Sciences **112**, 8684 (2015).

[26] A. B. Phillimore and T. D. Price, *Density-Dependent Cladogenesis in Birds,* PLoS Biology **6**, e71 (2008).

[27] R. A. Pyron and J. J. Wiens, *Large-scale phylogenetic analyses reveal the causes of high tropical amphibian diversity,* Proceedings of the Royal Society B: Biological Sciences **280**, 20131622 (2013).

[28] D. H. Erwin, *The end and the beginning: Recoveries from mass extinctions,* Trends in Ecology & Evolution **13**, 344 (1998).

[29] M. J. Benton, *The Red Queen and the Court Jester: Species Diversity and the Role of Biotic and Abiotic Factors Through Time,* Science **323**, 728 (2009).

[30] R. W. Meredith, J. E. Janecka, J. Gatesy, O. A. Ryder, C. A. Fisher, E. C. Teeling, A. Goodbla, E. Eizirik, T. L. L. Simão, T. Stadler, D. L. Rabosky, R. L. Honeycutt, J. J. Flynn, C. M. Ingram, C. Steiner, T. L. Williams, T. J. Robinson, A. Burk-Herrick, M. Westerman,

N. A. Ayoub, M. S. Springer, and W. J. Murphy, *Impacts of the Cretaceous Terrestrial Revolution and KPg Extinction on Mammal Diversification,* Science , 1211028 (2011).

[31] R. H. MacArthur and E. O. Wilson, *The Theory of Island Biogeography* (Princeton University Press, 1967).

[32] D. L. Rabosky and I. J. Lovette, *Density-dependent diversification in North American wood warblers,* Proceedings of the Royal Society B: Biological Sciences **275**, 2363 (2008).

[33] E. Lewitus and H. Morlon, *Characterizing and Comparing Phylogenies from their Laplacian Spectrum,* Systematic Biology **65**, 495 (2016).

[34] D. Moen and H. Morlon, *Why does diversification slow down?* Trends in Ecology & Evolution **29**, 190 (2014).

[35] A. L. Pigot, A. B. Phillimore, I. P. F. Owens, and C. D. L. Orme, *The Shape and Temporal Dynamics of Phylogenetic Trees Arising from Geographic Speciation,* Systematic Biology **59**, 660 (2010).

[36] J. S. Levinton, *A Theory of Diversity Equilibrium and Morphological Evolution,* Science **204**, 335 (1979).

[37] D. Schluter, *The Ecology of Adaptive Radiation.* (Oxford Univ. Press, Oxford, 2000).

[38] L. Van Valen, *A new evolutionary law,* Evolutionary Theory **1**, 1 (1973).

[39] C. Darwin, *On the Origin of Species by Means of Natural Selection, or the Preservation of Favoured Races in the Struggle for Life.* (John Murray, London, 1859).

[40] H. Morlon, M. D. Potts, and J. B. Plotkin, *Inferring the Dynamics of Diversification: A Coalescent Approach,* PLOS Biology **8**, e1000493 (2010).

2

BRANCHING PATTERNS IN PHYLOGENIES CANNOT DISTINGUISH DIVERSITY-DEPENDENT DIVERSIFICATION FROM TIME-DEPENDENT DIVERSIFICATION

Théo Pannetier, César Martinez, Lynsey Bunnefeld, Rampal S. Etienne.

οχι Γιαννης, Γιανναχης

Greek saying

Branching patterns in phylogenies cannot distinguish diversity-dependent diversification from time-dependent diversification. **Evolution**, 2020, **75-1:** 25–38 [1].

2

ABSTRACT

One of the primary goals of macroevolutionary biology has been to explain general trends in long-term diversity patterns, including whether such patterns correspond to an up-scaling of processes occurring at lower scales. Reconstructed phylogenies often show decelerated lineage accumulation over time. This pattern has often been interpreted as the result of diversity-dependent diversification, where the accumulation of species causes diversification to decrease through niche filling. However, other processes can also produce such a slowdown, including time-dependence without diversity-dependence. To test whether phylogenetic branching patterns can be used to distinguish these two mechanisms, we formulated a time-dependent, but diversity-independent model that matches the expected diversity through time of a diversity-dependent model. We simulated phylogenies under each model and studied how well likelihood methods could recover the true diversification mode. Standard model selection criteria always recovered diversity-dependence, even when it was not present. We correct for this bias by using a bootstrap method and find that neither model is decisively supported. This implies that the branching pattern of reconstructed trees contains insufficient information to detect the presence or absence of diversity-dependence. We advocate that tests encompassing additional data, e.g., traits or range distributions, are needed to evaluate how diversity drives macroevolutionary trends.

Keywords — maximum likelihood, simulations, time-dependence, diversity-dependence, macroevolution, birth-death models

2.1. INTRODUCTION

STANDING species diversity ultimately results from speciation and extinction events of lineages over millions of years. Investigating the dynamics of these events in the past can therefore help us understand the current distribution of species across the globe, as these dynamics provide a background against which more fine-grained ecological and evolutionary processes can be studied. Macroevolutionary research has taken a "nomothetic" approach to diversification, favoring the study of "cases and events as universals, with a view to formulating general laws" [2]. That is, studies have sought to identify consistent trends in past diversity dynamics, and to infer evolutionary processes that produced them, in the hope of identifying universal rules that govern long-term evolution across the tree of life.

A common empirical trend is the tendency of diversification to slow down over the evolutionary history of many groups. This was first identified in fossil data on high taxonomic levels [3–5], showing that the number of taxa rapidly accumulated after mass extinction events but eventually slowed down to reach an equilibrium level. Molecular phylogenies of extant species have also suggested a slowdown of branching events, with per capita branching events often being more densely distributed near the crown of a phylogenetic tree than near its tips [6–10].

Various explanations have been offered for this observed slowdown in lineage accumulation [11]. Here we focus on arguably the most important of these: diversity-dependent diversification. Parallels between diversity curves inferred from fossil data and plateau-like patterns of community assembly on islands [3, 12] have been interpreted as speciation and extinction following similar dynamics to immigration and extinction in the theory of island biogeography [13]. This suggests a model of diversity-dependent diversification, where the species of an evolving clade compete for ecological resources in a shared niche space. Competitive interactions inside the clade strengthen as diversification proceeds and species accumulate, hindering speciation, increasing extinction, or both [3], leading to the observed slowdowns. Diversity-dependent diversification thus provides an intuitive framework to interpret macroevolutionary patterns in ecological terms, for instance that long-term evolutionary trends can be understood by up-scaling competitive interactions. However, competition for niche space is not the only possible explanation behind diversity dependent diversification; it may also be induced by allopatric speciation and range size dynamics [14]. Furthermore, some mechanisms have been shown to produce diversification slowdowns that are independent from standing diversity, for example when diversification is influenced by the age of the clade [15] or by fluctuations in temperature [10]. In fact, any scenario where the rate of diversification declines over time (i.e., is time-dependent) will cause a slowdown and is sufficient to explain such a pattern. Hereafter, we refer to the wide range of scenarios where the rate of diversification declines over time, but independently of the dynamics of diversity as time-dependence. The simplest time-dependent models make no assumption regarding the underlying mechanism, and hence these constitute suitable statistical null models to control for decelerating, diversity-independent diversification [16]. Here we study to what extent phylogenetic branching patterns can inform us whether diversity-dependent diversification is operating or whether there is some other time-dependent, but diversity-independent factor

governing the decline of diversification over time.

Diversification models are usually compared by fitting the models to phylogenetic branching times using maximum likelihood methods, and then evaluating their performance with information criteria such as likelihood ratio tests or the Akaike information criterion (AIC). The method to compute the likelihood of time-dependent models has been available for a long time [17], but a method to compute the likelihood for diversity-dependent models has become available only relatively recently [18]. Previously employed diversity- and time-dependent models assume simple relationships between speciation and extinction rates and diversity or time, such as a linear or exponential function. The performance of each model may thus depend largely on the choice of these functions, rather than on whether the observed pattern is driven by diversity over time, or time alone. Here, we formulate a time-dependent model where the expected number of species over time is equal to the expectation under the diversity-dependent model at any point in time, leaving as the only difference between the two models the presence or absence of a mechanism linking species diversity and diversification. This formulation however underlies an important difference on how diversification is set to slow down in each model. While the two models share the same expectation, in the truly diversity-dependent process, the diversification rate adjusts dynamically to the number of species in the tree. In the time-dependent process by contrast, the diversification rate is set in advance and declines continuously, following the expected diversity-dependent process, but independently from the actual number of species in the tree. We used simulations to generate phylogenetic trees under both models and fitted both models to each set of trees using maximum likelihood to compare the models' performances. Additionally, we used a bootstrap likelihood method to correct for type I errors in the detection of diversity-dependence. We find that in most cases, we are unable to decisively recover the generating model, and conclude that diversity-dependence cannot be distinguished from explicit time-dependence from branching patterns alone.

2.2. METHODS

2.2.1. DIVERSIFICATION MODELS

DIVERSITY-DEPENDENT MODEL

Birth-death diversification models assume a (per capita) speciation rate, denoted by λ, and a (per capita) extinction rate, μ. Both rates can be constant, or depend on time or on other factors, including diversity itself. For the diversity-dependent (DD) model we use the formulation introduced in Etienne *et al.* [18], with a linear, negative diversity-dependent effect on speciation rate (λ_N):

$$\begin{aligned} \lambda_N &= \max(0, \lambda_0 - (\lambda_0 - \mu_0)\frac{N}{K}) \\ \mu_N &= \mu_0, \end{aligned} \tag{2.1}$$

where parameter λ_0 is the speciation rate when $N = 0$, μ_0 is the (constant) extinction rate and K denotes the carrying capacity, that is, the value of the diversity N for which

$\lambda_N = \mu_N$. The model can also be written in the following form:

$$\begin{aligned} \lambda_N &= \max(0, \lambda_0(1 - \frac{N}{K'})) \\ \mu_N &= \mu_0, \end{aligned} \tag{2.2}$$

where $K' = \frac{\lambda_0 K}{\lambda_0 - \mu_0}$ is the maximum number of species in the system (or, more precisely, the nearest integer larger than K' is this maximum).

TIME-DEPENDENT MODEL

For the TD model we require that it has the same expected behavior over time as the DD model, so that the only difference between the models is the presence or absence of a feedback of diversity on diversification (the N term in the expression of λ_N). To be precise, we required the expected number of lineages alive at time t under the TD process ($N_{TD}(t)$) to be the same as the expected number of lineages under the DD process ($N_{TD}(t)$), that is, we start both processes with N0 species at time $t = 0$, and we further require that for any later time before present ($t < T$):

$$E[N_{\mathrm{TD}}(t)] = E[N_{\mathrm{DD}}(t)]. \tag{2.3}$$

Either of the two processes can go extinct. Hence we need to find $\lambda_{TD}(t)$ and $\mu_{TD}(t)$ such that this condition is met.

From the general birth-death model [19], it follows that

$$E[N_{\mathrm{TD}}(t)]'(t) = E[N_{\mathrm{TD}}(t)](\lambda_{TD} - \mu_{TD}) \tag{2.4}$$

$$\lambda_{TD} = \frac{E[N_{\mathrm{TD}}(t)]'(t)}{E[N_{\mathrm{TD}}(t)]} + \mu_{TD} \tag{2.5}$$

We assume the time-dependent and the diversity-dependent model share the same, constant, extinction rate, so that $\mu_{TD} = \mu_{DD} = \mu_0$. The expression for λ_{TD} then becomes:

$$\lambda_{TD} = \frac{E[N_{\mathrm{DD}}(t)]'(t)}{E[N_{\mathrm{DD}}(t)]} + \mu_0. \tag{2.6}$$

$E[N_{\mathrm{DD}}(t)](t)$ and its derivative are obtained from the master system of the DD model, introduced in Etienne *et al.* [18] (see also Supporting Information). The first term in eq. (6) is initially high: early in the simulation, we expect $E[N_{\mathrm{DD}}]$ to be low, but its rate of change to be fast. As time passes the derivative decreases, and approaches zero when $E[N_{\mathrm{DD}}]$ reaches K. At this point, $\lambda_{\mathrm{TD}}(t)$ approaches μ_0 and the diversification process reaches a dynamic equilibrium.

Note that under this process, how λ_{TD} changes through time is independent of the actual diversity in the tree, and as a consequence all realizations of the process will share the same speciation (and, thereby, diversification) rate through time. This is in contrast with the DD model, where λ_{DD} tracks diversity in the tree, and therefore, can change from a realization of the process to the next.

The two models share the same set of parameters, $\{\lambda_0, \mu_0, K\}$. However, parameter K takes a slightly different interpretation in the TD model: rather than providing a limit on the number of species, it sets a time scale for the approach to equilibrium diversity. Parameter K thus modulates the progressive onset of the diversification slowdown in time.

2.2.2. SIMULATION PROCEDURE

We simulated DD and TD phylogenetic trees using the Gillespie algorithm, as implemented in functions `dd_sim` and `td_sim`, respectively, from the R package DDD 4.3 [18].

We set $\lambda_0 = 0.8$ and $K = 40$ following Etienne *et al.* [18], so that trees reach carrying capacity after around 10 myr in the absence of extinction. We then simulated trees for different crown ages, to capture different phases of the radiation relative to equilibrium diversity: exponential growth with little diversity-dependence (5 myr), equilibrium diversity reached recently (10 myr), or sometime in the recent (15 myr) or ancient (60 myr) past.
Varying the crown age with fixed λ_0 and K thus allowed us to consider trees with an increasing (DD or TD) slowdown signal.
For each age, we considered four scenarios with increasing levels of extinction ($\mu_0 = 0.1, 0.2, 0.3$ or 0.4), extinction being known to erase information in phylogenetic branching patterns [16]. Note that we did not vary the speciation rate λ_0, because this only changes how fast trees reach equilibrium diversity, and therefore affects the distribution of branching times only relatively to the crown age [18]. We also considered four additional settings (one for each level of extinction) with $K = 80$ (and crown age = 15 myr), to assess whether the inference would yield more power for larger trees. For each of these 20 scenarios, we simulated a set of 1000 phylogenetic trees.

We conditioned the simulation process on nonextinction of the trees: when either crown lineage went extinct during the simulation process, the simulation was stopped and the whole tree simulated anew. Note that this conditioning is likely to affect the expected number of species over time to some extent, and was not accounted for in the formulation of the TD model. It is not possible to choose a TD model for which the conditional expectation is similar to that of the DD model, because this requires knowledge of the probability distribution that we did not know yet, but in fact aimed to find through this procedure.

2.2.3. MODEL SELECTION

Our primary objective was to study whether the phylogenetic trees generated by either model are indeed best fit by the model that generated them, or whether both models fit the data. We therefore fitted both models to each set of phylogenetic trees, using maximum likelihood, and looked at the log-likelihood ratio (LLR) of DD versus TD. Note that this is equivalent to comparing AIC, because the models have the same number of parameters.

We used the likelihood formula introduced in Etienne *et al.* [18] for DD. In the Supporting Information, we derive the likelihood for the TD model with constant extinction

rate $\mu_{TD}(t) = \mu_0$ and the speciation rate given in equation (2.6), based on the general likelihood for time-dependent models introduced in Nee *et al.* [17]. The computation of both likelihoods are implemented in functions `dd_loglik` and `bd_loglik`, respectively, in R package DDD 4.3. The optimization routine for these two likelihood functions is based on the subplex algorithm, and is implemented respectively in R functions `dd_ML` and `bd_ML` of the same package. Initial parameter values were set to the true values to ensure relatively fast convergence of the likelihoods. Convergence however sometimes proved difficult, for example for large trees (i.e. more than a hundred tips), because the computation of the TD likelihood became challenging for trees of this size, and because of the presence of local optima in the likelihood landscape. In these cases, we initialized the optimization with a different value of K (the most influential parameter for the likelihood). First, TD trees were often larger than the carrying capacity would allow in DD (see "Results" section). In instances where $N > K'$, the likelihood of either model becomes 0 and we instead set the initial value of K to $N' = N\frac{\lambda_0-\mu_0}{\lambda_0}$. Second, to avoid local optima, we started the optimization at $K = N$, which we had observed to often be close to the maximum likelihood estimate for other trees.

2.2.4. BOOTSTRAP LIKELIHOOD-RATIO TEST

It has been shown in a previous comparison of DD with the constant-rate (CR) model [20] that DD tends to overfit the data, causing erroneous inference of diversity dependence when it is not the true model. Because the two models we compare here are by design much more similar than DD and CR, we expected to encounter the same issue. We addressed this problem by using a procedure similar to the parametric bootstrap procedure introduced in Etienne *et al.* [20]. Instead of using likelihood ratios as a direct model selection criterion, we used our simulated trees to generate distributions of likelihood ratios for DD and TD trees (Fig. 2.1). Although DD is expected to receive inflated support on both DD and TD trees, it is expected to fit better on DD trees, where it is the generating process, than on TD trees. This expectation can be used to set a model selection criterion based on the distribution of the LLR for DD and TD trees. We defined the threshold for the likelihood ratio of DD to TD above which the selected model would be DD to be the 95th percentile of the LLR distribution for TD trees (blue line in Fig. 2.1). This means that we allow a 5% error: by specification 5% of all TD trees would yield a higher LLR than this threshold. Similarly, LLR values below the 5th percentile of the LLR distribution of all DD trees (green line in Fig. 2.1) would be interpreted as evidence for TD; that is, we allow a 5% error in calling a tree a TD tree when it is actually a DD tree. If an empirical (or simulated) LLR value falls between these two thresholds, it is not possible to decisively select either model over the other (gray area in Fig. 2.1).
Furthermore, the fraction of DD trees that exceed the 95th percentile of the LLR distribution for TD trees is a measure of the power to detect DD. Conversely, the fraction of TD trees with a LLR below the 5th percentile of the LLR distribution for DD trees is a measure of the power to detect TD. We denote these two measures by P_{DD} and P_{TD}, respectively. If the two distributions largely overlap, then the power is very low. They are equal to our significance level in case the distributions completely overlap, in which case one can also conclude that the models are not distinguishable.

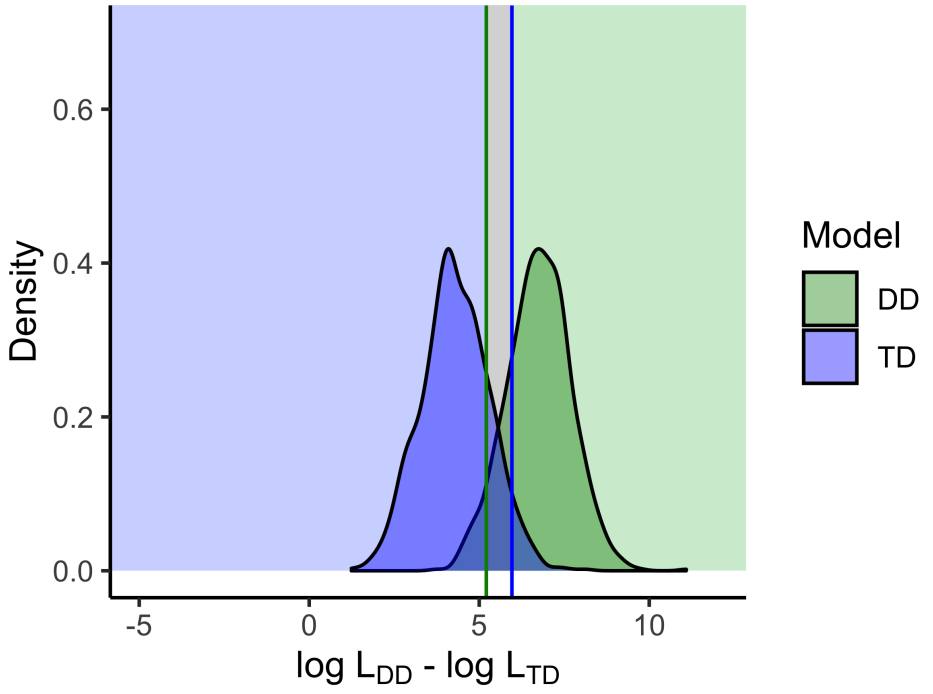

Figure 2.1 | Potential distribution of the logarithm of the likelihood ratios (or, equivalently, the log-likelihood differences) for diversity-dependent trees (green) and time-dependent trees (blue). For illustrative purposes, each curve was generated by sampling 1000 values in normal distributions with a standard deviation of 1 and mean 6.8 (DD) and 4.3 (TD). Vertical dashed lines represent the 5th and 95th percentiles of the DD and TD distributions, respectively. Empirical log-likelihood ratio values falling to the left of the green dashed line would point to support of the TD model (blue background), whereas empirical values falling to the right of the blue dashed line would point to support of the DD model (green background). For empirical values in the gray area, neither model can be selected and the test is inconclusive.

Family	Age	Clade size	λ_0		μ_0		K		LLR
			DD	TD	DD	TD	DD	TD	
Parulidae	10.8	115	0.820	0.756	0.110	0.068	118.9	170.821	1.851585
Canidae	7.0	34	7.592	8.770	0.596	0.552	33.3	30.924	2.604858
Pseudocheiridae	27.4	16	0.628	0.319	0.031	0.021	15.2	16.828	3.312996
Bucerotidae	48.6	59	0.199	0.156	0.052	0.034	60.5	85.756	1.325633
Indicatoridae	17.1	17	1.543	1.174	0.233	0.244	16.4	13.472	2.341508

Table 2.1 | Maximum likelihood DD and TD parameter estimates for each Family, and logarithm of the likelihood ratio (LLR) of the two models (DD over TD). DD estimates were taken from Condamine *et al.* [10], while TD estimates where obtained here (see Methods).

2.2.5. BOOTSTRAP LIKELIHOOD RATIO TEST ON EMPIRICAL PHYLOGENIES

To complement our simulation study, we applied the bootstrap procedure described above to a set of empirical phylogenies that bore a strong signal for diversity dependence.

We took the set of Tetrapod family-level phylogenies compiled from published literature by Condamine *et al.* [10], and selected five groups for which the linear diversity-dependent model with constant extinction (that is, the DD model we used for simulations) fitted best out of 26 birth-death models. The five groups included three bird families, Parulidae, Bucerotidae, and Indicatoridae, and two mammal phylogenies, Canidae and Pseudocheiridae. Bird phylogenies were assembled by Condamine et al. from the bird phylogeny published by Jetz *et al.* [21]; and mammal phylogenies were pruned from the mammalian tree of Rolland *et al.* [22], itself built from the tree of Bininda-Emonds *et al.* [23]). For each group, we extracted the estimated parameter values for the DD model reported in Condamine *et al.* [10], and used these as a starting point for fitting the TD model introduced in the "Time-dependent model" section to each phylogeny (see Table 2.1). We then obtained the LLR distribution for each model by simulating 1000 DD and TD trees from the corresponding parameter estimates, and fitting both models to each simulated tree. We computed the decision thresholds as described in the “Bootstrap likelihood ratio test” section and compared the LLR obtained for the original phylogeny to decide if DD, TD, or neither, could be selected.

2.3. RESULTS

2.3.1. PHYLOGENETIC PATTERNS OF TIME-DEPENDENT AND DIVERSITY DEPENDENT TREES

EXPECTED LINEAGES-THROUGH-TIME PLOTS OF TIME-DEPENDENT AND DIVERSITY DEPENDENT TREES ARE SIMILAR

Both TD and DD trees exhibited the typical pattern of a DD radiation, as described in Etienne *et al.* [18]: initial exponential growth (< 5 myr), followed by convergence to a plateau (> 5 myr) with the pull-of-the-present [17] visible for trees with extinction, resulting in the typical inverted S-shape. The shape of TD trees reflected our formulation of the TD model, as the mean TD lineage-through-time (LTT) curves closely matched the DD LTT curves across all parameter settings (Fig. 2.2).

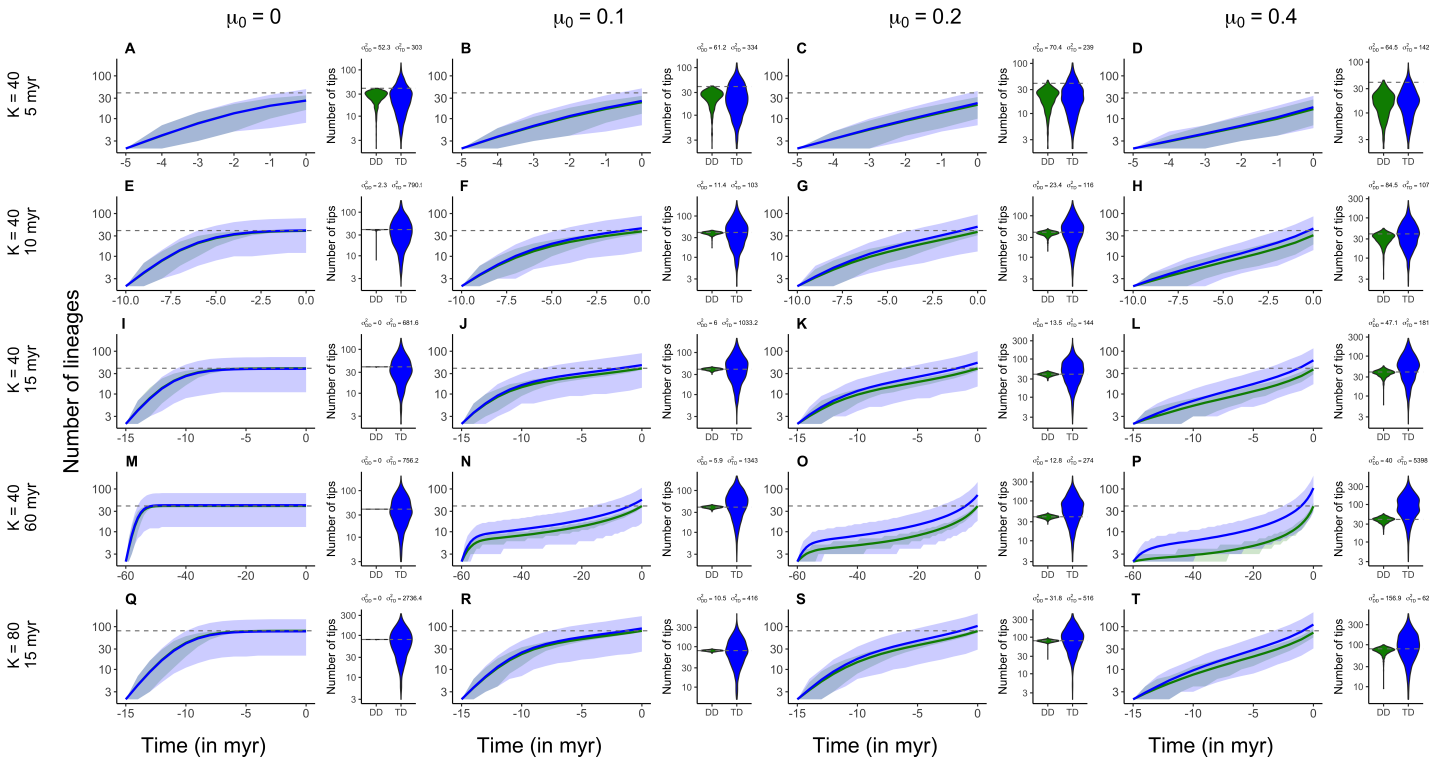

Figure 2.2 | Lineages-through-time (LTT) plots of trees simulated under the diversity-dependent (green) and time-dependent (blue) model. Curves were obtained by computing the average number of tips in the 1000 trees at every myr. The green curve is barely visible in most panels as it overlaps with the blue curve. Transparent areas in the background denote the 10th and 90th percentile of the number of species through time, coloured by model (blue for TD and green for DD). Violin plots represent the distribution of the number of species N at present ($t = 0$) for each model, and variance scores are noted above each plot. Horizontal dashed lines in both violin and LTT plots indicate the carrying capacity, K. Note that the y-axis on both LTT and violin plots is shown on a log-scale.

The difference between the two curves for parameter settings with extinction (Fig. 2.2, second through fourth columns, second through fifth rows) is a result of conditioning the phylogenies on survival during simulations (see the next section). Apart from this, average DD and TD LTT curves are qualitatively similar.

TIME-DEPENDENT TREES ARE MORE VARIABLE IN SIZE THAN DIVERSITY-DEPENDENT ONES
Despite both models producing similar trees on average, the distribution of tree sizes reveals a key difference between the two models (Fig. 2.2, right-hand side panels). The size of DD trees is narrowly distributed around the carrying capacity: virtually all trees without extinction and older than 10 myr had 40 (Fig. 2.2, E, I, M) or 80 (Q) tips by the end of the simulation. Extinction introduced more variance, but tree size remained closely constrained around the carrying capacity (Fig. 2.2, second through last columns). By contrast, the size of TD trees was broadly distributed for all parameter settings (note the log-scale on the y-axis), being skewed and having a long tail corresponding to large trees (especially on Fig. 2.2, M). Both simulation age (Fig. 2.2, fourth row, 60 myr vs. second and third rows) and extinction (Fig. 2.2, last columns vs. second and third columns) contributed to this variance. The TD model thus produced a much wider range of outcomes, with trees often smaller or larger than would be expected under diversity-dependence. This wider spectrum of realizations of the TD model is a consequence of the absence of a direct feedback of diversity on diversification and how the speciation rate changes in each model, as exposed in the “Time-dependent model” section.. In the DD model, rates are continually adjusted based on the discrepancy between the standing diversity and the carrying capacity. As a result, the effect of stochasticity is reduced compared to a TD process; should DD diversification be unusually fast or slow in a particular time window, then rates will be decreased and increased, respectively, in the next time window. Given enough time to grow to carrying capacity, the distribution of tree sizes will be tightly constrained around the carrying capacity (Fig. 2.2), akin to the dynamics of Ornstein-Uhlenbeck process. In a TD, diversity-independent process, by contrast, rates are blind to the state of the tree, and any stochastic burst or lag in time to speciation will alter the course of the radiation from its expected final state. As a result, tree size ends up more widely distributed around the carrying capacity, and variance in tree size increases over time, although in a decelerated way (as the speciation rate decreases over time). This is more akin to a Brownian motion process where drift would decrease over time toward zero.

This, along with conditioning on survival (see the "Methods" section), explains the large size of some TD trees in the settings with longer simulation times and a high extinction rate (Fig. 2.2, second to last columns, second to last rows). Trees that went entirely extinct through the simulation were simulated anew, pushing the sampled distribution of tree sizes upwards compared to that of DD trees. This difference increased with the age of the tree, as trees with longer simulation times were more likely to go extinct before the present.

2.3.2. MODEL SELECTION

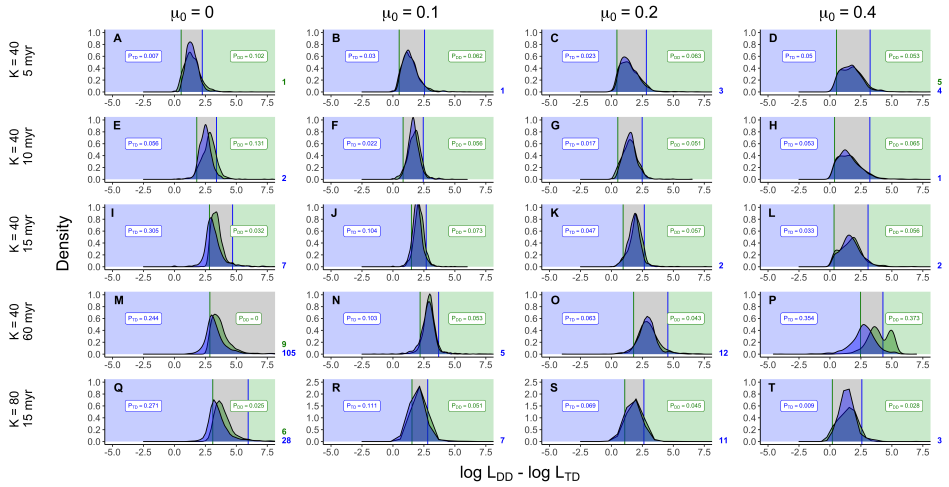

Figure 2.3 | Distributions of the logarithm of the likelihood ratios (or, equivalently, log-likelihood differences) for diversity-dependent (green) and time-dependent (blue) trees, respectively. Vertical lines represent the 5th and 95th percentiles of the distribution for DD and TD trees, respectively. Background colours indicate the result of the test as in Fig. 2.1. P_{DD} and P_{TD} labels denote the power of the analysis for DD trees and TD trees, respectively (see "Methods" section). Numbers right to the x-axis of each plot indicate the number of trees of each model outside of the plotting area ($LLR > 7.5$).

RAW LIKELIHOOD RATIOS ARE NOT ADEQUATE SELECTION CRITERIA FOR DISTINGUISHING DIVERSITY-DEPENDENCE FROM TIME-DEPENDENCE

LLRs were almost always found to be positive (Fig. 2.3), suggesting support for diversity-dependence over time-dependence even when the tree was simulated under time dependence. This was the case across all parameter settings, with the exception of a few TD trees of 60 myr with extinction, where LLR values were slightly negative (Fig. 2.3, N-P). The strongest support for DD diversification (most positive LLR scores) was obtained for older trees with no extinction (Fig. 2.3, E, I, M, Q), that is, trees that were at equilibrium diversity at present. For younger trees (Fig. 2.3, A) and trees with extinction (second through last columns), likelihood ratios were less pronounced, yet still positive. In short, based on likelihood ratios, diversity-dependent diversification is strongly supported, regardless of whether it was the simulated mode. Using raw likelihood ratios as a model selection criterion would then yield a frequency of type-I errors (false-positives) close to 1.

USING LIKELIHOOD RATIOS AS A STATISTIC IMPROVES TYPE-I ERRORS BUT THE MODELS CAN NO LONGER BE DISTINGUISHED

Using the bootstrap procedure described in the “Bootstrap likelihood ratio test” section reduced the rate of type-I error to 0.05, by design. However, the distribution of the likelihood ratio for DD and TD trees largely overlapped for most scenarios (Fig. 2.3), resulting in the test having a low power (P_{DD} and P_{TD}) to detect the model used to generate the trees. The effect of parameters across the different scenarios on the statistical power of this test appeared to be ambiguous. Without extinction, P_{DD} and P_{TD} increased slightly from 5 myr to 10 myr scenarios (Fig. 2.3, A vs. E). P_{DD} decreased when extinction

was introduced, but was comparable across extinction levels (Fig. 2.3, B-D and E-H), whereas P_{TD} was low with or without extinction (Fig. 2.3, A-D, E-H). P_{DD} did not increase from 10 myr to 15 myr trees (Fig. 2.3, E-H vs. I-L), despite the latter having been at equilibrium diversity for a long time (Fig. 2.2, I-L), and was low for all levels of extinctions (Fig. 2.3, I-L). By contrast, P_{TD} for 15 myr trees was initially relatively high (Fig. 2.3, I), but gradually decreased with higher extinction levels (Fig. 2.3, J-L). For 60 myr trees, without extinction, it was not possible to recover DD for any tree ($P_{DD} = 0$, Fig. 2.3, M), as the distribution of the LLR for TD trees displayed a very long tail, thus pushing the threshold of detection of DD well beyond the distribution of DD trees (Fig. 2.3, M). We discuss this issue further in the next paragraph, in relation to tree size. $P_{DD} = 0$ was then low for intermediate extinction levels (Fig. 2.3, N-O), and increased sharply for the highest extinction setting, yielding the highest power across all settings (Fig. 2.3, P). A relatively high P_{TD} was found for 60 myr trees with no extinction (Fig. 2.3, M). Intermediate extinction levels appeared to erode P_{TD} (Fig. 2.3, N-O), while, again, the highest power was found for the highest extinction settings (Fig. 2.3, P).

In summary, the power to detect both DD and TD was low overall, ranging between 0.05 to 0.1 for most settings (Fig. 2.3). Some settings yielded a higher power, but the power varied inconsistently between P_{DD} and P_{TD}, or with tree age or level of extinction. Perhaps surprisingly, the highest power to detect both DD and TD was found for the oldest trees (60 myr), with high extinction (Fig. 2.3, P), which stands in contrast to the argument that extinction erodes signal in phylogenetic trees [16, 24]. In this setting, the distribution of the LLR of DD and TD trees did not overlap much (Fig. 2.3, P). However, this is likely due to the large mismatch in the distribution of tree sizes we mentioned earlier, and the result of a different conditioning of the likelihood between the two models (see "Methods" section), rather than optimal conditions to distinguish the two models.

Tree size did not appear to have an effect on the power of the bootstrap likelihood ratio test. Despite the settings with $K = 80$ producing markedly larger trees than settings with $K = 40$ (Fig. 2.2, I-L vs Q-T), P_{DD} and P_{TD} were comparable between settings (given the same level of extinction), with even a slightly stronger signal for trees simulated with $K = 40$ (Fig. 2.3, I-L vs Q-T), suggesting that larger trees did not contain more information. We graphically inspected whether either model was easier to recover in larger trees, under the expectation that larger trees contain more information (Fig. 2.4). In this case, one would expect large trees to lie on the edges of the LLR distribution in Fig. 2.3, close to, or beyond the corresponding threshold value. That is, tree size should display a positive correlation with the LLR in the case of DD trees, and a negative one in the case of TD trees. We found no correlation between tree size and the LLR in DD trees (Fig. 2.4, top half). In the case of TD trees, we did find a curious apparent correlation between the size of the tree and the LLR (Fig. 2.4, bottom half). The correlation only started above a certain tree size (75 tips for settings with $\mu_0 = 0$, Fig. 2.4, E, I, M and Q), and for most parameter settings, appeared to be driven by a few outlying, exceptionally large trees (Fig 2.4, A, N-O, Q-T). Yet in at least one setting (Fig. 2.4, M) this set of large trees with high log-likelihood ratios was clearly part of the sample. Note that this is also visible in Fig. 2.3 (panel M), as the long tail to the right of the distribution (and causes a null P_{DD} for this setting). We fail to understand this result. Apart from this setting, the correlation only concerns a handful of trees in each setting, and thus does not impact the results of

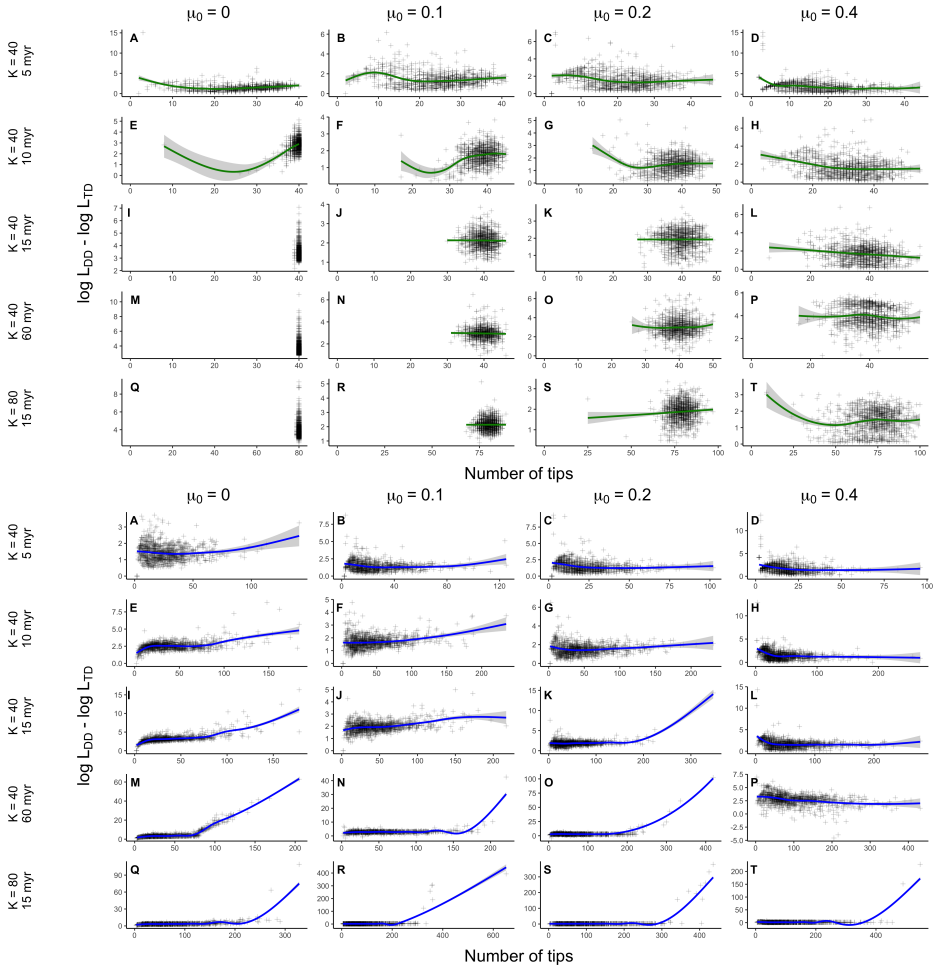

Figure 2.4 | Tree size (x axis) plotted against log-likelihood ratios for DD trees (top half) and TD trees (bottom half) for each scenario. Each point is a single tree. The smooth lines (green for DD trees, blue for TD trees), were present, computed with `ggplot2` (version 3.3.1) function `geom_smooth` with default settings, which performed either a GAM or a LOESS regression through the data. Labels match those of figure 2 and 3

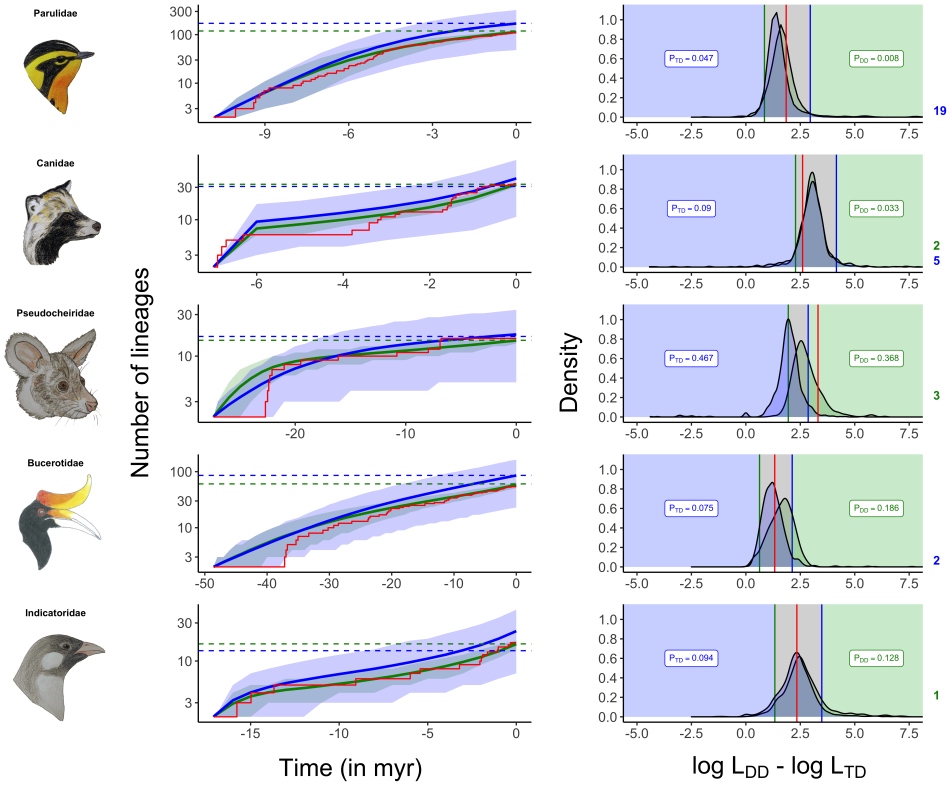

Figure 2.5 | Average lineages-through-time (LTT) curves (left column) and distribution of the logarithm of the likelihood ratio (right column) for simulated trees generated from empirical phylogenies. Color schemes follow those of Fig. 2.2 and Fig. 2.3, respectively. Red lines denote the LTT (left panels) and inferred likelihood ratio (right panels) of the empirical phylogenies. The pictures on the rightmost columns were drawn by the first author and represent a member species from each family. From top to bottom: *Setophaga fusca* (Müller, 1776)*Nyctereutes procyonoides* (Gray, 1834), *Petauroides volans* (Kerr, 1792), *Buceros rhinoceros* (Linnaeus, 1758), *Indicator indicator* (Sparrman, 1777)

the test. In any case, the correlation does not support larger trees containing a stronger signal for the original model: these trees are simulated with the TD model, and a high LLR denotes strong support for the DD model.

2.3.3. DD AND TD ARE INDISTINGUISHABLE FOR EMPIRICAL PHYLOGENIES ACCORDING TO BOOTSTRAP LIKELIHOOD RATIO TEST

The set of empirical phylogenies covered a broader range of values than the simulation study (Table 2.1). Yet, when we simulated trees from these parameter values, we found that the distribution of the LLR for DD and TD trees largely overlapped, in four out of the five examples (Fig. 2.5, right column), and the LLR for the empirical phylogeny fell between the decision thresholds (Fig. 2.5). Consequently, for these families (Parulidae,

Canidae, Bucerotidae, and Indicatoridae) it was not possible to select either model over the other.

In one instance (Pseudocheiridae) however, the empirical LLR was found to lie above the 95th percentile of the TD distribution, supporting that this group did experience DD diversification (Fig. 2.5, central row). Here, again, the power of the analysis did not appear to vary consistently with any of the parameters, and so the conditions leading to higher power in the case of Pseudocheiridae do not appear to be tied to this setting presenting favorable conditions. Pseudocheiridae had a lower carrying capacity ($K_{DD} = 15.2$, $K_{TD} = 16.8$) compared to our simulation settings, yet another family with a comparable inferred carrying capacity (Indicatoridae, $K_{DD} = 16.4$, $K_{TD} = 13.5$) did not yield a high statistical power for the test. Pseudocheiridae are relatively old (27.4 myr), but the older Bucerotidae (48.6 myr) show a weak statistical power. Pseudocheiridae show a discrepancy in the baseline speciation rate λ_0 and therefore the initial, net diversification rate ($r_0 = \lambda_0 - \mu_0$)(Table 2.1); the estimate for DD was about twice that for TD. There were two other phylogenies for which estimates for the net diversification rate diverged substantially between the two models as well: Canidae ($\Delta r_0 = -1.222$) and Indicatoridae ($\Delta r0 = 0.380$). In both cases, the power of the analysis was low (Fig. 2.5).

The average LTT plots for DD and TD trees (Fig. 2.5, left column) were quite different. This is not due to different conditioning as we described for the simulation study, but rather reflects that the two sets of trees were simulated from different parameter values (the maximum likelihood estimates for each model, see "Methods" section). This difference in the methods made it slightly easier to distinguish the two models in the empirical study, but it is the most appropriate choice to use the maximum likelihood estimates from each respective model. In an alternative set of results where we simulated both DD and TD trees from the maximum likelihood estimates of the DD model, we found that none of the five families were recovered as DD or TD (Fig. 2.6).

2.4. DISCUSSION

We used simulations to compare DD diversification with TD, diversity-independent diversification. We tailored our TD model to minimize differences between the two models to focus on differences arising from the contrasting diversification modes: presence or absence of negative diversity feedback on diversification. Our results indicate that, across much of the tested parameter space, diversity-dependence cannot be reliably distinguished from time-dependence without diversity-dependence.

We constrained our models to have a similar branching tempo in order to identify differences in the branching pattern caused solely by the presence or absence of diversity-dependence. We did this by equating the expected number of species through time in both models. We observed that the expected LTT plots were similar, only differing quantitatively due to conditioning on survival.

Although no differences were apparent at the level of individual trees, we found that DD diversification produced a much narrower range of branching patterns than the equivalent TD model. In an empirical context, this feature of DD diversification would not be observable in an individual phylogenetic tree, which is the typical object of macro evolutionary inference. Rather, this would only be observable if one considered

a collection of phylogenetic trees, under the assumption that each diversified with the same carrying capacity, speciation, and extinction rates. Therefore diversity-dependence could in principle be detected with data of various clades diversifying under the same parameters, a situation that is unlikely to occur in the real world. A notable example would be the scenario considered in the DAISIE model of island diversification [25], where the rates of speciation and extinction are assumed to be properties of an island, shared by all the lineages on the island. However, DAISIE typically considers a handful of trees with few tips, and such data are unlikely to provide the resolution of our simulated trees.

Using likelihood ratios for model selection, following the standard procedure for testing competing diversification models [26, 27], we found DD diversification to be better supported across all but a few trees, regardless of whether the trees were simulated under diversity-dependence or not, yielding consistent false-positives in the latter case. This confirms the systematic bias in favor of diversity-dependence found in an earlier comparison of DD and CR diversification [20], and indicates that a direct comparison of diversity-dependent models with other time-dependent models using likelihood ratios (or equivalently, AIC values) should be avoided. One may wonder what the origin of this bias is. Etienne *et al.* [20] mentioned a violation of the mathematical conditions for a reliable comparison: the CR model being a special, boundary case of diversity-dependence (where K is infinite). This violation does not apply here.

We observed that the final size of DD trees was strongly constrained around the carrying capacity, whereas TD trees varied widely in size (Fig. 2.2). We interpret this as diversity-dependence constraining the range of possible realizations of the diversification process. During DD diversification, the speciation rate is constantly modulated by the current diversity. That is, should stochasticity produce an excess of speciation or extinction events, the speciation rate is adjusted accordingly, allowing diversification to proceed following the expected tempo. Fewer realizations of the stochastic process are probable under diversity-dependence, so the likelihood that a DD model produced a given tree is higher than for the equivalent diversity-independent model, when evaluated at the maximum likelihood parameters. It is important to note that this is not specific to the models we used here. Rather, this result arises from the definition of diversity-dependence, and the use of maximum likelihood.

To address this issue, we followed a similar procedure to the bootstrap method suggested in Etienne *et al.* [20], which guarantees by construction that the type-I errors are low (they are set by the user). We considered the distribution of likelihood ratios for DD and diversity-independent trees, and defined thresholds beyond which we would be confident that a tree was produced under a DD or strictly TD process, akin to the distribution of a statistic. If the models are distinguishable, one would expect the distribution of likelihood ratios for DD trees to be right-shifted to some extent compared to TD trees (Fig. 2.1), the model fitting better on trees that were generated under it than on trees generated under the other model. This was not the case, however: the likelihood ratios were comparable for the two types of trees, and the distributions overlapped considerably as a result (Fig. 2.3). Only in the exceptional case of unusually old trees with high extinction was it relatively often possible to recover the generating model (Fig.2.3, panel P). In this case diversity-dependence is at its strongest: the speciation rate changes frequently as diversity drifts around equilibrium diversity, and frequent extinction events trigger new

speciation events. This result suggests that old groups that retained a stable diversity, with a high turnover for most of their evolutionary history provide the best power to distinguish diversity-dependence from a purely TD slowdown. Yet, for this scenario, we observed a large difference in the expected LTT plots (Fig. 2.2, panel P), and this may be the result of a differential conditioning on survival between the two models (see Methods). This difference might cause the gap between distributions observed in Fig.2.3, so we could not rule out the possibility that the better power to distinguish diversity-dependence from time-dependence observed for this setting might be the result of an assumption in our methods. For all other scenarios considered, neither the intensity of extinction, the amount of time the phylogeny stayed at equilibrium diversity (age of the tree), or tree size appeared to have a clear effect on the power of the bootstrap likelihood ratio test, and the chances of correctly inferring diversity-dependence or its absence remained low over the entire span of our simulations.

Because likelihood-based methods performed so poorly, alternative methods could be considered to distinguish the two models. One could consider likelihood-free methods. Approximate Bayesian Computation (ABC) [28–30] and neural network based methods [31, 32] have been applied to macroevolutionary inference, and have been shown to yield reliable parameter estimates. ABC estimation of evolutionary rates in particular has been shown to perform on a par with likelihood-based inference when coupled with the normalized lineage-through-time (nLTT) metric [28]. This method could be used to compare support for models, by comparing the average error made by trees simulated under either process compared to a reference tree for which the original process is known. We anticipate however that this approach would not be able to distinguish the two models either, because our likelihood-based analysis has shown that a tree produced by either model can be similarly generated by the alternative model with different parameters.

In conclusion, our failure to distinguish a DD model from a comparable diversity-independent model of diversification stems from a lack of information in the branching patterns of the simulated trees. Nee *et al.* [17] proved that for each CR birth-death process there is a pure birth process with a declining speciation rate which gives a mathematically identical likelihood. This proof has recently been generalized: each TD diversification model has an infinitely large family of other TD diversification models that have identical likelihoods [33]. Hence, phylogenetic branching times cannot distinguish between members of this family of models. Here we have shown that we can almost never distinguish statistically between the most often used DD model and a TD diversification model, and by virtue of the results of Louca and Pennell [33], all the TD models that are congruent with it. We note that our result is not a mathematical identity, but the models are virtually indistinguishable in practice.

It could be argued that the TD model we formulated for this comparison is artificial in construction, and unlikely to represent a realistic biological process. TD models encompass any diversification model where net diversification is formulated as a direct function of time [6]. Simple TD models specifying linear or exponential changes in rates have been used efficiently to characterize the temporal features of diversification in empirical trees [9]. We could have used a similar model here as a control for diversity-independent diversification slowdowns, as has been done before [16, 34]. Yet, there is no clear biological reason for a DD or diversity-independent decline to follow simple rules. TD,

but diversity-independent diversification could be driven by the complex fluctuations of an environmental variable [35, 36], and the strength of diversity-dependence could change as the carrying capacity changes over time [37]. For example, consider the situation where an investigator tests a phylogeny for diversity-dependence by comparing the fit of the linear DD model used here against a model specifying a linear decline of diversification over time. Unknown to the investigator, the phylogeny was shaped by long-term climatic changes (i.e., is TD), but the effects on the branching pattern more closely match the DD model than the specified linear TD decline, leading to the incorrect conclusion of diversity-dependence. For this reason, we have based our comparisons on models that generate the same predictions for the timing of branching. We found that, in this situation, diversity-dependence does not produce any distinctive feature on a single tree that would distinguish it from a diversity-independent process with the same expectation for the number of species over time. Note that, throughout this study, we only consider the case of negative diversity-dependence, as we are interested in disentangling the potential causes of diversification slowdowns. Our conclusions would not apply to a positive DD process [38, 39], where "diversity-begets-diversity." In this case, there would not be an equilibrium point in the number of species, and variance in tree size would not be constrained by diversity-dependence.

DD diversification is expected to arise under an evolutionary scenario where diversification is driven by competitive interactions, either through ecological opportunities [40], or the partitioning of resources between related taxa [41, 42]. This simple model generates predictions beyond the distribution of branches in a phylogeny [11]. For instance, classic verbal models of adaptive radiation [40, 43] predict that the rate of trait evolution should slow down over time along with the speciation rate, as progressive niche filling precludes further innovation [34, 44]. Similarly, the accumulation of trait disparity over time should follow a damped increase [45]. Studies have reported evidence for joint slowdowns in lineage and disparity accumulation, [34, 46, 47], but trait evolution slowdowns have also been reported from groups that do not exhibit diversification slowdowns [44, 48], and a meta-analysis [49] showed that slowdowns in trait evolution were far from ubiquitous, even in classic examples of adaptive radiation. This suggests that the interplay between competition, trait evolution and phylogenetic branching may be complex, and that rates of speciation and trait evolution are not necessarily coupled [50, 51].

Tests of the expected distributions of traits and branching events through time under the classic verbal model can be developed using mechanistic models that explicitly incorporate how radiating species are expected to compete based on trait similarity. Aristide and Morlon [52] have recently simulated adaptive radiation under such a model and found that although diversification slowdowns indeed appeared as a result of competition, rates of trait evolution seldom slowed down, and disparity only stopped increasing when hard bounds on trait space were imposed. Incorporating how species interact in space may however change expectations and the outcomes of any model, for example, range overlap of competitors is expected to modulate the effect of competition on trait evolution [53].

Models incorporating trait evolution could make use of tests based on tree topology to infer diversification mode, particularly as empirical phylogenies have been noted

to be highly unbalanced [54]. Such an option was not available to us as our models are "species-exchangeable" [26], that is, the identity of each lineage does not affect the diversification process (as opposed to, for example, trait-dependent processes). It is, however, available for models where trait values [52] or the spatial distribution [55] of each lineage is inherited along the branches.

We note that branch-based methods such as the ones used here are still powerful tests for distinguishing models predicting different tempos of diversification. Should more precise, biologically grounded predictions for DD patterns be derived beyond simple linear or exponential relationships, we expect it may also be possible to adapt existing methods to test for the role of competition in phylogenies. Mechanistic models considering the underlying ecological and geographic components of diversification [52, 56, 57] are likely to help test the predictions of verbal models and formulate joint predictions of patterns across branching, traits and distributions.

2.5. CONCLUSIONS

We constrained the tempo of diversification to be the same across two models of diversification. There is little information in the branching pattern that would allow us to detect the presence or absence of diversity-dependence. This implies that the mode of diversification alone hardly leaves a diagnostic signature on the branches of a phylogeny. We have provided a bootstrap likelihood ratio test to properly identify the presence or absence of diversity-dependence. This can be used by empiricists, but we have shown that one will only rarely detect diversity-dependence even if it is present; failure to detect either presence or absence of diversity-dependence is very likely. We call for the derivation of more precise predictions for DD diversification, perhaps encompassing multiple data types, and based on explicit ecological processes. Mechanistic, eco-evolutionary models that have emerged in the recent literature offer a promising framework for deriving such predictions.

SUPPORTING INFORMATION

COMPUTATION OF $\lambda(t)$ UNDER THE TD MODEL

The speciation rate under the TD model is:

$$\lambda_{TD}(t) = \frac{E(N_{\mathrm{DD}}(t))'}{E(N_{\mathrm{DD}}(t))} + \mu_0 \tag{2.7}$$

Evaluating this expression requires knowledge of the expectation N_{DD} and its derivative.

The expected value of N for the DD model is

$$E(N_{\mathrm{DD}}(t)) = \sum_{n=1}^{\lceil K' \rceil} nP_n(t) \tag{2.8}$$

where $P_n(t)$ is the probability of having n species in the phylogeny at time t [18]. The derivative of the first order moment is

$$\frac{\mathrm{d}E(N_{DD}(t))}{\mathrm{d}t} = \sum_{n=1}^{\lceil K' \rceil} n\frac{\mathrm{d}P_n(t)}{\mathrm{d}t}. \tag{2.9}$$

where $\lceil K' \rceil$ is the ceiling value of K'. The equation for $\frac{\mathrm{d}P_n(t)}{\mathrm{d}t}$ is (see Etienne *et al.* [18]):

$$\frac{\mathrm{d}P_n(t)}{\mathrm{d}t} = P_{n-1}(t)\lambda_{n-1}(n-1) + P_{n+1}(t)\mu_{n+1}(n+1) - (\lambda_n + \mu_n)P_n(t)n \tag{2.10}$$

where

$$\lambda_n = \lambda_0(1 - \frac{n}{K'}) \tag{2.11}$$

Inserting Eq.(2.10) in Eq.(2.9) we find that

$$\frac{\mathrm{dE}(N_{DD}(t))}{\mathrm{d}t} = (\lambda_0 - \mu_0)\mathrm{E}(N_{DD}) - \frac{\lambda_0}{K'}\mathrm{E}(N_{DD}^2) \tag{2.12}$$

Replacing K' with $\lambda_0 K/(\lambda_0 - \mu_0)$, the equation becomes:

$$\begin{aligned}
\frac{\mathrm{dE}(N_{DD}(t))}{\mathrm{d}t} &= (\lambda_0 - \mu_0)\mathrm{E}(N_{DD}) - \frac{(\lambda_0 - \mu_0)}{K}\mathrm{E}(N_{DD}^2) \\
&= (\lambda_0 - \mu_0)\mathrm{E}(N_{DD})(1 - \frac{\mathrm{E}(N_{DD}^2)}{K\mathrm{E}(N_{DD})}) \\
&= (\lambda_0 - \mu_0)\mathrm{E}(N_{DD})(1 - \frac{\mathrm{Var}(N_{DD}) + (\mathrm{E}(N_{DD}))^2}{K\mathrm{E}(N_{DD})}) \\
&= (\lambda_0 - \mu_0)\mathrm{E}(N_{DD})(1 - \frac{\mathrm{E}(N_{DD})}{K} - \frac{\mathrm{Var}(N_{DD})}{K\mathrm{E}(N_{DD})})
\end{aligned} \tag{2.13}$$

Hence, this equation differs from the deterministic differential equation (i.e. the logistic equation) by the term $\frac{(\lambda_0-\mu_0)\mathrm{Var}(N)}{K\mathrm{E}(N)}$. It is a good approximation when the variance is small compared to K^2. However, we do not make use of an approximation because we can compute the variance, or more directly, $\mathrm{E}(N^2)$, from the solution of the master equation Eq. (2.10) and

$$E(N_{\mathrm{DD}}^2(t)) = \sum_{n=1}^{\lceil K' \rceil} n^2 P_n(t) \tag{2.14}$$

Demonstration:

$$\begin{aligned}
\frac{\mathrm{d}E(N_{DD})(t)}{\mathrm{d}t} &= \sum_{n=0}^{\infty} n \frac{\mathrm{d}P_n(t)}{\mathrm{d}t} \\
&= \sum_{n=1}^{\infty} n\left(P_{n-1}(t)\lambda_{n-1}(n-1) + P_{n+1}(t)\mu_{n+1}(n+1) - (\lambda_n+\mu_n)P_n(t)n\right) \\
&= \sum_{n=1}^{\infty} nP_{n-1}(t)\lambda_{n-1}(n-1) - \sum_{n=1}^{\infty} n^2\lambda_n P_n(t) \\
&+ \sum_{n=1}^{\infty} nP_{n+1}(t)\mu_{n+1}(n+1) - \sum_{n=1}^{\infty} n^2\mu_n P_n(t)
\end{aligned}$$

Two changes in indices are set: , $k = n-1$ in the first sum and $l = n+1$ in the third sum.

$$= \sum_{k=0}^{\infty} (k+1)kP_k(t)\lambda_k - \sum_{n=1}^{\infty} n^2\lambda_n P_n(t) + \sum_{l=2}^{\infty} (l-1)lP_l(t)\mu_l - \sum_{n=1}^{\infty} n^2\mu_n P_n(t)$$

The indices in the second and fourth sums are then re-labelled as k and n, respectively.

$$\begin{aligned}
&= \sum_{k=0}^{\infty} (k+1)kP_k(t)\lambda_k - \sum_{k=1}^{\infty} n^2\lambda_n P_n(t) + \sum_{l=2}^{\infty} (l-1)lP_l(t)\mu_l - \sum_{l=1}^{\infty} n^2\mu_n P_n(t) \\
&= \sum_{k=0}^{\infty} (k+1)kP_k(t)\lambda_k - \sum_{k=0}^{\infty} n^2\lambda_n P_n(t) + \sum_{l=1}^{\infty} (l-1)lP_l(t)\mu_l - \sum_{l=1}^{\infty} n^2\mu_n P_n(t) \\
&= \sum_{k=0}^{\infty} \left((k+1)kP_k(t)\lambda_k - k^2\lambda_k P_k(t)\right) + \sum_{l=1}^{\infty} \left((l-1)lP_l(t)\mu_l - l^2\mu_l P_l(t)\right) \\
&= \sum_{k=0}^{\infty} k\lambda_k P_k(t) - \sum_{l=1}^{\infty} l\mu_l P_l(t) \\
&= \sum_{k=0}^{\infty} k\lambda_k P_k(t) - \sum_{l=0}^{\infty} l\mu_l P_l(t)
\end{aligned}$$

With the rates of the dd logistic model, (λ_0, μ_0, K') this formula becomes:

$$\begin{aligned}\frac{\mathrm{d}E(N_{DD})(t)}{\mathrm{d}t} &= \sum_{k=0}^{\infty} k\lambda_0(1-\frac{k}{K'})P_k(t) - \sum_{l=0}^{\infty} l\mu_0 P_l(t) \\ &= \lambda_0 \sum_{k=0}^{\infty} kP_k(t) - \frac{\lambda_0}{K'}\sum_{k=0}^{\infty} k^2 P_k(t) - \mu_0 \sum_{l=0}^{\infty} lP_l(t) \\ &= \lambda_0 \mathrm{E}(k) - \frac{\lambda_0}{K'}\mathrm{E}(k^2) - \mu_0 \mathrm{E}(l) \\ &= (\lambda_0 - \mu_0)\mathrm{E}(N) - \frac{\lambda_0}{K'}\mathrm{E}(N^2)\end{aligned}$$

where in the last line we replaced the indices by N

LIKELIHOOD OF THE TD MODEL

The likelihood of a reconstructed phylogeny with branching times $t_i, i = 2...N$ and current time T, for a general time-dependent model with rates $\lambda(t)$ and $\mu(t)$, and conditioned on survival of the clade from the crown to the present, is derived in Nee *et al.* [17]:

$$L = f(t_2, t_3, \ldots, t_N; \lambda(t), \mu(t) | \text{survival, crown age}) \tag{2.15}$$

$$= (N-1)!(1-u(t_2,T))^2 \prod_{k=3}^{N} \lambda(t_k)P(t_k,T)\,(1-u(t_k,T)) \tag{2.16}$$

where

$$u(t,T) = 1 - P(t,T)e^{\rho(t,T)} \tag{2.17}$$

and

$$P(t,T) = (1+\sigma(t,T))^{-1} \tag{2.18}$$

where we have defined

$$\sigma(t,T) = \int_t^T \mu(s)e^{\rho(t,s)}\,\mathrm{d}s. \tag{2.19}$$

and

$$\rho(t,T) = \int_t^T (\mu(s)-\lambda(s))\,\mathrm{d}s, \tag{2.20}$$

To perform likelihood maximization, it is convenient to use the log likelihood, which is (ignore the first, constant, term $\log(n-1!)$:

$$\log L = 2\left(\log(P(t_2,T)+\rho(t_2,T))\right)+\sum_{k=3}^{N}\left(\log(\lambda(t_k))+2\log(P(t_k,T))+\rho(t_k,T)\right). \tag{2.21}$$

We then need to evaluate the terms $\rho(t,T)$, $\lambda(t)$, $\sigma(t,T)$ and $P(t,T)$. We know from Eq. (11) that

$$\rho(t,T)=\ln\left(\frac{E(N_{DD}(t))}{E(N_{DD}(T))}\right) \tag{2.22}$$

and from Eq. (20) and (2.12) that

$$\lambda(t)=\mu_0+\frac{(\lambda_0-\mu_0)\mathrm{E}(N_{DD})-\lambda_0\mathrm{E}(N\times\min(1,\frac{N_{dd}}{K'}))}{E(N_{DD})(t)} \tag{2.23}$$

and

$$K'=\frac{\lambda_0}{\lambda_0-\mu_0}\times K \tag{2.24}$$

$\lambda(t)$ and $\rho(t,T)$ can both be determined from the knowledge of the first and second order moments at the different branching times and at the present time. $\sigma(t,T)$ and $P(t,T)$ can in turn be derived from $\rho(t,T)$.

Recall that the time-dependent model is built from the corresponding diversity dependent model. Because the solution of the diversity-dependent model is heavy to compute, we evaluate $\sigma(t,T)$ along with $\frac{\mathrm{d}P_n}{\mathrm{d}t}$:

$$\begin{cases}\dfrac{\mathrm{d}P_n}{\mathrm{d}t}=P_{n-1}\lambda_{n-1}(n-1)+P_{n+1}\mu_{n+1}(n+1)-(\lambda_n+\mu_n)P_n n\,;\ K'_+>n\geq 1\\ \dfrac{\mathrm{d}P_0}{\mathrm{d}t}=\mu_1 P_1\\ \dfrac{\mathrm{d}P_{\lceil K'\rceil}}{\mathrm{d}t}=(\lceil K'\rceil-1)\lambda_{\lceil K'\rceil-1}P_{\lceil K'\rceil-1}-\lceil K'\rceil(\lambda_{\lceil K'\rceil}+\mu_{\lceil K'\rceil})P_{\lceil K'\rceil}\\ \dfrac{\mathrm{d}\sigma(t_i,t)}{\mathrm{d}t}=\dfrac{\mu_0\mathrm{E}(N_{DD}(t_i))}{\mathrm{E}(N_{DD}(t))}\end{cases} \tag{2.25}$$

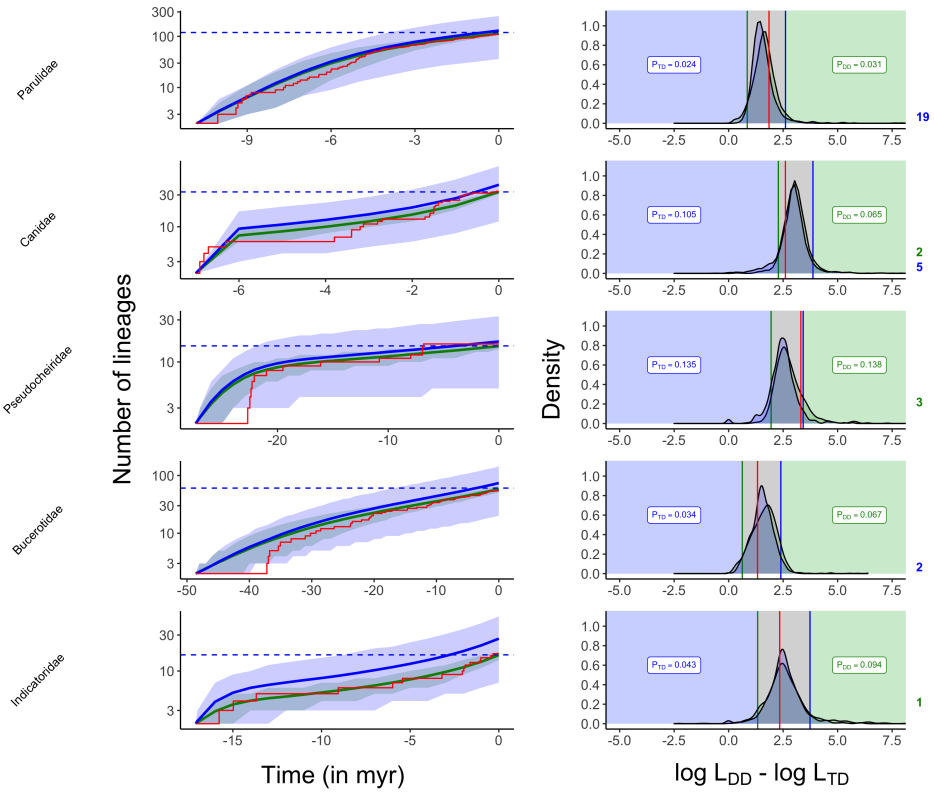

Figure 2.6 | Average lineages-through-time curves (left column) and distribution of the logarithm of the likelihood ratio (right column) for simulated trees generated from empirical phylogenies. Here TD trees were simulated from DD maximum likelihood estimates of the parameters (instead of TD estimates in Fig.5), so that both DD and TD trees are simulated from the same values. All the legends and colour schemes are identical between the two figures.

REFERENCES

[1] T. Pannetier, C. Martinez, L. Bunnefeld, and R. S. Etienne, *Branching patterns in phylogenies cannot distinguish diversity-dependent diversification from time-dependent diversification,* Evolution **75**, 25 (2021).

[2] D. M. Raup, S. J. Gould, T. J. M. Schopf, and D. S. Simberloff, *Stochastic Models of Phylogeny and the Evolution of Diversity,* The Journal of Geology **81**, 525 (1973).

[3] J. J. Sepkoski, *A kinetic model of Phanerozoic taxonomic diversity I. Analysis of marine orders,* Paleobiology **4**, 223 (1978).

[4] S. M. Stanley, *Effects of Competition on Rates of Evolution, With Special Reference to Bivalve Mollusks and Mammals,* Systematic Zoology **22**, 486 (1973).

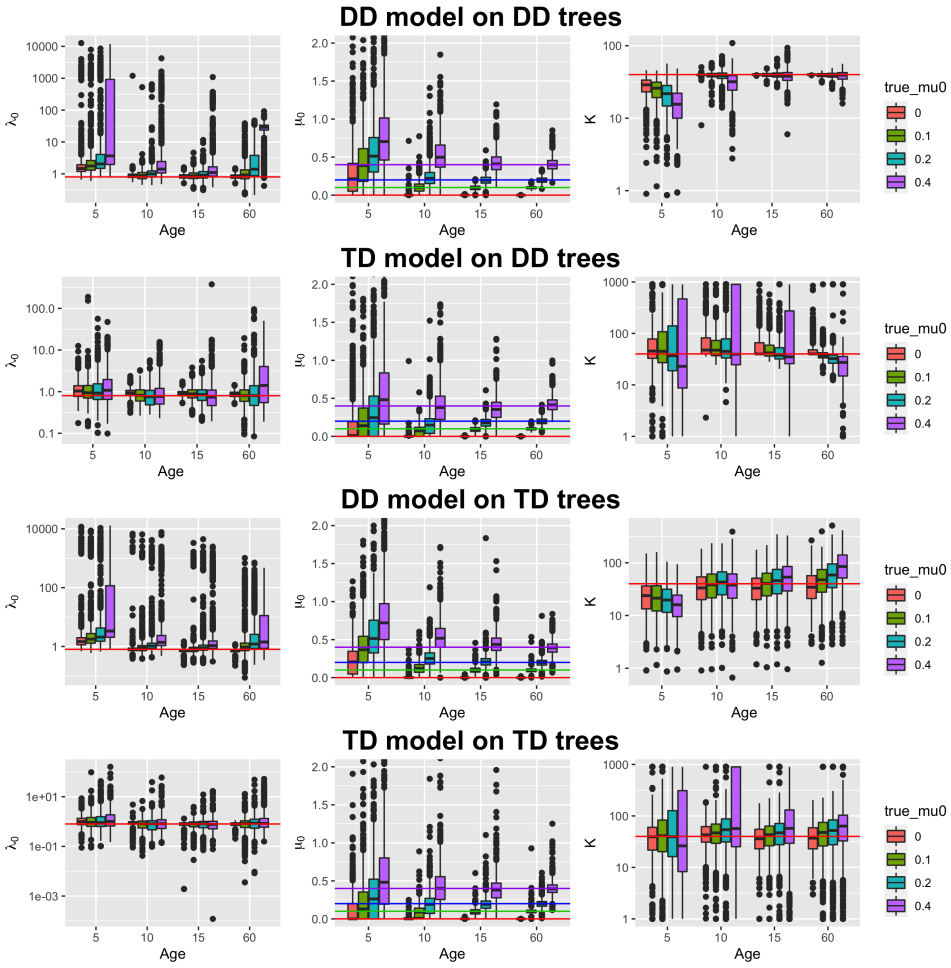

Figure 2.7 | Accuracy of parameter estimation by model and type of tree. Each individual boxplot represents the distribution of maximum likelihood estimates of the corresponding parameter for one scenario, across 1,000 simulated trees. Horizontal bars denote the true value used to simulate trees, coloured by value in the case of μ_0 (central column). Values of λ_0 (right column) and K (left column) are plotted on a log scale.

[5] J. J. Sepkoski, *Ten years in the library: New data confirm paleontological patterns,* Paleobiology **19**, 43 (1993).

[6] S. Nee, A. O. Mooers, and P. H. Harvey, *Tempo and mode of evolution revealed from molecular phylogenies,* Proceedings of the National Academy of Sciences **89**, 8322 (1992).

[7] A. B. Phillimore and T. D. Price, *Density-Dependent Cladogenesis in Birds,* PLoS Biology **6**, e71 (2008).

[8] M. A. McPeek, *The Ecological Dynamics of Clade Diversification and Community Assembly,* The American Naturalist **172**, E270 (2008).

[9] H. Morlon, M. D. Potts, and J. B. Plotkin, *Inferring the Dynamics of Diversification: A Coalescent Approach,* PLOS Biology **8**, e1000493 (2010).

[10] F. L. Condamine, J. Rolland, and H. Morlon, *Assessing the causes of diversification slowdowns: Temperature-dependent and diversity-dependent models receive equivalent support,* Ecology Letters **22**, 1900 (2019).

[11] D. Moen and H. Morlon, *Why does diversification slow down?* Trends in Ecology & Evolution **29**, 190 (2014).

[12] D. S. Simberloff and E. O. Wilson, *Experimental Zoogeography of Islands. A Two-Year Record of Colonization,* Ecology **51**, 934 (1970).

[13] R. H. MacArthur and E. O. Wilson, *The Theory of Island Biogeography* (Princeton University Press, 1967).

[14] A. L. Pigot, A. B. Phillimore, I. P. F. Owens, and C. D. L. Orme, *The Shape and Temporal Dynamics of Phylogenetic Trees Arising from Geographic Speciation,* Systematic Biology **59**, 660 (2010).

[15] O. Hagen, T. Andermann, T. B. Quental, A. Antonelli, D. Silvestro, and M. Alfaro, *Estimating Age-Dependent Extinction: Contrasting Evidence from Fossils and Phylogenies,* Systematic Biology **67**, 458 (2018).

[16] D. L. Rabosky and I. J. Lovette, *Explosive evolutionary radiations: Decreasing speciation or increasing extinction through time?* Evolution **62**, 1866 (2008).

[17] S. Nee, R. M. May, and P. H. Harvey, *The reconstructed evolutionary process,* Phil. Trans. R. Soc. Lond. B **344**, 305 (1994).

[18] R. S. Etienne, B. Haegeman, T. Stadler, T. Aze, P. N. Pearson, A. Purvis, and A. B. Phillimore, *Diversity-dependence brings molecular phylogenies closer to agreement with the fossil record,* Proceedings of the Royal Society B: Biological Sciences **279**, 1300 (2012).

[19] D. G. Kendall, *On the Generalized "Birth-and-Death" Process,* **19**, 1 (1948).

[20] R. S. Etienne, A. L. Pigot, and A. B. Phillimore, *How reliably can we infer diversity-dependent diversification from phylogenies?* Methods in Ecology and Evolution **7**, 1092 (2016).

[21] W. Jetz, G. H. Thomas, J. B. Joy, K. Hartmann, and A. O. Mooers, *The global diversity of birds in space and time,* Nature **491**, 444 (2012).

[22] J. Rolland, F. L. Condamine, F. Jiguet, and H. Morlon, *Faster Speciation and Reduced Extinction in the Tropics Contribute to the Mammalian Latitudinal Diversity Gradient,* PLOS Biology **12**, e1001775 (2014).

[23] O. R. P. Bininda-Emonds, M. Cardillo, K. E. Jones, R. D. E. MacPhee, R. M. D. Beck, R. Grenyer, S. A. Price, R. A. Vos, J. L. Gittleman, and A. Purvis, *The delayed rise of present-day mammals,* Nature **446**, 507 (2007).

[24] T. B. Quental and C. R. Marshall, *Diversity dynamics: Molecular phylogenies need the fossil record,* Trends in Ecology & Evolution **25**, 434 (2010).

[25] L. M. Valente, A. B. Phillimore, and R. S. Etienne, *Equilibrium and non-equilibrium dynamics simultaneously operate in the Galápagos islands,* Ecology Letters **18**, 844 (2015).

[26] T. Stadler, *Recovering speciation and extinction dynamics based on phylogenies,* Journal of Evolutionary Biology **26**, 1203 (2013).

[27] H. Morlon, *Phylogenetic approaches for studying diversification,* Ecology Letters **17**, 508 (2014).

[28] T. Janzen, S. Höhna, and R. S. Etienne, *Approximate Bayesian Computation of diversification rates from molecular phylogenies: Introducing a new efficient summary statistic, the nLTT,* Methods in Ecology and Evolution **6**, 566 (2015).

[29] Y. Haba and N. Kutsukake, *A multivariate phylogenetic comparative method incorporating a flexible function between discrete and continuous traits,* Evolutionary Ecology **33**, 751 (2019).

[30] D. L. Rabosky, *Heritability of Extinction Rates Links Diversification Patterns in Molecular Phylogenies and Fossils,* Systematic Biology **58**, 629 (2009).

[31] F. Bokma, *Artificial neural networks can learn to estimate extinction rates from molecular phylogenies,* Journal of Theoretical Biology **243**, 449 (2006).

[32] F. Bokma, *Time, Species, and Separating Their Effects on Trait Variance in Clades,* Systematic Biology **59**, 602 (2010).

[33] S. Louca and M. W. Pennell, *Extant timetrees are consistent with a myriad of diversification histories,* Nature **580**, 502 (2020).

[34] J. T. Weir and S. Mursleen, *Diversity-Dependent Cladogenesis and Trait Evolution in the Adaptive Radiation of the Auks (aves: Alcidae),* Evolution **67**, 403 (2013).

[35] F. L. Condamine, J. Rolland, and H. Morlon, *Macroevolutionary perspectives to environmental change,* Ecology Letters **16**, 72 (2013).

[36] E. Lewitus and H. Morlon, *Detecting Environment-Dependent Diversification From Phylogenies: A Simulation Study and Some Empirical Illustrations,* Systematic Biology **67**, 576 (2018).

[37] L. McInnes, C. D. L. Orme, and A. Purvis, *Detecting shifts in diversity limits from molecular phylogenies: What can we know?* Proceedings of the Royal Society of London B: Biological Sciences **278**, 3294 (2011).

[38] B. C. Emerson and N. Kolm, *Species diversity can drive speciation,* Nature **434**, 1015 (2005).

[39] D. H. Erwin, *Increasing returns, ecological feedback and the Early Triassic recovery,* Palaeoworld Contributions to Permian and Carboniferous Stratigraphy, Brachiopod Palaeontology and End-Permian Mass Extinctions, In Memory of Professor Yu-Gan Jin, **16**, 9 (2007).

[40] D. Schluter, *The Ecology of Adaptive Radiation.* (Oxford Univ. Press, Oxford, 2000).

[41] M. L. Rosenzweig, *Competitive speciation,* Biological Journal of the Linnean Society **10**, 275 (1978).

[42] U. Dieckmann and M. Doebeli, *On the origin of species by sympatric speciation,* Nature **400**, 354 (1999).

[43] G. G. Simpson, *Tempo and Mode in Evolution* (Columbia University Press, New York, 1944).

[44] G. J. Slater, S. A. Price, F. Santini, and M. E. Alfaro, *Diversity versus disparity and the radiation of modern cetaceans,* Proceedings of the Royal Society B: Biological Sciences **277**, 3097 (2010).

[45] L. J. Harmon, J. A. Schulte, A. Larson, and J. B. Losos, *Tempo and Mode of Evolutionary Radiation in Iguanian Lizards,* Science **301**, 961 (2003).

[46] F. T. Burbrink and R. A. Pyron, *How Does Ecological Opportunity Influence Rates of Speciation, Extinction, and Morphological Diversification in New World Ratsnakes (tribe Lampropeltini)?* Evolution **64**, 934 (2010).

[47] J. D. Kennedy, J. T. Weir, D. M. Hooper, D. T. Tietze, J. Martens, and T. D. Price, *Ecological Limits on Diversification of the Himalayan Core Corvoidea,* Evolution **66**, 2599 (2012).

[48] E. P. Derryberry, S. Claramunt, G. Derryberry, R. T. Chesser, J. Cracraft, A. Aleixo, J. Pérez-Emán, J. V. R. Jr, and R. T. Brumfield, *Lineage Diversification and Morphological Evolution in a Large-Scale Continental Radiation: The Neotropical Ovenbirds and Woodcreepers (aves: Furnariidae),* Evolution **65**, 2973 (2011).

[49] L. J. Harmon, J. B. Losos, T. J. Davies, R. G. Gillespie, J. L. Gittleman, W. B. Jennings, K. H. Kozak, M. A. McPeek, F. Moreno-Roark, T. J. Near, A. Purvis, R. E. Ricklefs, D. Schluter, J. A. S. Ii, O. Seehausen, B. L. Sidlauskas, O. Torres-Carvajal, J. T. Weir, and A. Ø. Mooers, *Early Bursts of Body Size and Shape Evolution Are Rare in Comparative Data,* Evolution **64**, 2385 (2010).

[50] N. M. A. Crouch and R. E. Ricklefs, *Speciation Rate Is Independent of the Rate of Evolution of Morphological Size, Shape, and Absolute Morphological Specialization in a Large Clade of Birds,* The American Naturalist **193**, E78 (2019).

[51] A. Machac, C. H. Graham, and D. Storch, *Ecological controls of mammalian diversification vary with phylogenetic scale,* Global Ecology and Biogeography **27**, 32 (2018).

[52] L. Aristide and H. Morlon, *Understanding the effect of competition during evolutionary radiations: An integrated model of phenotypic and species diversification,* Ecology Letters **22**, 2006 (2019).

[53] J. A. Tobias, C. K. Cornwallis, E. P. Derryberry, S. Claramunt, R. T. Brumfield, and N. Seddon, *Species coexistence and the dynamics of phenotypic evolution in adaptive radiation,* Nature **506**, 359 (2014).

[54] M. E. Alfaro, F. Santini, C. Brock, H. Alamillo, A. Dornburg, D. L. Rabosky, G. Carnevale, and L. J. Harmon, *Nine exceptional radiations plus high turnover explain species diversity in jawed vertebrates,* Proceedings of the National Academy of Sciences **106**, 13410 (2009).

[55] M. Pontarp, J. Ripa, and P. Lundberg, *The Biogeography of Adaptive Radiations and the Geographic Overlap of Sister Species,* The American Naturalist **186**, 565 (2015).

[56] M. Pontarp, J. Ripa, and P. Lundberg, *On the origin of phylogenetic structure in competitive metacommunities,* Evolutionary Ecology Research **14**, 269 (2012).

[57] R. Aguilée, F. Gascuel, A. Lambert, and R. Ferriere, *Clade diversification dynamics and the biotic and abiotic controls of speciation and extinction rates,* Nature Communications **9**, 3013 (2018).

3

COMRAD – A MORE MECHANISTIC APPROACH TO DIVERSITY-DEPENDENT DIVERSIFICATION

Théo Pannetier, A. Brad Duthie, Rampal S. Etienne.

Tlaalahui, tlapetzcahui in tlalticpac

Nahuatl saying

ABSTRACT

A long-standing question in macroevolution is whether diversification is governed by the same processes that structure diversity at ecological scales, particularly competition. This competition has led to the development of a model where diversification rates depend on diversity, analogous to density-dependence in population growth models. Various versions of this model have been widely used for inference, where the rate of speciation and/or extinction can be either a linear or a power function of species number. It is, however, unknown if either approximates the diversification process that arises from the general ecological setting proposed to lead to diversity-dependence. This is of concern for inference, as failure to include a model that appropriately represents the hypothesized scenario is likely to lead to erroneous inference. Here we use an individual-based model adapted from adaptive dynamics, where fitness is governed by resource availability and the density of competitors, to determine the shape of the diversity-dependence functions. We find that the diversity-dependent rate of speciation produced by the individual-based model is best approximated by an exponential function of species diversity, consistent with a view of macroevolution where diversity increases rapidly after mass extinctions or when new adaptive space becomes available. Although we do find diversity-dependence in the extinction rate, it remains low over the entire process and erases its own signal, so it cannot be recovered from reconstructed phylogenies. The support for a linear relationship for diversity-dependent diversification found in many empirical phylogenies suggests that either our adaptive dynamics model of speciation is inadequate or there is too little information contained in reconstructed phylogenies. We indeed find evidence for the latter when pruning extinct species from our simulated phylogenies, but this does not rule out the former.

3.1. INTRODUCTION

WHETHER and how multi-million year evolutionary trends observed in fossil diversity and reconstructed molecular phylogenies are related to the eco-evolutionary processes taking place within contemporary communities is a challenging question that has been the focus of many studies [1–4]. The model of evolution through competition and exclusion between closely related forms as described by Darwin attests that it was already a central concern in the Origin of Species [5, 6]. To this day, it remains unclear how ecological interactions among organisms and their environment scale up to shape the rates of speciation and extinction that are central to macroevolutionary studies. Paleobiologists of the 1970s through 1980s proposed that the diversification of taxa within clades behaves analogously to community assembly [1, 7], as described in the then-recent theory of island biogeography [8]. Closely related taxa are assumed to exploit a common pool of resources available to the clade and occupy exclusive niches. If niche space is assumed to be limited, expansion of the clade results in saturation of this niche space, in turn impeding the successful establishment of new species and increasing the risk of extinction through increased competition intensity. Conversely, extinction of a taxon relaxes some of the competition pressure and provides the ecological opportunity for other species to diversify, so that in the long term, the clade tends to reach an equilibrium diversity. Under this view, diversity feeds back on diversification; i.e., diversification is diversity-dependent. The model provides a simple, intuitive explanation for how competitive interactions among individuals may have cascading effects on the formation of clades. Because it is based on the universal ecological principle of competitive exclusion, it is also applicable to any study system.

Implementations of diversity-dependence as a birth-death model have been widely used to test for a primary role of competition in a clade's evolutionary history, both using reconstruction of fossil diversity [9–11] or the branching patterns of a molecular phylogeny [12–15]. Although the verbal model outlined above makes the intuitive predictions that the rate of speciation should generally decline with the number of species in the clade, and the rate of extinction should increase, it does not describe any precise relationship between the rates and the number of species, as this would require making a number of assumptions regarding the ecological setting, the nature of competitive interactions, and the mode of evolution of the species considered. Instead, it is usually assumed that the relationship between the respective per-capita rates of speciation and extinction and the number of species is simple, most often a linear function. Originating from Sepkoski [7]'s influential study of temporal patterns of diversity in the marine fossil clades, a linear function was chosen because of tractability, and in analogy with contemporary models of island biogeography [8]. Sepkoski himself acknowledged that this constituted an approximation, justified by the ease of analysis and interpretation such a model permits (for example, it is easy to predict the equilibrium diversity of the clade). Less frequently, power functions of the number of species have been used instead, often somewhat confusingly referred to as the "exponential" [12, 13], or "hierarchical" [16, 17] diversity-dependent model. Linear and power models predict similar diversity growth curves, but differ in important aspects as a result of the curvature of both rates in the power model. First, the initial speciation rate is typically much higher in the power model, resulting in rapid

("explosive") initial growth of the clade [17]. Second, in the power model, species diversity has a strong effect on the per capita rates when the clade contains only a few species, and a weak effect when diversity approaches equilibrium, whereas in the linear model these effects are constant throughout the diversification process [12, 16]. Finally, the dynamics of the rates beyond equilibrium diversity differ. In the linear model, speciation becomes zero, such that there exists a theoretical maximum to the possible size of the clade. By contrast, in the power model both rates are asymptotic, so that the strength of diversity-dependence itself reaches a maximum. The power diversity-dependent model has a more substantial biological background, as it was originally derived from a population-level model of "energy flow" (i.e, resource allocation), in order to establish a mechanistic foundation instead of simply assuming the shape of the relationship [16]. These underlying population-level processes have however seldom been referred to in later uses of the model [12, 13, 17].

For the purpose of statistical tests for diversity-dependence against alternative evolutionary scenarios in reconstructed molecular phylogenies, both versions of the model are often included in the set of candidate models as alternative implementations of the same hypothesis (a primary role of competition in driving diversification) [13, 15, 18]. In this context, linear diversity-dependence is often selected over power diversity dependence. For example, Condamine *et al.* [18] found that linear diversity-dependence in speciation was selected for 35 phylogenies (out of 218 phylogenies of Tetrapod families), while power diversity-dependence in speciation was only selected for 1. The choice of the form of diversity-dependence may rarely matter for the detection of diversity-dependence from branching patterns in molecular phylogenies: model selection tends to rank models with linear and power functions of diversity-dependence close to one another compared to other birth-death models [13, 18], implying that omitting either model is unlikely to change the qualitative conclusions. Yet, the selection of either model over the other leads to different interpretations of the ecological mechanisms underlying diversity-dependence [12]. Importantly, other mechanisms can lead to slowdowns in the rate of diversification [6, 19], making it unclear whether what is recovered is indeed the contribution of competition, or an unrelated evolutionary scenario. Time-variable birth-death models are known to be subject to the issue of unidentifiability, where independent models representing unrelated evolutionary scenarios will have the same likelihood if they predict the same average growth of the clade [20, 21]. This issue has been recently shown to extend to diversity-dependent birth-death models [22]. Because of this, the inclusion of several models representing the same evolutionary scenario increases the risk of inferring diversity-dependence when it is in fact absent, should the "true" scenario be congruent with either of the diversity-dependent models. This issue is not unique to macroevolution, but instead applies to model selection in general. Burnham and Anderson [23] famously argued against automated selection procedures, and instead insisted that much attention should be given to the careful formulation of the set of candidate models. That is, the size of the set should be limited, and each model should be sufficient in itself to represent a given hypothesis. This policy has recently been advocated to address unidentifiability in molecular phylogenies [24]. Unfortunately, there is no clear justification for either form of diversity-dependence, as it remains unclear which, if any, of the models appropriately represents the effect of competition between individuals on evolutionary rates [3, 6]. Here,

we aim to address this gap, and establish what form of diversity-dependence emerges from the scenario described above. We use an evolutionary individual-based model (IBM) where differences in reproductive success depend on the profitability of a resource matched by a trait, modified by Lotka-Volterra-like competition between individuals [25]. The model can be considered a stochastic, finite-population version of the deterministic models used in adaptive dynamics [26–28], and such models have been used extensively to study the ecological and evolutionary conditions that lead to the formation of species [29, 30]. In this context, emphasis has been placed on the first branching event, and comparatively few studies have studied the macroevolutionary dynamics of such models. Yet, given enough time and depending on the model parameters, further branching may occur, such that a clade forms from an initially monomorphic population. Previous studies have described the interplay between competition and landscape dynamics on the phylogenetic structure of the resulting communities [25] and the shape of phylogenetic trees [31], and the effect of trait dimensionality on the speed of (trait) evolution [32]. We are aware of only one study describing the relationship between the rates of speciation and extinction and the number of species in the community [33]. Aguilée et al. provided a thorough description of the effect and interplay of biotic (competition, and the build-up of genetic differentiation) and abiotic (structure and dynamics of the landscape) factors on diversity-dependence. They found that diversity-dependence proceeded in three phases, corresponding to distinct phases of the building of communities: an initial adaptive radiation corresponding to the colonisation of all patches, followed by in-situ competition-driven diversification, and saturation of the local and global communities. Here, we consider a simpler scenario, with asexual reproduction, a 1-to-1 genotype-to-phenotype map, a unidimensional ecological trait and no spatial structure. By doing so, we seek to limit the evolutionary process to the minimal mechanisms described in the verbal model of diversity-dependence: evolutionary branching proceeds through competition-induced divergent selection and the partitioning of niche space between the resulting species, while extinction occurs as a result of stochasticity [28]. Total niche space and population sizes are limited, such that only a limited number of species can coexist in the final community, and diversity reaches a dynamic equilibrium [25]. We run the simulation and measure the rates of speciation and extinction as functions of the number of species. We use the phylogenies of the resulting communities to assess whether the linear, power, or exponential function best approximates the diversity-dependent diversification process that emerges from our evolutionary individual-based model.

3.2. METHODS

3.2.1. INDIVIDUAL-BASED MODEL

We simulated evolving communities using an individual-based version of the Lotka-Volterra competition model (hereafter, LVIBM).

In this model, individuals are characterised by an ecological trait matching a resource. The fitness $W(z)$ of an individual with trait value z depends on the density of competitors

with a similar trait value, and on the resource abundance corresponding to this value:

$$W_z = e^{r\left(1-\frac{A(z)}{K(z)}\right)},$$

where r is the baseline growth rate, $A(z)$ is the total competition intensity for an individual with trait value z, and $K(z)$ is the abundance of the resource available for individuals with this trait value. $K(z)$ is modeled as a Gaussian distribution:

$$K(z) = K_{opt} e^{-\frac{(z-z_{opt})^2}{2\sigma_K^2}},$$

where K_{opt} is the maximum abundance, corresponding to optimal trait value z_{opt}, and the standard deviation σ_K controls how fast the abundance of the resource declines away from z_{opt}. The total competition intensity at trait value z is

$$A(z) = \sum_{i=1}^{N} \alpha(z, z_i),$$

where N is the number of individuals in the community and,

$$\alpha(z, z_i) = e^{-\frac{(z-z_i)^2}{2\sigma_\alpha^2}},$$

is the competition intensity experienced by a focal individual with trait value z, caused by individual i with trait value z_i; $1 \geq \alpha(z, z_i) \geq 0$. Parameter σ_α controls how fast competition between individuals declines as the trait distance between them increases.

Generations are discrete and non-overlapping, and reproduction is asexual. In each generation, the number of offspring each individual produces is drawn from a Poisson distribution with the fitness of this individual as the mean parameter. Offspring inherit the trait value of their parent, modified due to mutation; their trait value is sampled from a normal distribution with the parental trait values as mean and standard deviation σ_μ,

$$z_{\text{offspring}} = \mathcal{N}(z_{\text{parent}}, \sigma_\mu)$$

Our formulation of this Lotka-Volterra model is based on the one used by Pontarp *et al.* [25], although we modified the fitness function. In Pontarp *et al.* [25], the fitness function is of the form

$$W(z) = 1 + r\left(1 - \frac{A(z)}{K(z)}\right)$$

Here, we instead used the Ricker model, $W(z) = e^{r(1-\frac{A(z)}{K(z)})}$, in order to avoid fitness becoming negative when $\frac{A(z)}{K(z)} > \frac{r+1}{r}$, which, although unlikely and probably without much consequence for the simulation, may happen at the edges of the resource distribution. A key feature of the model is the presence of an unstable attractor in the fitness landscape, at point $z = z_{opt}$. The phenotypes of individuals are first attracted to this point, but are eventually pushed away from it as frequency-dependence turns this fitness maximum into a local minimum. This frequency-dependence causes the population to split into two phenotypic clusters on either side of the optimum, i.e. evolutionary branching. Here,

we treat such clusters as species (see next section). The new species may branch further or not, depending on $K(z)$ and $\alpha(z_i, z_j)$, and the values of their parameters (here, σ_α and σ_K). Determining the conditions that lead to branching of the initial population has been the focus of many adaptive dynamics studies, and this has led to key advances in the understanding of how ecological interactions may cause speciation even in conditions of sympatry or incomplete isolation. A robust result is that in an asexual reproduction setting, branching occurs if $\sigma_\alpha < \sigma_K$. In the deterministic version of the model, branching will keep occurring indefinitely as a result of the symmetric structure of the fitness landscape [28]. By contrast, stochasticity in the IBM occasionally causes species to go extinct and smoothens the fitness landscape, increasingly slowing branching (see Chap. 3 in [28] for a further description of the process). As a result, the community eventually reaches a stochastic equilibrium. Here, we are primarily interested in determining the speciation rate (that is, the pace of the branching events), as well as the rate of extinction, and how they change with the number of species in the community. This has, to our knowledge, received comparatively little attention. Similarly, while the existence of an equilibrium diversity is known, its value and how it changes with the parameters of the model has not been described, and appears hard to anticipate in a stochastic setting. To help interpreting our results, we approach this quantity empirically by measuring it from the output of the simulations. More precisely, in each simulation, we measured the average diversity at 10 equally distant points in time in the last sixth of total simulation time. We denote the average of this quantity over all replicate simulations in a set by $\hat{K}$, the "estimated equilibrium diversity".

3.2.2. SPECIES DEFINITION

Although branching in the trait z is an emergent feature of the model, species need to be labelled as we do not explicitly model reproductive isolation. Through the course of simulations, we used morphological divergence along the ecological trait axis for translating branching events into speciation events. Specifically, speciation was triggered whenever the two morphologically closest individuals i and j from the same species were found to diverge in their trait values by more than θ_z (that is, $|z_i - z_j| \geq \theta_z$). Upon speciation, we (arbitrarily) assigned the smallest population (cluster) on either side of the morphological gap between i and j to a new species, or either population at random if both had the same size. In the resulting phylogenies, this had no influence on the length of branches and thus did not affect any of the downstream results. Note that incipient speciation is a feature of the model, as speciation happens some time after two populations start diverging. Incidentally, speciation may fail, for example if the morphological gap collapses as a result of external competition pressures, or if either population goes extinct. However, when speciation does happen, it is permanent: even if the two species become closer in trait value, they are still assumed to be distinct species. Extinction happens when all living individuals of a species fail to produce offspring for the next generation. Note that in our simulations species identity is only a label used to keep track of phylogenetic relationships between individuals and branches, that is, two individuals i and j respectively belonging to species A and B have strictly the same fitness if $z_i = z_j$. Importantly, both speciation and extinction are driven by (scramble)

competition between individuals: speciation results from branching driven by changes in fitness optima as a result of accumulating local competition intensity, while extinction happens as a result of species being pushed in low-fitness areas of the adaptive landscape.

3.2.3. SIMULATION PROCEDURE

In order to study whether diversity-dependent diversification and the signal it leaves in the phylogenetic tree changes with community size, we ran the LVIBM for an array of values of σ_K (controlling the width of resource distribution and therefore community size) and σ_α (modulating competition intensity, and therefore the number of individuals that can coexist in a community given σ_K [25]). Specifically, the parameter values we considered were $\sigma_K \in \{1, 2, 3, 4, 5\}$ and $\sigma_\alpha \in \{0.1, 0.2, ..., 1\}$, resulting in a set of 50 parameter combinations. We set all other parameters to the following values: $r = 1$, $z_{opt} = 0$, $K_{opt} = 1000$, following Pontarp *et al.* [25], and $\sigma_\mu = 0.001$, $\sigma_z = 0.1$. For each parameter setting, we ran 100 replicate simulations (thus 5000 simulations in total). Starting communities contained 10 individuals of the same species, each with trait value $z = z_{opt}$.

We ran each simulation long enough to allow the community approach equilibrium diversity (here an emergent feature of the model), based on visual examination of the lineage-through-time (LTT) plots of preliminary simulations. In each simulation, we sampled 5% of all individuals in the community at random in every generation where one or more speciation or extinction event happened. For every individual, we saved its generation, its species and the ancestral species it originated from to build a phylogenetic tree of the community.

3.2.4. ESTIMATION OF DIVERSITY-DEPENDENT DIVERSIFICATION

We used the phylogenies obtained from the LVIBM to study what form of diversity dependent diversification emerges from competition among individuals. To be consistent with diversity dependent birth-death models (hereafter, DDBD models), we made the assumption that both the rate of speciation ($\lambda(N)$) and the rate of extinction ($\mu(N)$) are functions of the number of species N. We followed the assumptions made in DDBD models that the rates were not affected by any other factor, such as (generation) time, the affected species' population size, or the distribution of trait values within it, and that all species in the community were equally likely to be subject to speciation or extinction. For rate reconstruction, we only retained combinations of σ_α and σ_K that produced communities larger than or equal to the arbitrary threshold of 8 species ($\hat{K} \geq 8$), trees below this size probably lack the statistical power to yield reasonable estimates of the rates of speciation and extinction. To estimate the rates, we recorded the waiting times to speciation and extinction events and pooled them by the number of species in the community before the event, across all 100 replicate phylogenies for a given setting. We used two methods to estimate the rates from waiting times, both based on maximum likelihood. First, by estimating the rates at each value of N separately, maximizing the likelihood of the mean waiting times for each value of N. Second, by a standard model selection approach: we assumed a relationship between the rates and diversity, and then estimated the coefficients of this relationship by maximizing the likelihood of the waiting times for all N simultaneously, and finally compared the performance of various relationships specified

by the models. We then compared the rates estimated from both approaches.

3.2.5. ESTIMATION FOR EACH VALUE OF N SEPARATELY

If we assume that the waiting times for the next event are exponentially distributed we can write down the likelihood for observing, in the simulations, a set of M waiting times for each diversity value N,

$$L = \prod_{i}^{M} e^{(-(\lambda_N+\mu_N)Nt_i)} \lambda_N^{(p_i)} \mu_N^{1-p_i} = e^{-(\lambda_N+\mu_N)N\sum_i^M t_i} \lambda_N^{pM} \mu_N^{(1-p)M},$$

where p_i equals 1 if event i is a speciation event and 0 if it is an extinction event, p is the proportion of M waiting times that lead to a speciation event, t_i is the waiting time until the ith event, λ_N is the speciation rate at diversity N and μ_N is the extinction rate at diversity N. By maximizing the logarithm of this likelihood with respect to both λ_N and μ_N, we can get maximum likelihood estimators for these parameters:

$$\lambda_N = \frac{p}{Nt_N},$$

$$\mu_N = \frac{1-p}{Nt_N}.$$

This approach provides estimates of the rates of speciation and extinction corresponding to each value of N, and allows us to characterize the main features of the mode of diversity-dependence produced by the LVIBM. However, this approach requires knowledge of the number of species alive in the community through time, and thus is only available for complete trees. We treat the rates estimated from this direct approach as close to the "true" diversity-dependent rates, and use them as a baseline to compare with the rates estimated with the approach below.

3.2.6. ESTIMATION OF THE COEFFICIENTS OF RELATIONSHIP BETWEEN THE RATES AND N USING BIRTH-DEATH MODELS

To assess what type of diversity-dependent functions were most consistent with the patterns produced by the LVIBM, we maximized the likelihood of the waiting times for all N simultaneously for various functions. We considered the linear and power (also known as "exponential" diversity-dependence) functions frequently used in the literature (e.g. [13, 14]). To investigate the form of diversity-dependence produced by an actual exponential form of diversity-dependence, we also considered an exponential function of the number of species. Diversity-dependence of this form is somewhat intermediate between the linear and power forms, showing asymptotic rates but slower changes in both rates with diversity than in the power function. We used these functions to formulate diversity-dependent speciation and extinction functions (for example, exponential diversity-dependence on speciation, linear diversity-dependence on extinction). In addition, we also considered constant-rate (i.e, diversity-independent) extinction, but not constant-rate speciation, as it is clear from preliminary simulations and previous work

using similar IBMs [25, 28] that speciation slows down as the community grows. Speciation and extinction functions were then paired together to constitute a set of candidate diversity-dependent models covering all the 12 possible functions (3 speciation functions times 4 extinction functions). We parameterized all diversity-dependent functions to share the same set of four parameters: λ_0, μ_0, K and ϕ. λ_0 and μ_0 are, respectively the initial speciation and extinction rates when $N = 0$ (or when $N = 1$ in the case of the power functions). K is the equilibrium diversity (i.e., the unique value of N for which $\lambda_N = \mu_N$). Finally, ϕ controls the value of both rates at equilibrium as a weighted mean of the initial values of both rates,

$$\phi = \frac{\lambda_K - \mu_0}{\lambda_0 - \mu_0},$$

such that

$$\lambda_K = \mu_K = \phi\lambda_0 + (1-\phi)\mu_0.$$

Note that $\phi = 0$ implies constant-rate extinction, while $\phi = 1$ implies constant-rate speciation. Thus, ϕ measures the relative contribution of speciation and extinction to diversity dependence in the model. We bounded $0 \leq \phi \leq 1$, and thus assumed that diversity-dependence on speciation is always negative (speciation declines as the community grows), or absent, and that diversity-dependence on extinction is always positive (extinction increases as the community grows), or absent. Below, we refer to this equilibrium rate as λ_K, although this is, by definition, identical to μ_K.

Function	**Speciation rate**	**Extinction rate**
Constant	-	$\mu(N) = \mu_0$
Linear	$\lambda(N) = \lambda_0 - (\lambda_0 - \lambda_K)\frac{N}{K}$	$\mu(N) = \mu_0 + (\lambda_K - \mu_0)\frac{N}{K}$
Power	$\lambda(N) = \lambda_0 N^{-\frac{\log\left(\frac{\lambda_0}{\lambda_K}\right)}{\log(K)}}$	$\mu(N) = \mu_0 N^{\frac{\log\left(\frac{\lambda_K}{\mu_0}\right)}{\log(K)}}$
Exponential	$\lambda(N) = \lambda_0 e^{-\log\left(\frac{\lambda_0}{\lambda_K}\right)\frac{N}{K}}$	$\mu(N) = \mu_0 e^{\log\left(\frac{\lambda_K}{\mu_0}\right)\frac{N}{K}}$

Table 3.1 | Speciation and extinction functions used in the birth-death models fitted to the phylogenetic trees produced by the LVIBM.

In all models with constant-rate extinction, we fixed $\phi = 0$ in the speciation function.

3.2.7. COMPLETE PHYLOGENIES

We fitted each of the 12 models to the entire set of 100 replicate complete trees for a given parameter setting of the LVIBM, that is, the entire set of waiting times, for all N together, by likelihood maximization.

We used the optimizer function implemented in R package DDD [14], with 1,000 sets of random initial parameter values to minimize the chances of finding only a local likelihood optimum. To restrict the initial values to a range of sensible values, we sampled them in a preset distribution for each parameter. We defined an auxiliary parameter $\Lambda = \frac{log(N_{max})}{t_p}$ which is an approximation of the average growth rate of the phylogeny assuming constant-rate diversification, with N_{max} denoting the maximum number of species in the simulation and t_p the simulation time, in generations. We then sampled initial values for λ_0 in uniform distribution $U(0.5\Lambda, 2\Lambda)$, so that λ_0 was roughly consistent with the size of the tree and the time frame of the simulation. μ_0 was sampled from $U(0, 0.75\lambda_0)$, to avoid a high probability of the tree going extinct early (which can be expected if $\lambda_0 \approx \mu_0$). Values of $K < N_{max}$ would make the tree implausible, so we sampled K in $N_{max}(1 + \Gamma(0.5, 0.3))$, where Γ is the Gamma distribution, yielding initial values that were most often equal or slightly larger than N_{max}, with occasionally larger to much larger initial values. Finally, ϕ was sampled in $U(0, 1)$. For each model, we then selected the parameter values with the largest maximum likelihood out of the 1,000 optimizations, and computed AIC scores and the corresponding AIC weights.

3.2.8. RECONSTRUCTED PHYLOGENIES

While the model selection approach outlined above gives insight into the type of diversity dependence produced by competition, its results are not directly comparable to an experimental situation where one would seek to estimate diversity-dependence from a single reconstructed phylogeny, where there is no information from extinct lineages. Therefore, we repeated the model selection procedure on single, reconstructed phylogenies in order to estimate how much information is lost as a result of competition-driven extinction. The likelihood for complete trees above cannot be used for reconstructed phylogenies because past diversity in the clade is not directly accessible from the tree. Instead, we used the likelihood and optimization procedure introduced in Etienne *et al.* [14] and implemented in the R package DDD. We expanded DDD to include the diversity-dependent functions introduced above that were not already available.

3.3. RESULTS

3.3.1. DIVERSITY-DEPENDENCE EMERGES FROM INDIVIDUAL-LEVEL COMPETITION

Consistent with expectations from adaptive dynamics theory, diversification (i.e., evolutionary branching) occurred in all communities simulated with the LVIBM if $\sigma_\alpha < \sigma_K$ (that is, all but one setting). Equilibrium community size ranged from a median of $\hat{K} = 2$ species to a median of $\hat{K} = 153$ (Fig. 3.2). $\hat{K}$ is strongly linked to the model parameters: wider resource distributions (larger values of σ_K), and smaller competition kernels (smaller values of σ_α) results in larger communities, with very little variability across replicates (Fig. 3.2). We note, however, that not all communities completely reached equilibrium diversity by the end of simulations. Equilibrium diversity, as measured by $\hat{K}$, appears to be entirely predictable from the values of parameters σ_K and σ_α (Fig. 3.2). We found $\hat{K}$

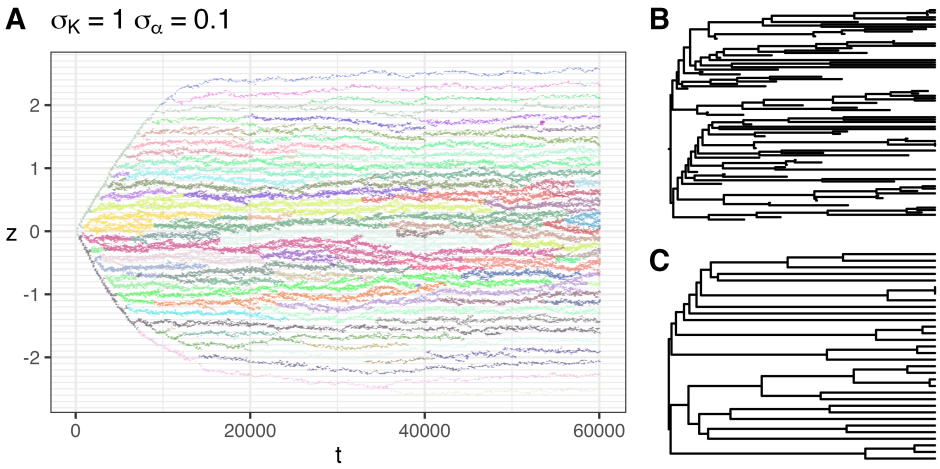

Figure 3.1 | Example output of the individual-based model for parameters $\sigma_K = 1$, $\sigma_\alpha = 0.1$, displaying diversification. (A) Sample of the distribution of phenotypic clusters (species) in trait space over 60,000 generations. 5% percent of all individuals in the community were sampled every 200 generations, and coloured by their species identity. (B) Complete and (C) reconstructed phylogenies built from the community displayed in (A).

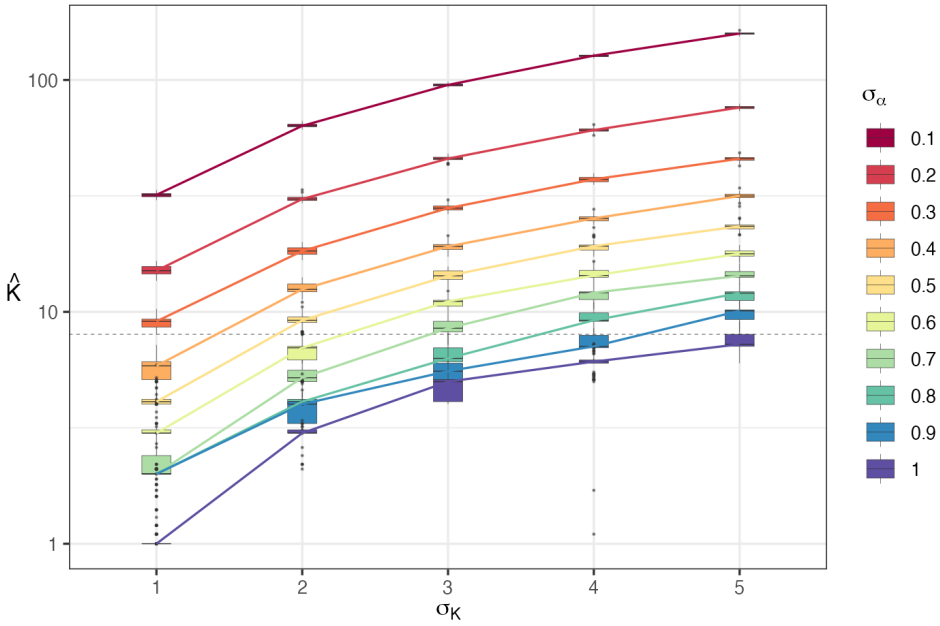

Figure 3.2 | Estimated equilibrium diversity ($\hat{K}$) at the end of simulations from communities simulated with a range of resource abundance widths (σ_K) and competition kernel widths (σ_α), shown on a log10-scale. Boxplots represent the distribution of $\hat{K}$ for each of the 100 replicates from the same parameter set, with lines representing the medians for each parameter set. Parameter sets with a median equilibrium diversity under $\hat{K} = 8$ species (dashed line) were discarded from subsequent analysis.

is proportional to the ratio between σ_K, which controls the total amount of phenotype space (through the total area under $K(z)$, $\sigma_K K_{opt}\sqrt{2\pi}$), and σ_α, which controls the width of low-fitness gaps between branches (and thus, how many species can coexist under $K(z)$ while maintaining non-negative growth). We also note that σ_α also affected $\hat{K}$ negatively independently beyond this ratio, although we could not establish the exact relationship linking $\hat{K}$ with the two parameters. This is consistent with the results of Doebeli and Ispolatov [32] in the context of a multidimensional $K(z)$; they reported the equilibrium diversity to scale exponentially with the dimensionality of $K(z)$ and to decrease with increasing σ_α. We found that fair predictions of $\hat{K}$ can be obtained in our results with the empirical relation,

$$\hat{K} = 0.056\,\sigma_\alpha^{-1.4} + (5.5\,\sigma_\alpha^{-0.89} - 4.1\,\sigma_\alpha^{-0.5})\,\sigma_K.$$

This relation is not entirely satisfactory however, as it does not capture important predictions from adaptive dynamics: $\hat{K}$ should equal 1 if $\sigma_\alpha = \sigma_K$, and the number of species should increase towards infinity as σ_α approaches zero, independently of the value of σ_K.

Diversification is definitely diversity-dependent in our simulations. Species- (Fig. 3.3) and lineage-through-time (Fig. 3.4) plots of the phylogenies built from simulated communities have a shape consistent with diversity-dependent diversification, with initially fast branching followed by a slowdown of diversification, and the eventual saturation of the community around $\hat{K}$ (see [14, 22] for comparison with phylogenies simulated under a diversity-dependent birth-death model). The average rate of speciation across replicate communities, as measured from the mean waiting time between successive events, decreases with species diversity, while the extinction rate tends to increase (Fig. 3.5, Fig. 3.6). The restricted variation in tree size across replicates (Fig. 3.2) is unusual for a diversity independent process, and instead supports a structuring effect as induced by the feedback between diversity and diversification in diversity-dependent models [22].

The relationship between species diversity and the per-capita rates of speciation and extinction is more complex than a simple increase or decrease (Fig. 3.5, Fig. 3.6). The decline of speciation progresses in two phases. Speciation is initially very high and decreases quickly with the number of species. During this first phase, the speciation rate oscillates as it declines (Fig. 3.5, Fig. 3.6). This is a result of the synchronous nature of this initial phase of the diversification process: branching tends to occur simultaneously on both crown lineages (Fig. 3.1), causing rapid speciation from e.g. 2 to 4 species. Such simultaneous branching of crown lineages is typical of the deterministic version of the model [28]. Oscillations dampen after the few first branching events as stochasticity causes speciation events to decouple (Fig. 3.1). Remarkably, the average rate of speciation in this first phase is identical across all values of σ_K (but not σ_α, Fig. 3.5, Fig. 3.6). Then, the decline of speciation with diversity itself slows down, and the speciation rate enters a second phase where it keeps declining at a constant pace with the number of species. The slope of the decline in that second phase depends on the value of σ_K and σ_α, with low values of σ_K and high values of σ_α being associated with a steeper slope (Fig. 3.5, Fig. 3.6). Low σ_K limits the width of exploitable trait space, while high σ_α pushes species further apart from one another in trait space. Both thus contribute to limiting the number of species that can coexist at equilibrium, and increasing the

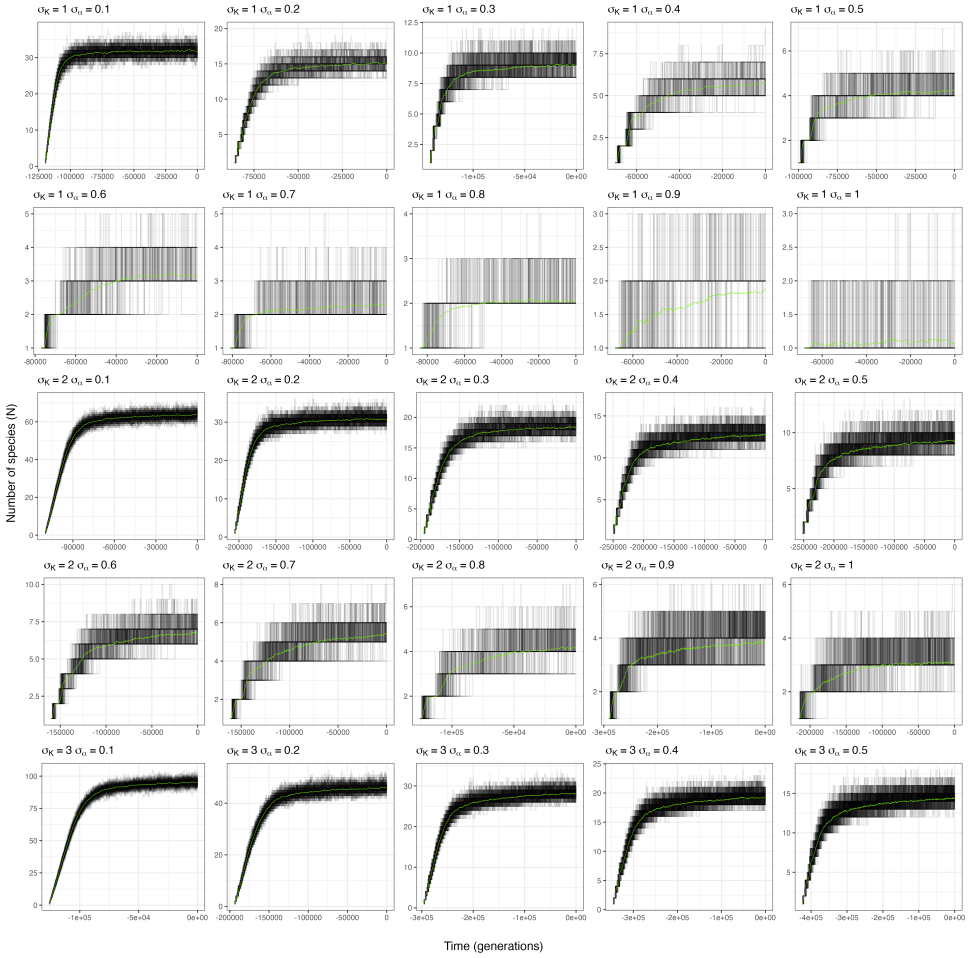

Figure 3.3 | Species-through-time plots (STT, that is the number of species in the clade at a given time in the past) of the phylogenies produced by the LVIBM. Each panel displays the individuals STTs for each of the 100 replicate simulations (black lines), and the average STT (green curve), computed at 1,000 equidistant points in time, for a given parameter setting.

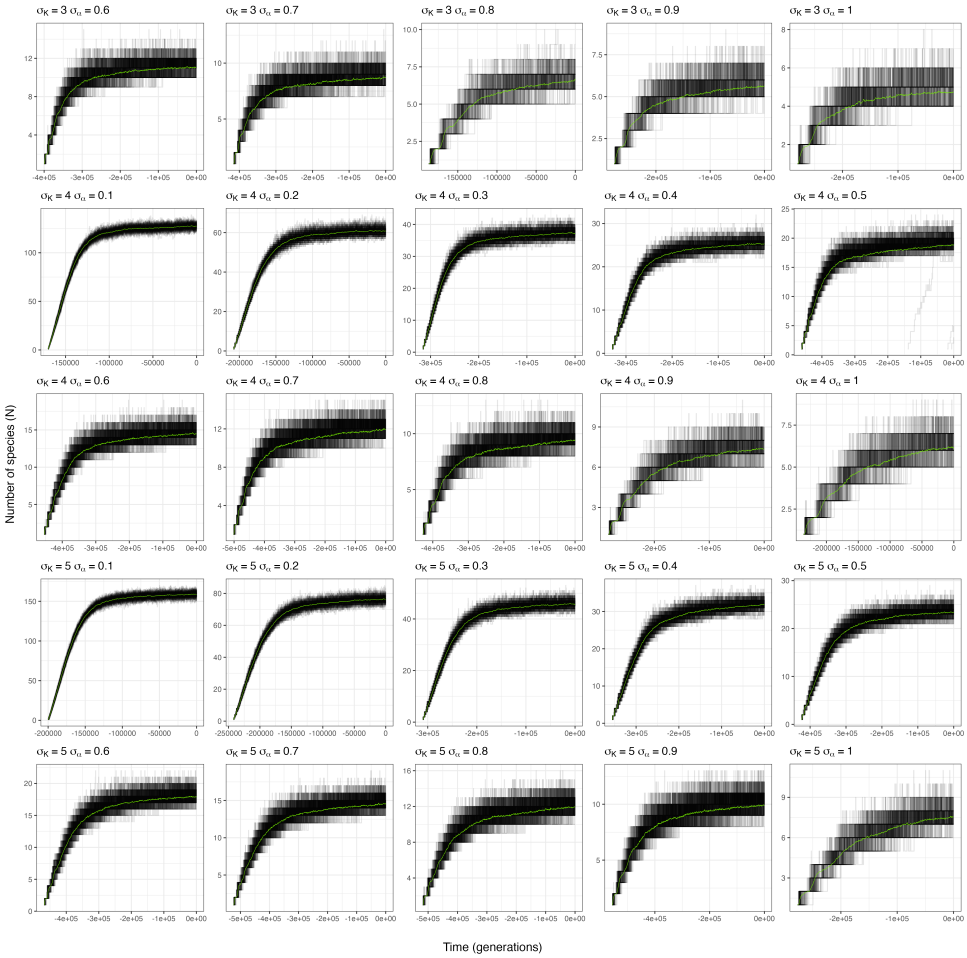

Figure 3.3 | Species-through-time plots (STT, that is the number of species in the clade at a given time in the past) of the phylogenies produced by the LVIBM. Each panel displays the individuals STTs for each of the 100 replicate simulations (black lines), and the average STT (green curve), computed at 1,000 equidistant points in time, for a given parameter setting.

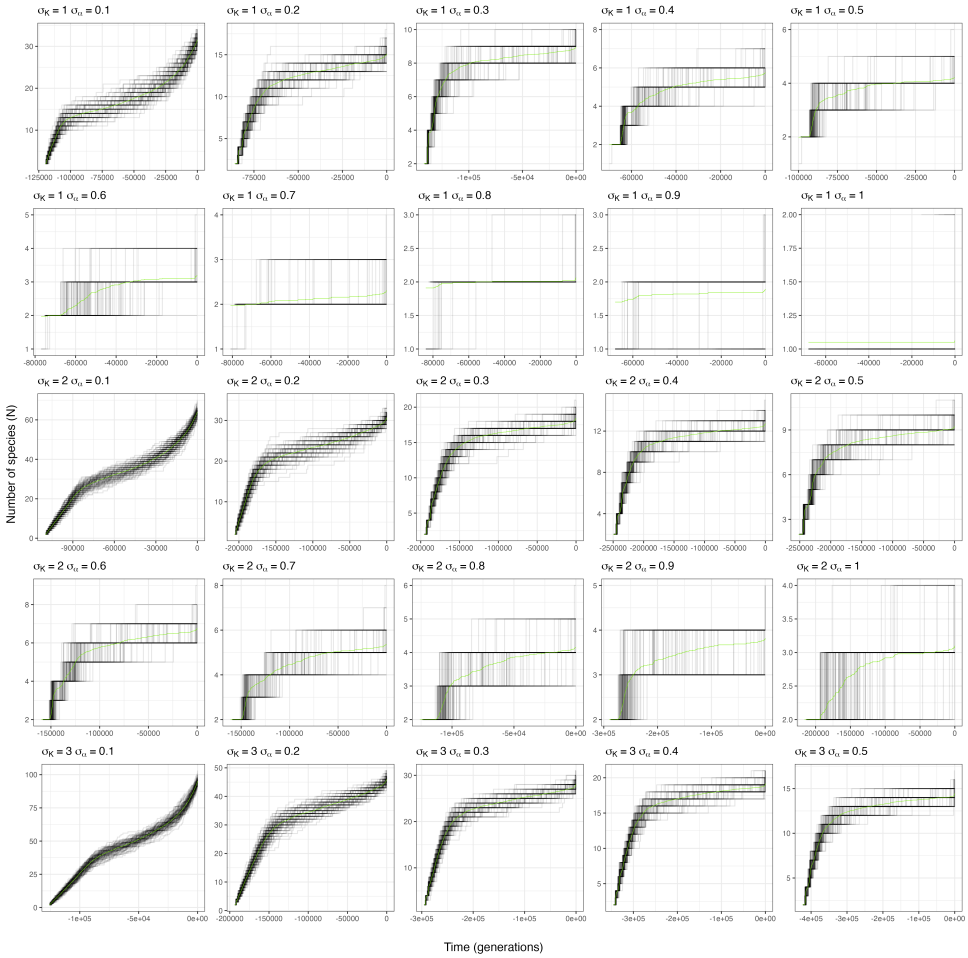

Figure 3.4 | Lineage-through-time plots (LTT, that is the number of lineages at a given time in the past that have extant descendants at the present) of the phylogenies produced by the LVIBM. Each panel displays the individuals LTTs for each of the 100 replicate simulations (black lines), and the average LTT (green curve), computed at 1,000 equidistant points in time, for a given parameter setting.

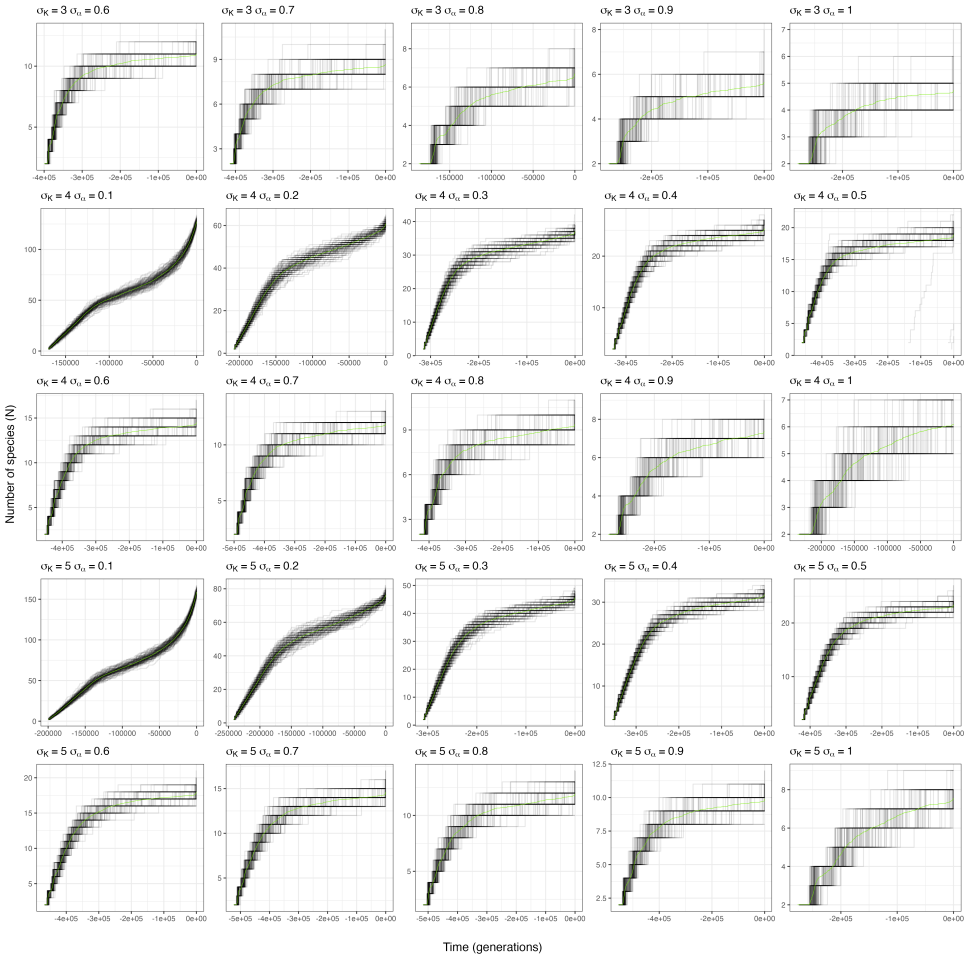

Figure 3.4 | Lineage-through-time plots (LTT, that is the number of lineages at a given time in the past that have extant descendants at the present) of the phylogenies produced by the LVIBM. Each panel displays the individuals LTTs for each of the 100 replicate simulations (black lines), and the average LTT (green curve), computed at 1,000 equidistant points in time, for a given parameter setting.

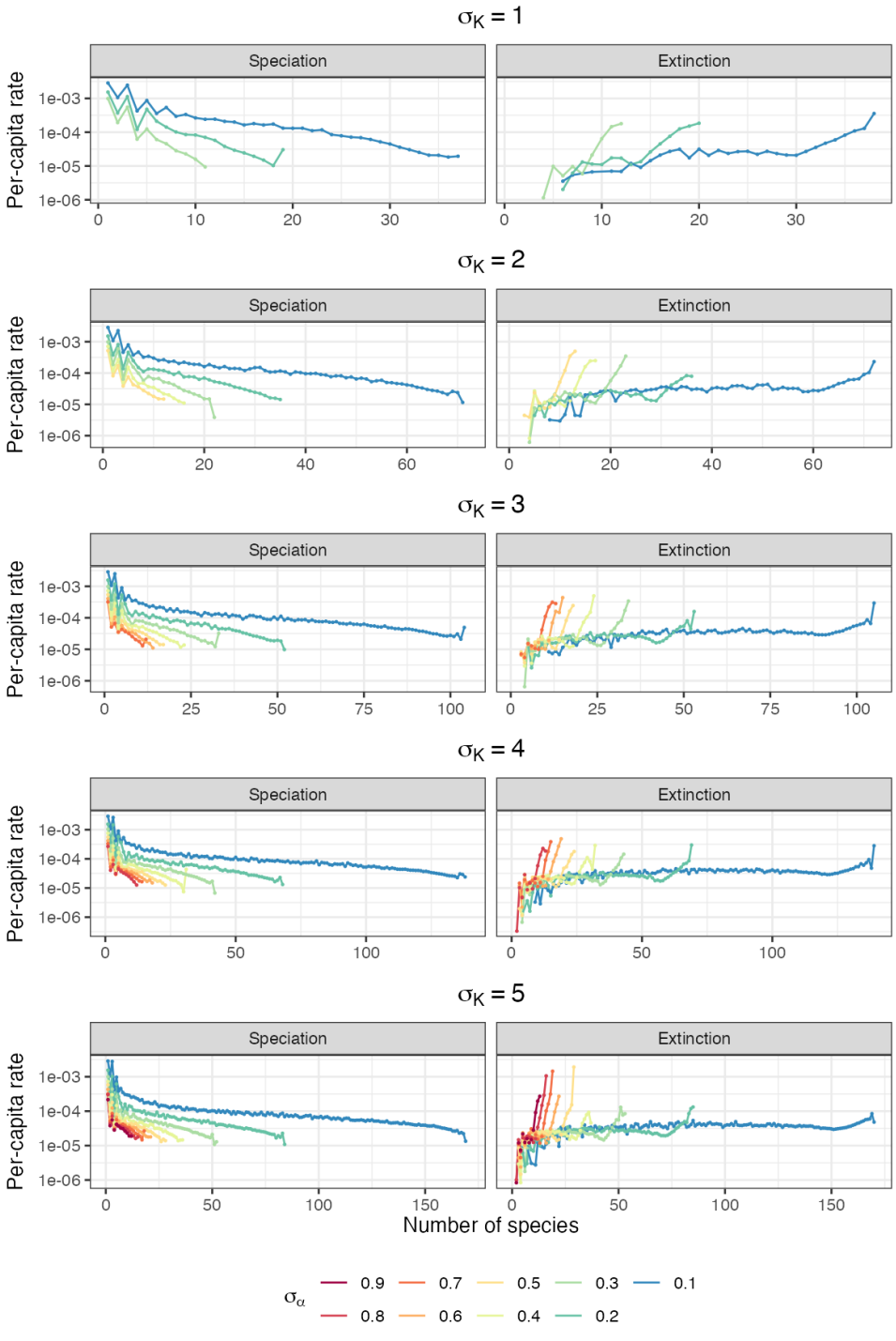

Figure 3.5 | Per-capita rates of speciation and extinction across values estimated independently for each value of N, from the inverse of the mean waiting time between events. Note the log10-scale of the y-axis.

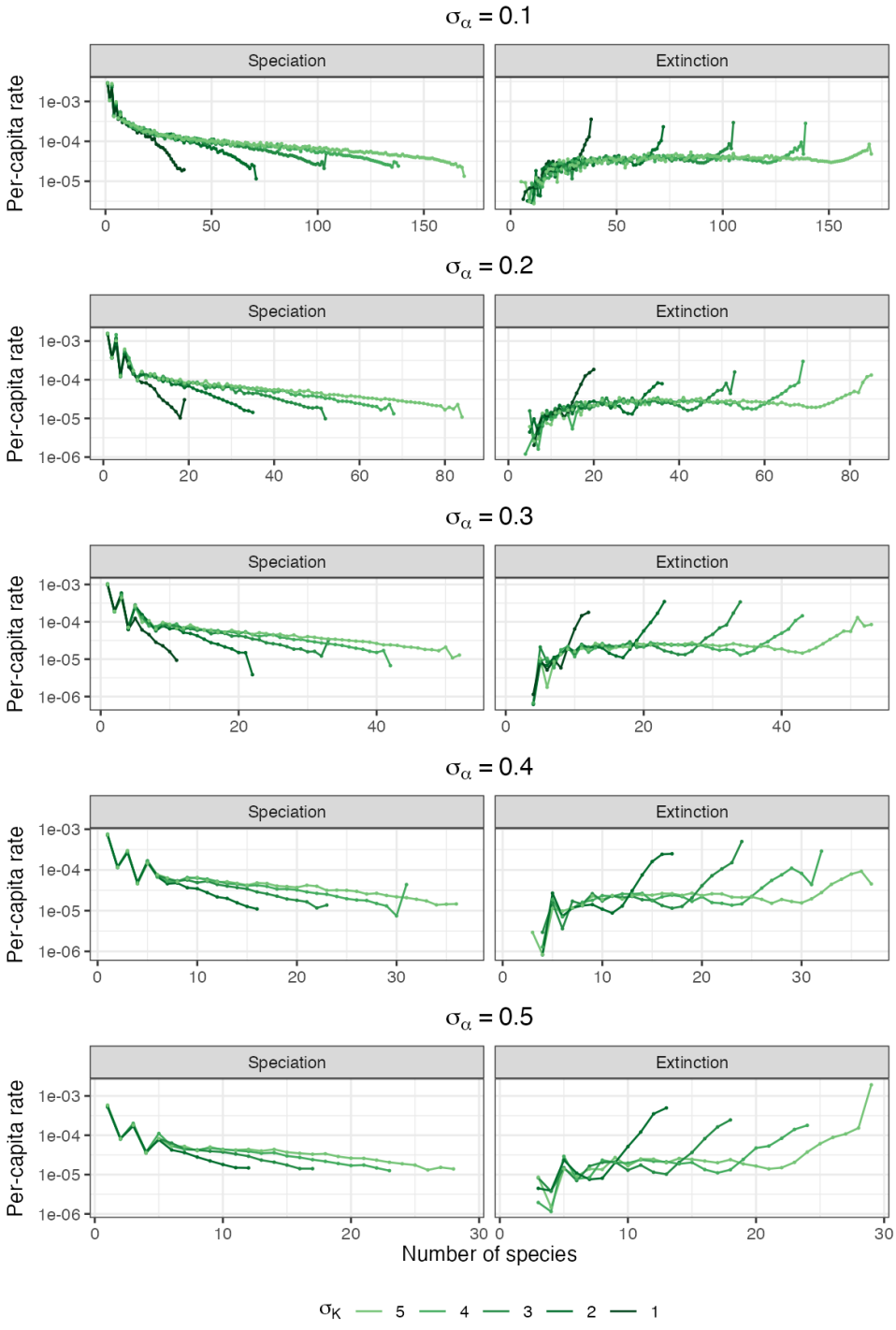

Figure 3.6 | Per-capita rates of speciation and extinction across values estimated independently for each value of N. The values are the same as in Fig.3.5, but are displayed by value of σ_K instead of σ_α.

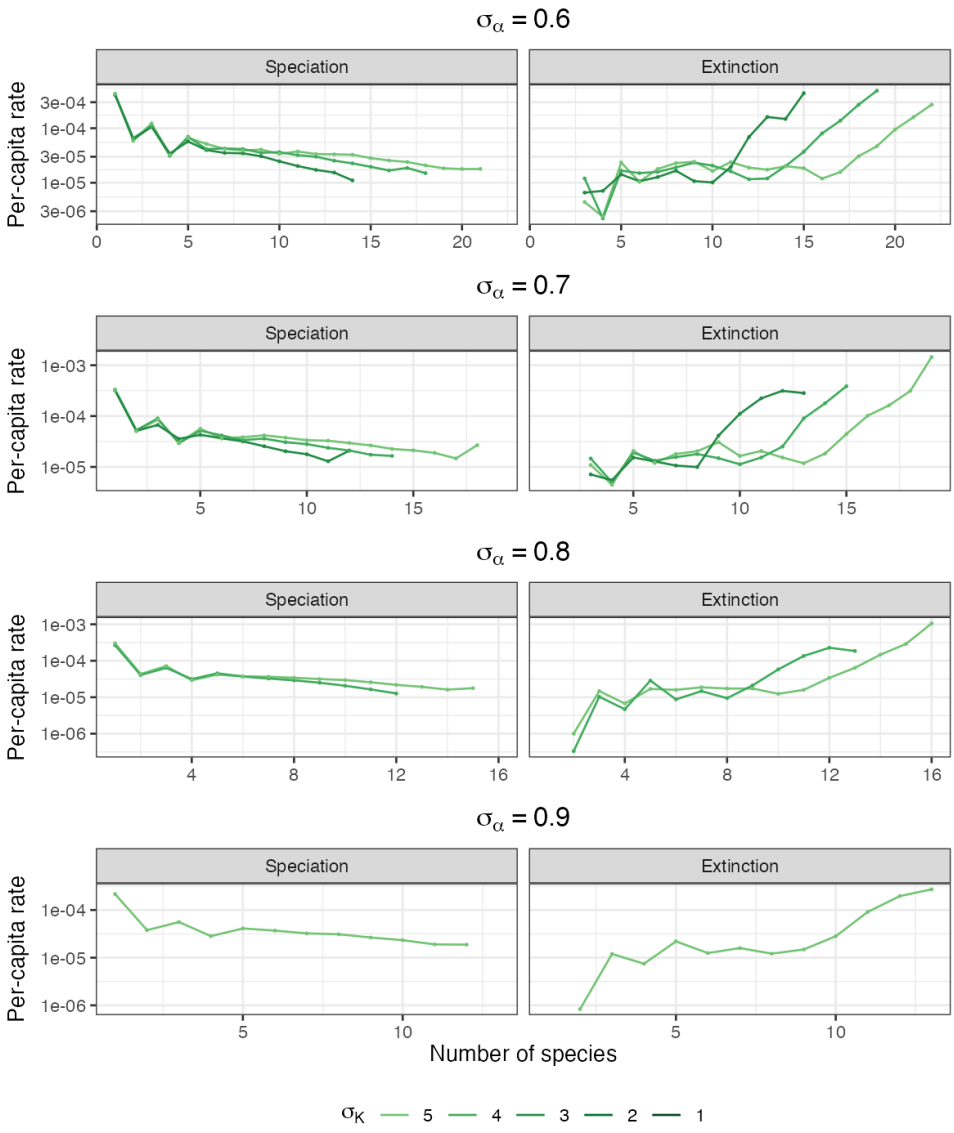

Figure 3.6 | Per-capita rates of speciation and extinction across values estimated independently for each value of N. The values are the same as in Fig.3.5, but are displayed by value of σ_K instead of σ_α.

intensity of diversity-dependent effects on speciation. In addition, σ_α also affects the absolute value of the speciation rate: higher competition intensities results in an overall lower speciation rate (Fig. 3.5, Fig. 3.6). Extinction is initially absent, and only starts occurring after a few species have branched (Fig. 3.5, Fig. 3.6). On its onset, the rate of extinction initially increases very fast, but this fast increase also slows down quickly as more species accumulate in the community. Upon diversity reaching a certain value, the extinction rate starts increasing quickly again, exceeding the speciation rate (and thus, setting equilibrium diversity), and keeps increasing steeply beyond this point.

Between these two phases, we observe an intermediate phase of diversity dependence where the extinction rate is about constant, or follows a hump, increasing at a slower pace than previously, then decreasing with the number of species shortly before the start of the second phase of acceleration of extinction. Interestingly, this decrease in the extinction rate appears to match the pace of the decrease in the speciation rate, such that the net rate of diversification (speciation - extinction) in this phase is about constant. This intermediate phase is hard to observe and may not be present in the smallest communities, where extinction instead seems to increase without interruption, but in all communities with more than about 20 species, the occurrence of extinction at a constant-rate is clear. This intermediate phase is only visible in settings producing large communities. For smaller communities, only a continuous, steep increase of the extinction rate is visible, as equilibrium diversity is reached quickly after the initial onset of extinction. Neither σ_K nor σ_α appear to have an effect on the absolute rate of extinction, or the extent of its increase, although this is not clear due to the relatively small number of extinction events at low levels of diversity (Fig. 3.5, Fig. 3.6). Both parameters appear to have an effect on how early extinction started to increase, and the duration of the different phases, through their effect on equilibrium diversity.

Thus, despite important quantitative differences in the diversity-dependent rates across parameter settings, the form of diversity-dependence emerging from the LVIBM can be described as a single process, with parameters σ_K and σ_α controlling (through equilibrium diversity) the diversity at which the process transits from one form to the next. In summary, σ_K and σ_α modulate the speciation and extinction rates through their effect on setting the equilibrium diversity of the community: higher values of σ_K increase it, while higher values of σ_α decrease it. This in turn influences the slope of the speciation rate, and the diversity at which the extinction rate accelerates towards infinity (Fig. 3.5, Fig. 3.6). Independently of the equilibrium diversity, smaller values of σ_α also increase the speciation rate overall, while no such effect is visible on the extinction rate.

3.3.2. EXTINCTION MOSTLY CONCERNS EXCLUSION BETWEEN SISTER LINEAGES

It has been suggested that diversity-dependence happens through competitive exclusion, a view consistent with Darwin's own proposed process of diversification, and that thus has been referred to as Darwinian diversity-dependence [6]. In our simulations, we do observe that species are at a much higher risk of extinction after branching: the distribution of the length of branches leading to extinction is strongly skewed to the left (Fig. 3.7). This concerns both the new daughter lineage appearing with the speciation event, and the

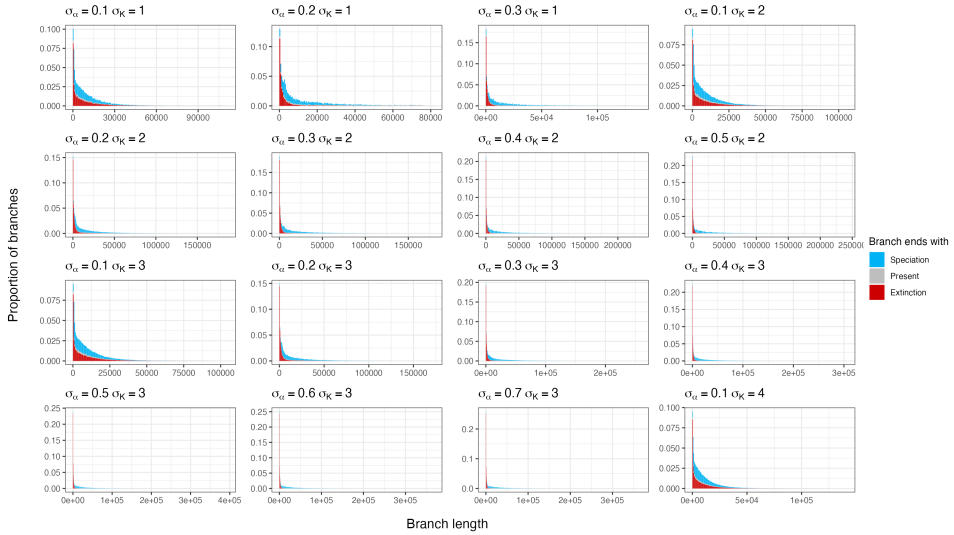

Figure 3.7 | Distribution of the length of branches appearing at a given point in time, coloured by the event terminating the branch.

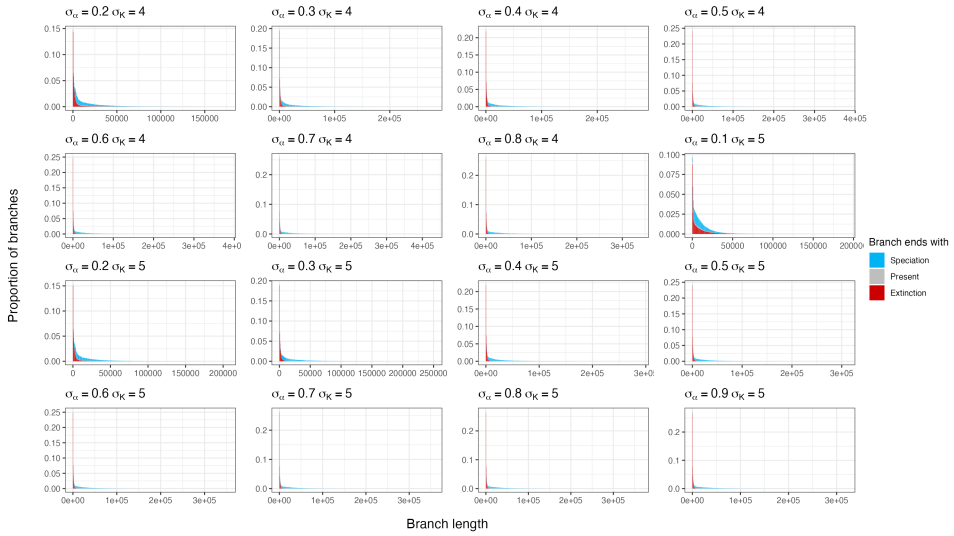

Figure 3.7 | (continued) Distribution of the length of branches appearing at a given point in time, coloured by the event terminating the branch.

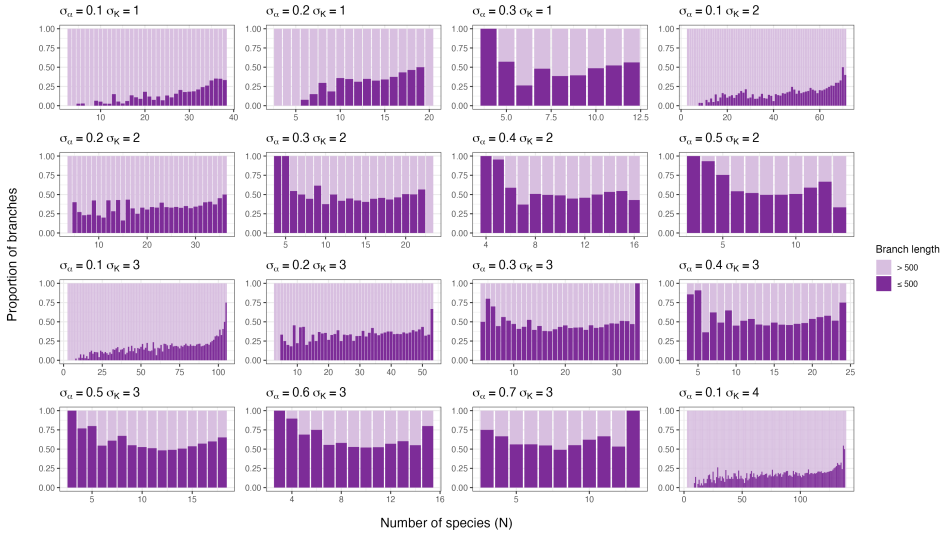

Figure 3.8 | Proportion of short branches (< 500 generations) among branches leading to extinction, plotted as a function of N.

mother lineage undergoing speciation. Extinction events concerning branches younger than 500 generations concern over 20% of all extinction events, in all parameter settings (Fig. 3.7). Competition intensity has an important effect on the proportion of these early extinction events, which made up around 20% of all extinction events as stated above for $\sigma_\alpha = 0.1$, and up to 56-57% in settings with $\sigma_\alpha > 0.6$. We examined the contribution of these short branches to diversity-dependence in the extinction by observing how the proportion of short-branch extinction events (out of all extinction events) changes with the value of N (Fig. 3.8). Overall, changes in the proportions have a small amplitude, staying about constant for much of the range of values of N. A continuous increase of the proportion of short-branch extinctions with increasing diversity is visible for settings with $\sigma_\alpha \leq 0.2$. In those cases, short-branch extinction represents a very low proportion of extinction events at low diversity, suggesting that competition is sparse enough for allowing both sister lineages to survive after divergence. For settings with $\sigma_\alpha > 0.2$, the pattern is instead U-shaped: short-branch extinctions represent the majority to totality of all extinctions when N is low. Excluding short branches from the data decreases both the speciation and extinction rate significantly (Fig 3.9). Yet, we observe that diversity-dependence remains largely unaffected: changes in both rates with values of N are virtually identical whether short-lived species are excluded from data or not. In summary, while a significant part of all extinction events concerns the extinction of recently diverged species as a result of competitive exclusion by their sister lineage, the proportion these events represent is fairly uniform across diversity bins, and thus does not contribute to diversity-dependence substantially.

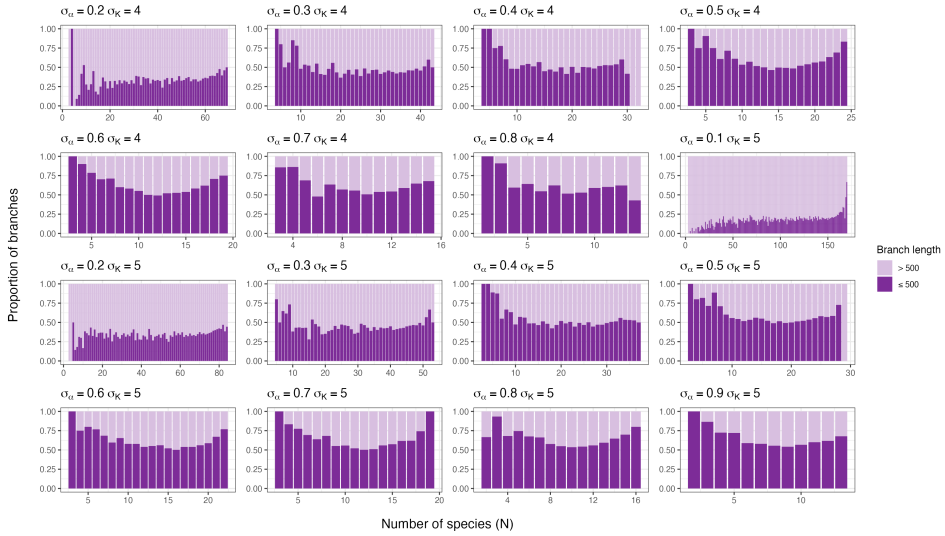

Figure 3.8 | Proportion of short branches (< 500 generations) among branches leading to extinction, plotted as a function of N.

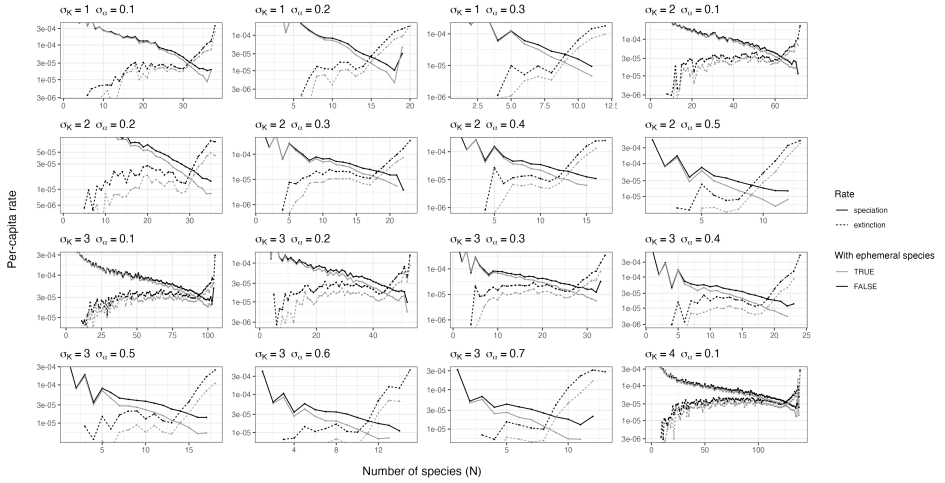

Figure 3.9 | Per-capita rates of speciation (full lines) and extinction (dashed lines), estimated independently for each value of N, including (black lines) or excluding (grey lines) ephemeral species (defined as species that survive for less than 500 generations). Black lines are the same curves as in Fig. 3.5 and Fig. 3.6

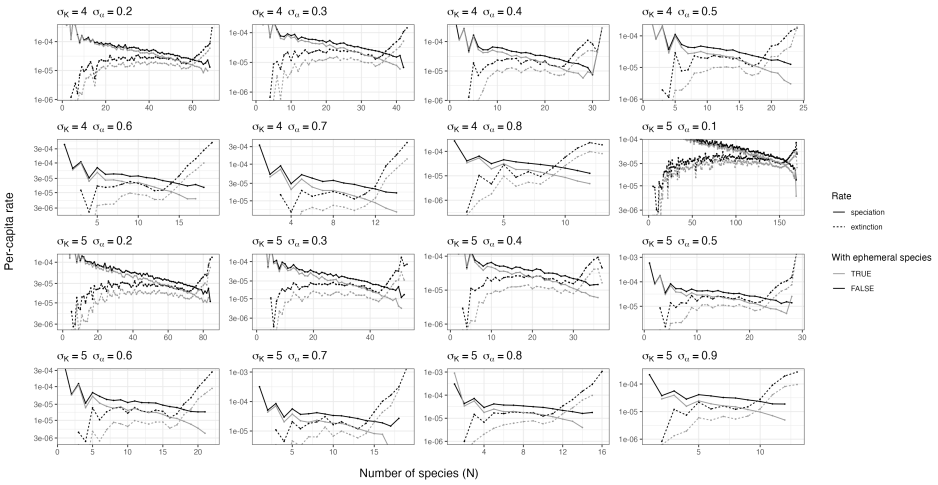

Figure 3.9 | (continued) Per-capita rates of speciation (full lines) and extinction (dashed lines), estimated independently for each value of N, including (black lines) or excluding (grey lines) ephemeral species (defined as species that survive for less than 500 generations). Black lines are the same curves as in Fig. 3.5 and Fig. 3.6

3.3.3. MODEL SELECTION ON COMPLETE TREES

In all settings, one single model was decisively supported over all others, although this best model itself varied across parameter settings. The AIC weight for the best model was over 0.95 in all but one setting ($\sigma_K = 4$, $\sigma_\alpha = 0.2$ where $AIC_w = 0.71$ for the best model) (Fig. 3.10). Rather than a much-improved performance in approximating the LVIBM from the best model compared to others, these large scores appear to be a result of the large number of observations in the data (i.e., all waiting times between successive events across 100 replicate simulations, 9.103 to 9.105 observations) and the small variability across replicates (Fig. 3.2). Reducing the number of observations to solve this issue would make little sense, as AIC_w scores would then reflect sample size rather than the relative performance of each model. Below, we interpret the selected model as providing the best approximation, but rely on inspection of the rates predicted by each function to interpret how well each type of diversity-dependence approximates the rates emerging from the LVIBM.

EXPONENTIAL- OR POWER DIVERSITY-DEPENDENCE BEST APPROXIMATES THE FORM OF DIVERSITY-DEPENDENCE EMERGING FROM THE LVIBM

For all but one combination of σ_K and σ_α, the best fitting model contains either exponential or power diversity-dependence on the speciation rate, and either exponential or power diversity-dependence on the extinction rate (Fig. 3.10). Linear diversity-dependence in the speciation rate was supported in only one setting ($\sigma_K = 4$, $\sigma_\alpha = 0.5$), while constant-rate extinction was never supported (Fig. 3.10). The selection of exponential or power diversity dependence in the speciation rate appears to be driven by the early, explosive phase of speciation that can be observed from the rates estimated separately (black lines in Fig. 3.11). Explosive speciation was indeed absent from the speciation rate

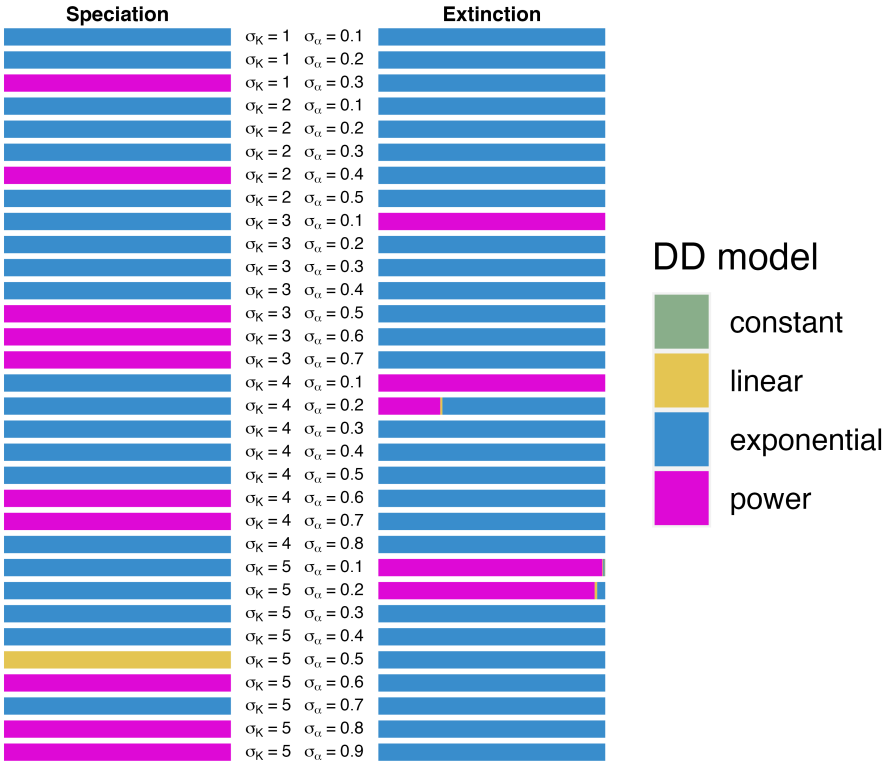

Figure 3.10 | Results of model selection using birth-death models and maximum likelihood, for complete trees. The width of the bars denotes the total AIC weight for each diversity-dependent function, taken as the sum of AIC weights of all birth-death models that included that function.

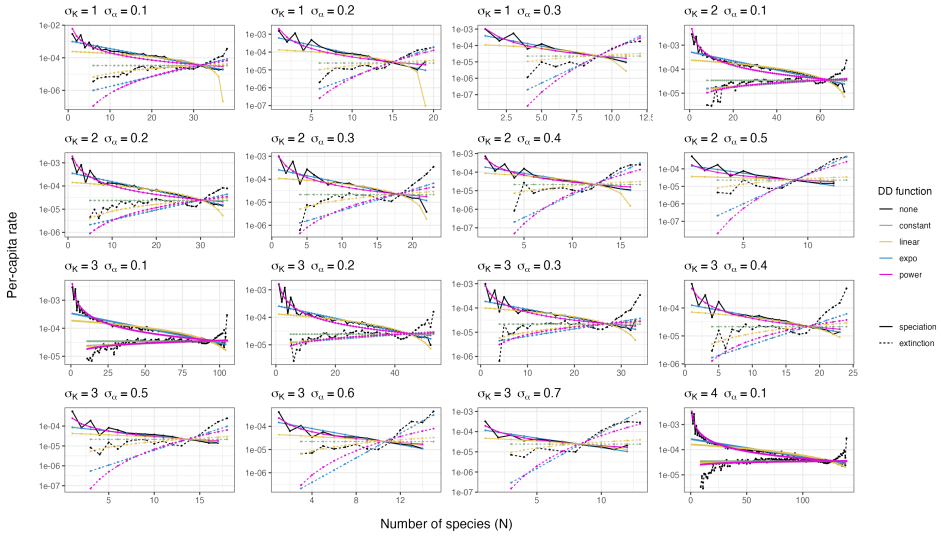

Figure 3.11 | Maximum-likelihood estimates of the speciation and extinction rates obtained from complete trees (coloured lines). Rates estimated independently for each value of N (Fig. 3.6) are plotted as well (black lines) for comparison.

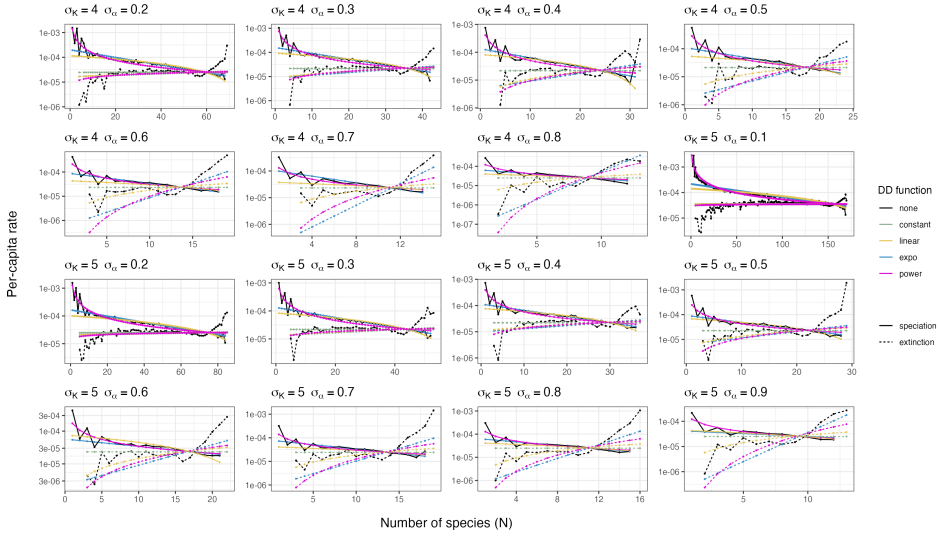

Figure 3.11 | (continued) Maximum-likelihood estimates of the speciation and extinction rates obtained from complete trees (coloured lines). Rates estimated independently for each value of N (Fig. 3.6) are plotted as well (black lines) for comparison.

predicted by the linear model (yellow lines in Fig. 3.11). This pattern was instead best approximated by power diversity-dependence, and to a lesser extent, by exponential diversity-dependence (Fig. 3.11, pink and blue lines, respectively). This early phase appears to have a strong influence on the differences in likelihood between the models, as power diversity-dependence otherwise tended to consistently underestimate the rate of speciation compared to linear diversity-dependence, particularly in the largest communities. The selection of exponential diversity-dependence seems to be the result of this model providing estimates intermediate between power and linear diversity-dependence. For the smallest communities ($\hat{K} < 20$ species), estimates of the speciation rate after the initial phase are closer to those of other models, which may explain why power diversity-dependence in speciation tends to be selected over exponential diversity-dependence in these cases (Fig. 3.10).

Exponential diversity-dependence in the extinction rate was selected for all parameter settings except the four that produced the largest communities (Fig. 3.10), where power diversity-dependence was instead preferred. Here again, the selection of these two models over linear diversity-dependence and constant-rate extinction appears to result from the rapid (rather than gradual) onset of extinction. Without this feature, linear diversity-dependence, or constant-rate extinction appears to better approximate the extinction rate observed in the LVIBM (Fig. 3.11), suggesting that model selection is strongly influenced by these early extinction events. This is particularly visible in the largest communities, where power diversity-dependence is selected over constant-rate extinction despite the extinction rate being close to constant for a large part of the diversification process (see previous section).

The shared features of power and exponential diversity-dependence allow highlighting important aspects of the mode of diversity-dependent diversification that emerges from competition at the level of individuals: the speciation rate decreases, and the extinction rates decrease with the number of species. The decline of speciation and onset of extinction are initially steep, but the rate of change itself declines quickly with the number of species, although it did not reach zero for the range of values of N covered in the community data.

DIVERSITY-DEPENDENCE IS MOSTLY MEDIATED BY THE SPECIATION RATE

Estimates of parameter ϕ are well below 0.5 for most parameter settings, indicating a more important contribution of the speciation rate than the extinction rate to overall diversity-dependence in diversification, although the value of ϕ increased with higher values of σ_α (Fig. 3.15). That is, for settings with low competition intensity ($\sigma_\alpha = 0.1, 0.2$), ϕ was estimated as close to zero, such that the extinction rate changed little with the number of species compared to the speciation rate. Intriguingly, in such settings, estimates of ϕ for models containing exponential or power diversity-dependence in the speciation rate lie close to zero, suggesting nearly-constant extinction. This is consistent with the rates estimated separately for each N: in settings with low σ_α, extinction tends to change very little over intermediate values of N (Fig. 3.6). Yet, the rates associated with these estimates do differ from constant-rate extinction by an initial rapid increase (Fig. 3.11), and this appears to be sufficient to prompt their selection over constant-rate extinction. In communities with high competition intensity (e.g, $\sigma_\alpha = 0.7, 0.8, 0.9$), by

contrast, estimates of ϕ are higher, and in some instances, close to 0.5 (Fig. 3.15), indicating that increasing N increases the extinction rate about as much as it decreases the speciation rate. Again, this is consistent with the rates estimated separately (Fig. 3.10 and black lines on Fig. 3.11), where the fast saturation of niche space resulted in a steep, uninterrupted increase of the extinction rate from its onset. To summarise, the same evolutionary scenario (i.e., the LVIBM) leads to a varying degree of diversity-dependence in the speciation rate versus extinction rate. In general, diversity-dependence affects the speciation rate more than the extinction rate. Yet if equilibrium diversity is low enough to be reached quickly, diversity-dependence affects both rates more evenly.

3.3.4. MODEL SELECTION ON RECONSTRUCTED TREES

MODEL SELECTION RECOVERS LINEAR DIVERSITY-DEPENDENCE IN THE SPECIATION RATE

We find that the exponential and power diversity-dependence in the speciation rate are not recovered in reconstructed trees. Instead, linear diversity-dependence was decisively supported by average AIC weights across all settings (Fig. 3.12). Contrary to the case of complete trees, the large support observed cannot be attributed to the large size of the datasets (models were fitted to each tree separately). Summarising support with an alternative method, by counting the number of occurrences across replicates of each model being selected as the best model yields even stronger support for linear diversity-dependence in speciation (Fig. 3.13). This is in contrast with the very strong support for exponential and power diversity-dependence found in the case of complete trees, and suggests that the strong signal for initially explosive speciation that appears to drive the fit of the model in the complete tree case is lost with extinct lineages in reconstructed trees.

In many cases, maximum likelihood estimates of K associated with power speciation models appear unreasonable, taking values over 1,000 species for many trees (Fig. 3.15). This concerned all parameter settings with $\sigma_\alpha > 0.1$. The implication of these values would be the near constancy (i.e., no diversity-dependence) of the speciation rate (pink lines in Fig. 3.14), a conclusion that should be dismissed given the clear deceleration of speciation observed in the corresponding lineage-through-time plots (Fig. 3.3). Exponential speciation models display the same issue, to a lesser degree, with estimates of $K > 100$, recovering diversity-dependence but still overestimating the equilibrium diversity by a large factor (Fig. 3.15). By contrast, estimates of K associated with linear speciation models are always close to the values estimated from the complete trees and estimates of $\hat{K}$ (Fig. 3.15). This issue is however insufficient to explain the better fit of the linear model: in cases where all three speciation models yield credible estimates for K (that is, settings with $\sigma_\alpha = 0.1$), power and exponential diversity-dependence on speciation remain poorly supported (Fig. 3.12). Surprisingly, further examination of the estimated values of the parameters associated with each model does show that explosive speciation is detected by the exponential and power models in cases where reasonable values were estimated for K (pink and blue lines in Fig. 3.14). Estimated values of λ_0 for reconstructed trees are indeed close to those estimated from complete trees, for all speciation functions (Fig. 3.15). Estimates from the linear speciation models are particularly consistent with the values estimated from complete trees. While λ_0 tends to be overestimated in the

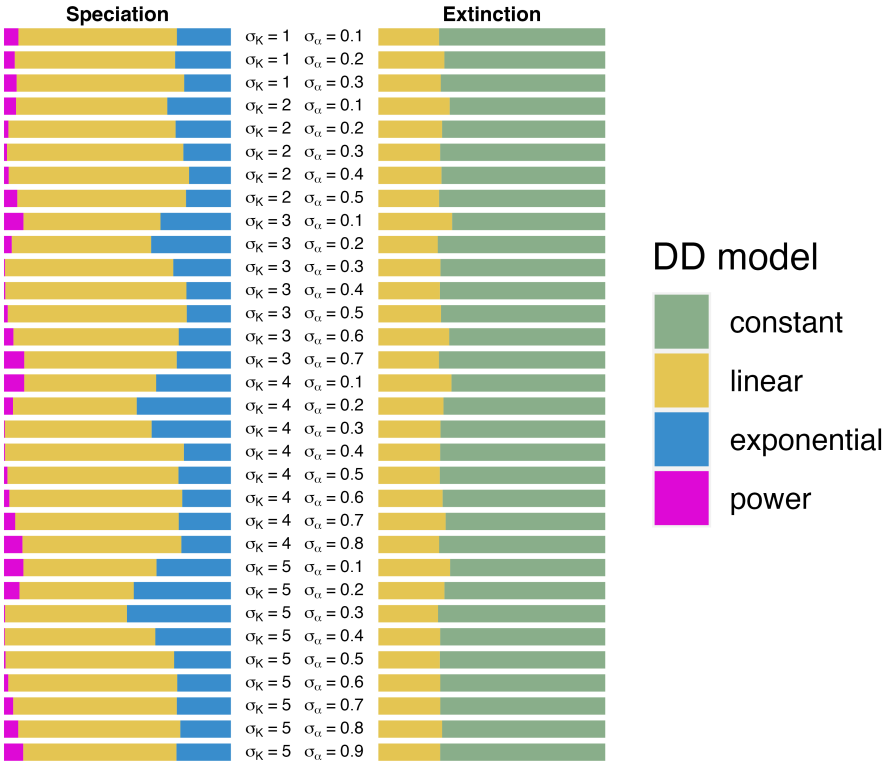

Figure 3.12 | Results of model selection using birth-death models and maximum likelihood, for reconstructed trees. The width of the bars denotes the total AIC weight for each diversity-dependent function, taken as the sum of average AIC weights (across all 100 trees) of all birth-death models that included that function.

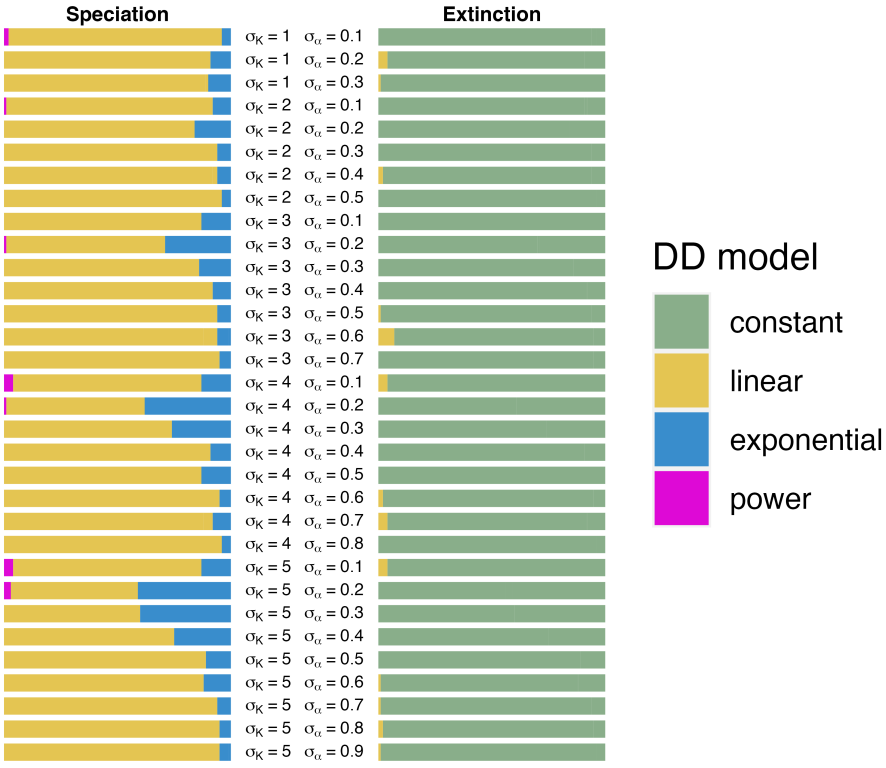

Figure 3.13 | Results of model selection using birth-death models and maximum likelihood, for reconstructed trees. By contrast with 3.12, support for a model is measured as the total number of occurrences of this model as the best model among the 100 replicate trees.

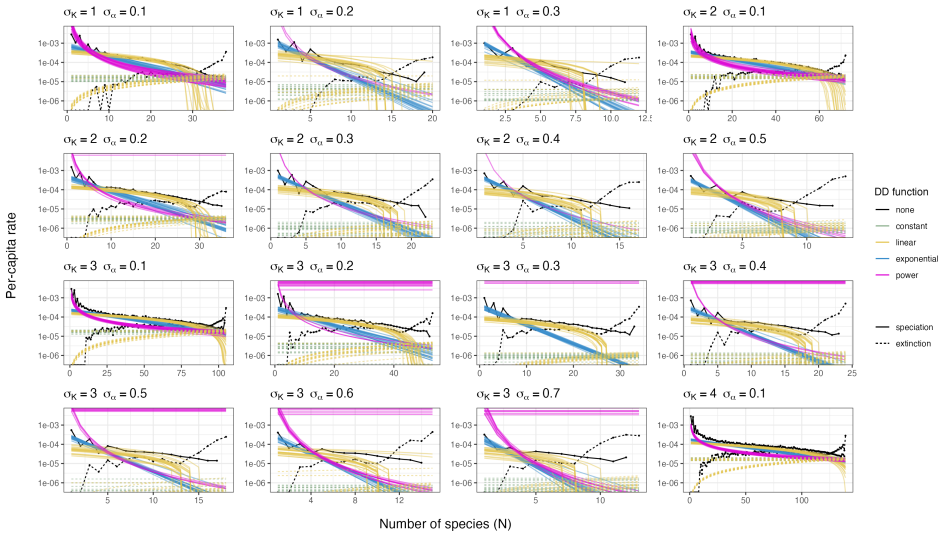

Figure 3.14 | Maximum-likelihood estimates of the speciation and extinction rates obtained from reconstructed trees (coloured lines). Since models were fitted separately on every tree, plotted are the maximum-likelihood estimates corresponding to a random sample of 20 trees among the 100 replicates. Rates estimated independently for each value of N (Fig. 3.6) are plotted (black lines) for comparison.

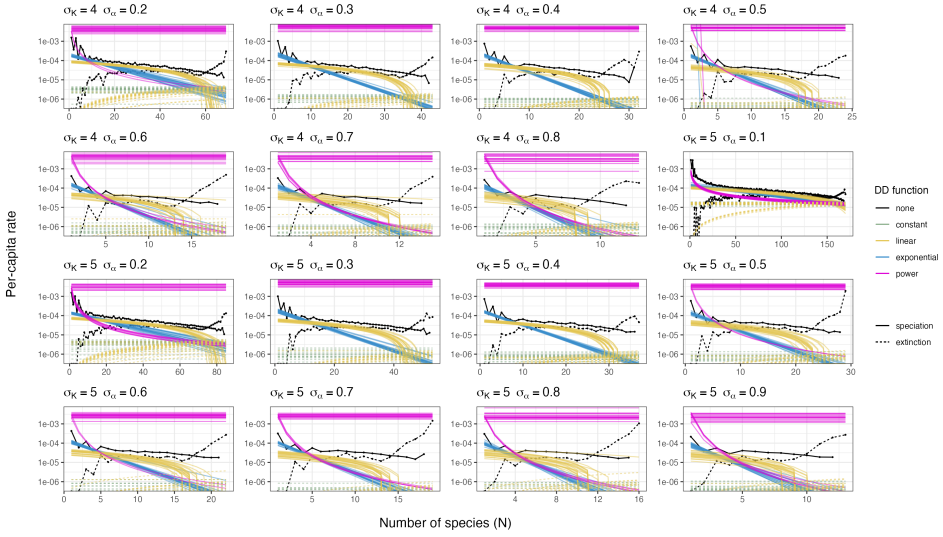

Figure 3.14 | (continued) Maximum-likelihood estimates of the speciation and extinction rates obtained from reconstructed trees (coloured lines). Since models were fitted separately on every tree, plotted are the maximum-likelihood estimates corresponding to a random sample of 20 trees among the 100 replicates. Rates estimated independently for each value of N (Fig. 3.6) are plotted (black lines) for comparison.

case of exponential and power speciation models (up to half an order of magnitude for exponential models and up to an order of magnitude for power models), the importance of this bias is reduced by the curvature of the speciation rate specified in those models: in the end, early explosive speciation is a feature of the resulting speciation rates, and those match the early phase of the rates estimated separately for all values of N well. Estimates of the speciation rate in the second phase of its decline with diversity tend to decouple from the rates estimated from complete trees, largely as a result of extinction being estimated as absent (see next section). With the exception of settings with $\sigma_\alpha = 0.1$, both μ_0 and ϕ are always estimated as close to zero (Fig. 3.15). In those settings and models where estimates of K are accurate, the consequence is that the estimated rate suggests a much steeper decline of speciation with N, and a lower rate of speciation at equilibrium ($N = K$) than what is observed in complete trees.

DIVERSITY-DEPENDENCE IN EXTINCTION IS NOT RECOVERED IN RECONSTRUCTED TREES

Maximum likelihood optimization proved challenging for exponential- or power diversity dependence models. For all models that included either exponential or power diversity dependence on extinction, solving the ODE numerically became computationally intractable for some values of the parameters of the birth-death models, effectively putting the optimisation algorithm to a halt. We could not link the occurrence of this issue with any particular condition of the parameter set. We chose to exclude these models from the analysis, and proceed with a comparison of linear diversity-dependence on extinction against constant-rate extinction (right panels in Fig. 3.12). As a result, we were not able to infer what form of diversity-dependence on extinction would be inferred from the molecular phylogeny of a clade evolving under a scenario similar to the LVIBM, as we did for speciation above.

It can however be anticipated that the likelihood of models with the two missing forms of extinction would be close to models with linear diversity-dependence on extinction (all of them specifying that extinction should generally increase), rather than constant-rate extinction. Indeed, we observed this for complete trees (Fig.3.10). We thus treat the linear model as a proxy for diversity-dependence in general, and model selection becomes a test for the detection of diversity-dependence in the extinction rate against its absence.

In this perspective, we find that the diversity-dependence in extinction observed in complete trees is not recovered in reconstructed trees: constant-rate extinction is decisively supported in all parameter settings (Fig. 3.12). The lack of signal for diversity-dependent extinction is further confirmed by the values of parameter ϕ estimated for the three models with linear diversity-dependence in extinction (Fig. 3.15). Despite substantial variation in the estimated value of ϕ in the complete tree case (see previous sections), in reconstructed trees ϕ is almost always found to be zero (Fig. 3.15). This implies that diversity-dependence is carried entirely through the decline of the speciation rate, and the rate of extinction is effectively constant even in those models that assume diversity-dependence in extinction (dashed lines in Fig. 3.14).

Furthermore, many models did not recover extinction at all: values estimated for both parameters ϕ and μ_0 were virtually zero (Fig. 3.15). This included models specifying diversity-dependent extinction, in all settings, as well as models with constant-rate extinction and either power or exponential diversity-dependence in speciation, in settings

with $\sigma_\alpha > 0.1$. Only the model with linear diversity-dependence in speciation rate and constant-rate extinction (that is, the best fitting model in most scenarios) consistently recovered non-zero extinction ("lc" in Fig. 3.15). Note that the selection of this model cannot be attributed to the failure of other models to infer extinction: in those settings ($\sigma_\alpha = 0.1$) where power or exponential diversity-dependent speciation models also infer non-zero extinction ("xc" and "pc" in Fig. 3.15), the linear model is still strongly preferred (Fig. 3.12).

3.4. DISCUSSION

Diversity-dependence in the net rate of diversification is expected to arise in an ecological scenario where resources limit diversity through increasing competition. Diversification is expected to decrease as the number of species in the community increases [34], but the quantitative relationship between diversity and diversification is not known. Recognizing a general decrease of diversification as a clade grows does not constitute satisfying evidence for a central role of competition in the evolution of the clade, because many unrelated, ecology- and non-ecology-based processes may also produce this pattern [22, 35]. Yet, only a handful of studies have attempted to measure what form of diversity-dependence would emerge from an ecological scenario featuring competition [16, 33], and most studies seeking diversity-dependence in empirical clades assume a linear and/or power function of the number of species (though see [10] for more mechanistic models of diversity-dependence). In order to find out what form of diversity-dependence would be expected if competition indeed drives and limits diversification, and what simple function best approaches it, we used a simple individual-based model derived from adaptive dynamics and tracked how the rates of speciation and extinction change with the number of species in the community. In a first approach, separating the times between events and estimating the per-capita rates of speciation and extinction independently for each value of N allowed us to observe variation in the rates without any assumption regarding the larger trends, and lead us to make two important observations.

First, we obtained qualitative expectations for how the rates of speciation of extinction should change with the number of species in an evolutionary system where competition drives evolution. This relation features transitions between different phases rather than a straightforward, uniform function. The rate of speciation presents two phases: a first phase presenting initially explosive speciation, followed by a quick but decelerating decrease, and a second phase where speciation keeps decreasing at a slower, steady pace. After the first few branching events, the rate of extinction starts increasing quickly, but at a decelerating pace. When diversity has built up to a certain level, the rate of extinction accelerates quickly, equalling the speciation rate, which sets equilibrium diversity. The rate of extinction keeps accelerating if diversity exceeds equilibrium, and at an increasing rate as diversity while the rate of speciation keeps decreasing at the same pace. Between these two phases of acceleration of the extinction rate, extinction is either about constant or increases first and then decreases at a slow pace. Overall, the amount of change in the speciation rate as diversity accumulates greatly exceeds the amount of change in the extinction rate, such that diversity-dependence is overall, primarily carried by the deceleration of speciation. Yet, diversity-dependence in extinction is present, and not

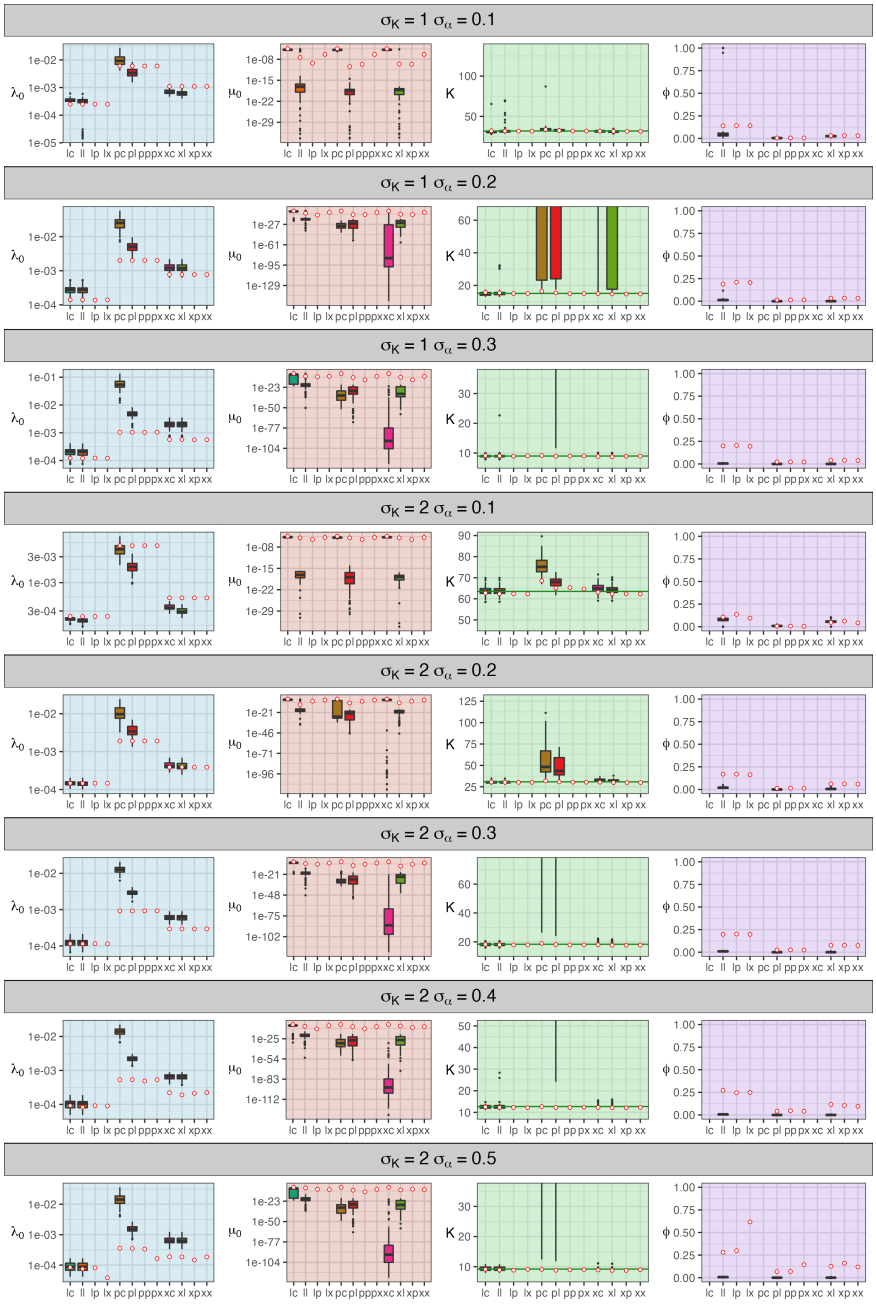

Figure 3.15 | Maximum likelihood estimates of the birth-death model parameters, shown separately for each model. Models are named after the speciation and extinction function that compose them ("c" for constant, "l" for linear, "p" for power, "x" for exponential). Estimates obtained from complete trees are shown as red circles (one estimate per model and set), and estimates obtained from reconstructed trees are shown as box-plots (one estimate per model and tree). The green horizontal bar in the K panels denotes $\hat{K}$. Note that estimates for models "lp", "lx", "px", "pp", "xp", and "xx" are missing for reconstructed trees as we could not obtain estimates for these models (see main text).

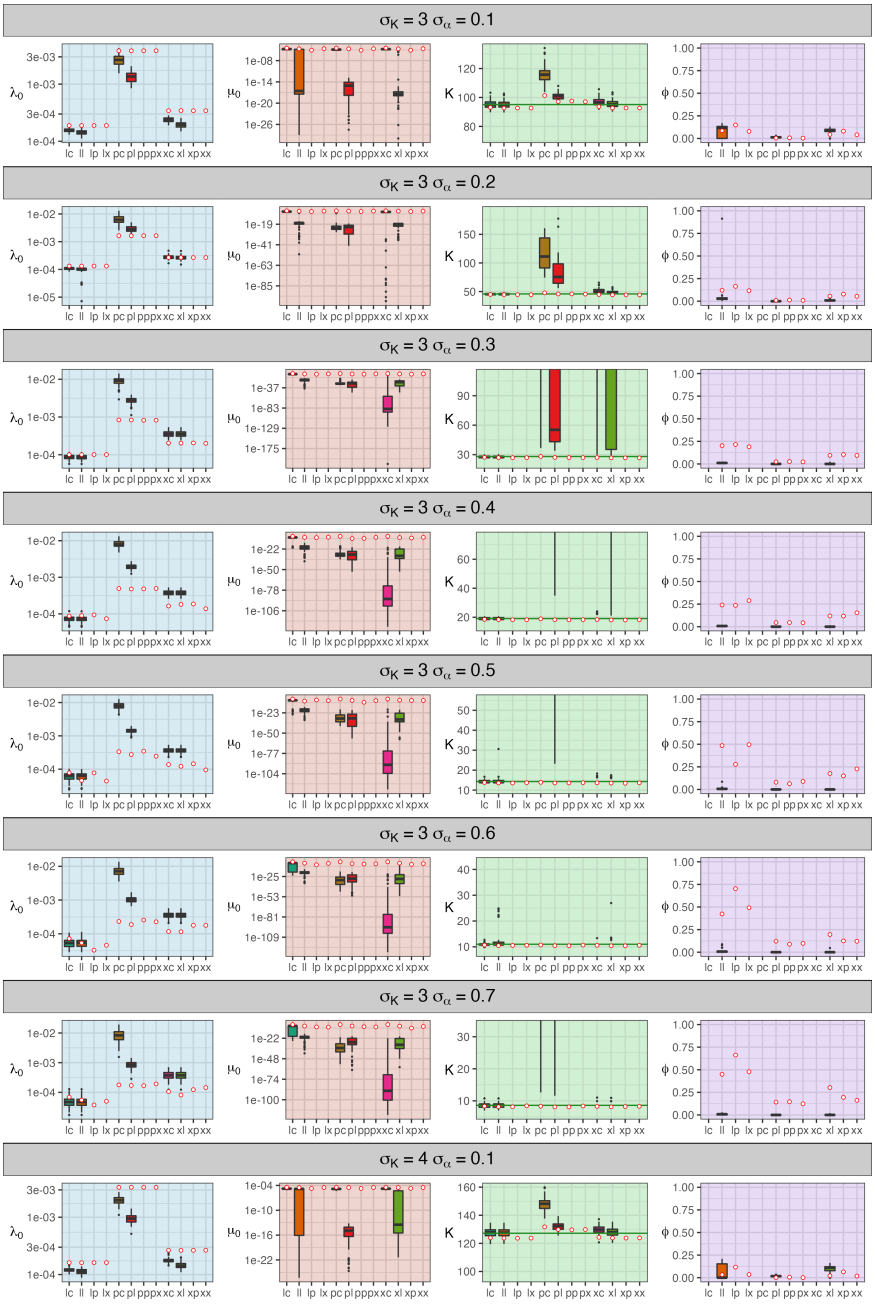

Figure 3.15 | (continued) Maximum likelihood estimates of the birth-death model parameters, shown separately for each model. Models are named after the speciation and extinction function that compose them ("c" for constant, "l" for linear, "p" for power, "x" for exponential). Estimates obtained from complete trees are shown as red circles (one estimate per model and set), and estimates obtained from reconstructed trees are shown as box-plots (one estimate per model and tree). The green horizontal bar in the K panels denotes $\hat{K}$. Note that estimates for models "lp", "lx", "px", "pp", "xp", and "xx" are missing for reconstructed trees as we could not obtain estimates for these models (see main text).

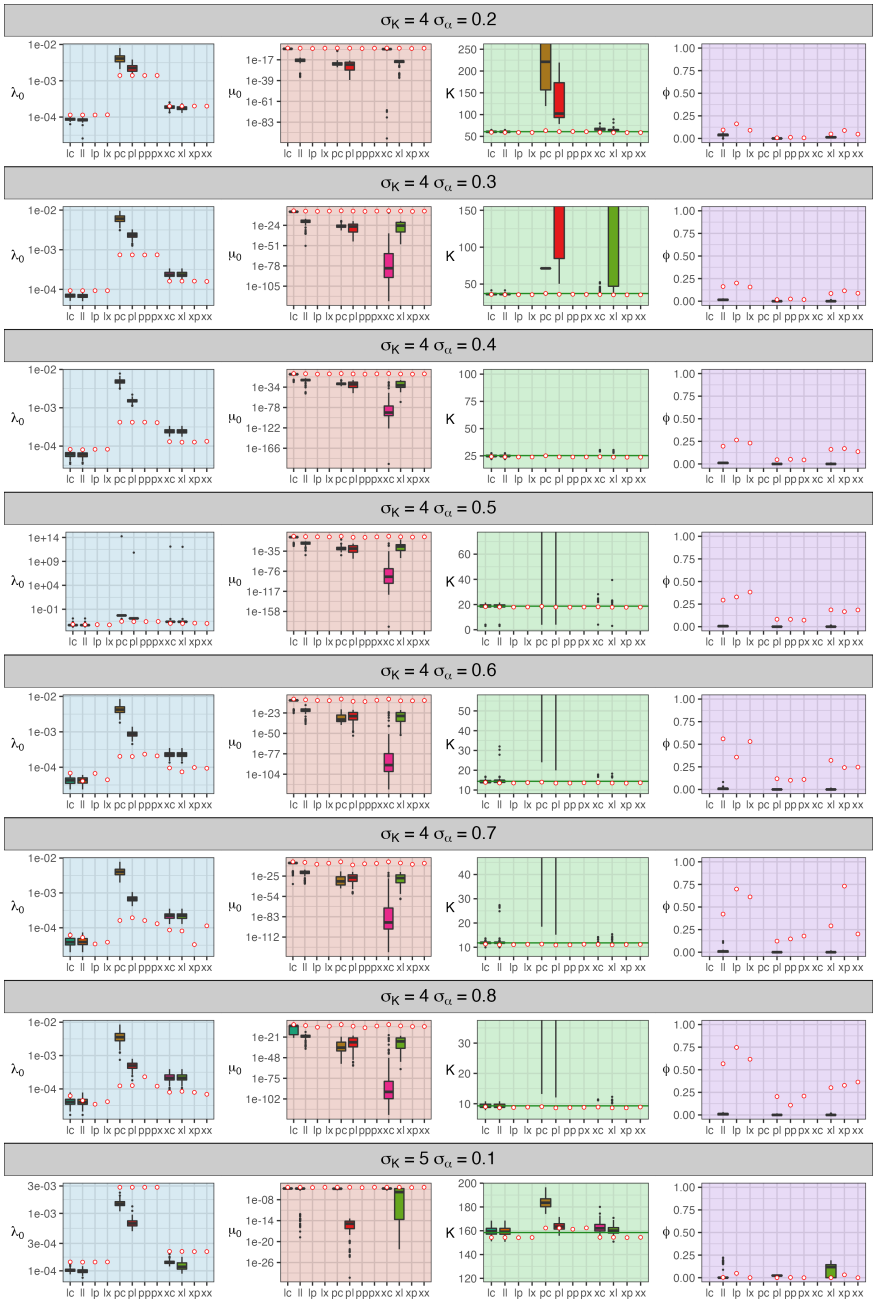

Figure 3.15 | (continued) Maximum likelihood estimates of the birth-death model parameters, shown separately for each model. Models are named after the speciation and extinction function that compose them ("c" for constant, "l" for linear, "p" for power, "x" for exponential). Estimates obtained from complete trees are shown as red circles (one estimate per model and set), and estimates obtained from reconstructed trees are shown as box-plots (one estimate per model and tree). The green horizontal bar in the K panels denotes $\hat{K}$. Note that estimates for models "lp", "lx", "px", "pp", "xp", and "xx" are missing for reconstructed trees as we could not obtain estimates for these models (see main text).

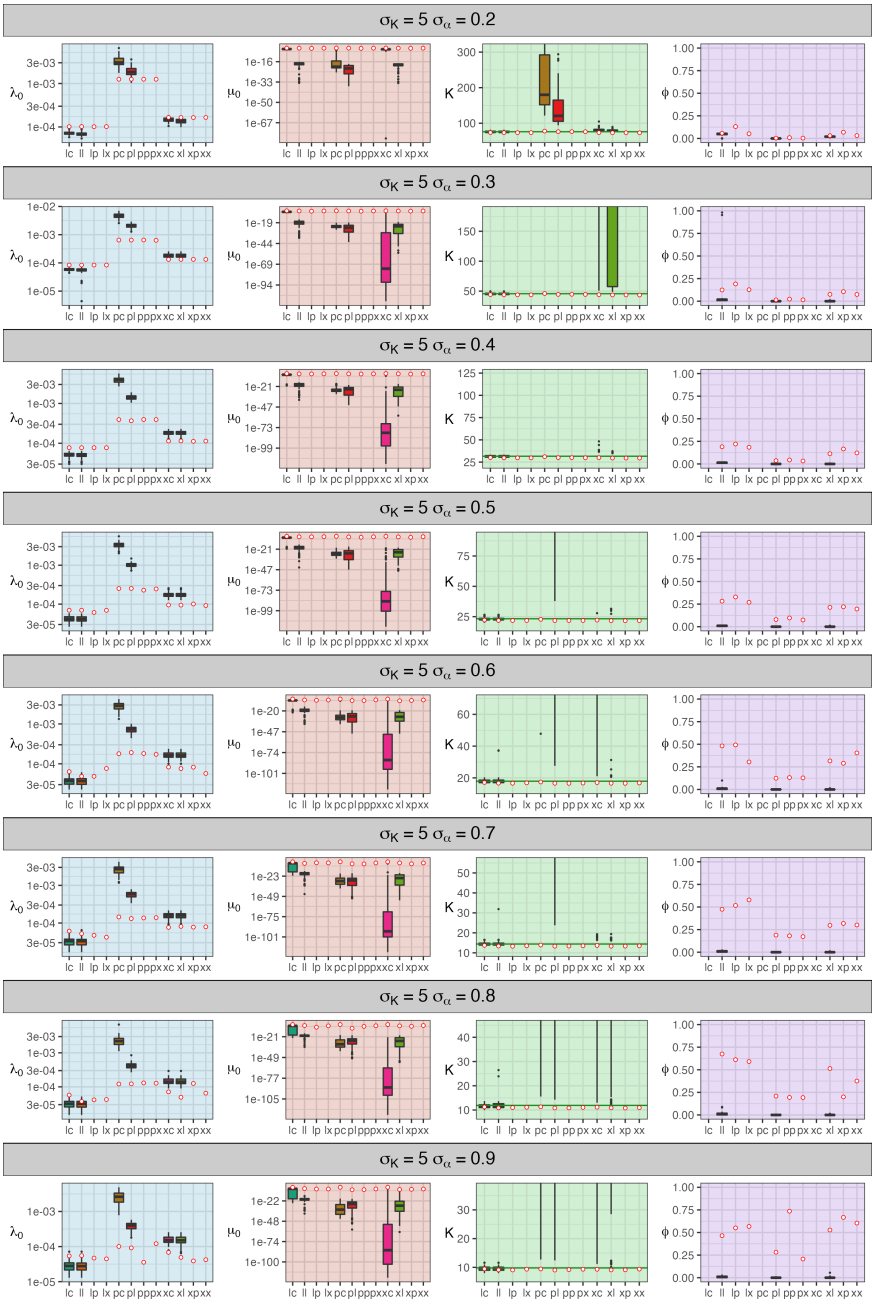

Figure 3.15 | (continued) Maximum likelihood estimates of the birth-death model parameters, shown separately for each model. Models are named after the speciation and extinction function that compose them ("c" for constant, "l" for linear, "p" for power, "x" for exponential). Estimates obtained from complete trees are shown as red circles (one estimate per model and set), and estimates obtained from reconstructed trees are shown as box-plots (one estimate per model and tree). The green horizontal bar in the K panels denotes $\hat{K}$. Note that estimates for models "lp", "lx", "px", "pp", "xp", and "xx" are missing for reconstructed trees as we could not obtain estimates for these models (see main text).

negligible. Diversity-dependence in extinction has been observed in the fossil record [11, 17, 36, 37], but has been poorly supported in molecular phylogenies. Here we show that competition indeed generates diversity-dependent extinction, although only for the lower and higher ranges of values of N. Extinction is otherwise roughly constant through a range of intermediate values of N. The duration of that constant-rate, intermediate phase relative to the two increasing extinction phases depends on how large is the equilibrium diversity, which in turn is determined by the ratio $\frac{\sigma_K}{\sigma_\alpha}$. As a result, the degree of diversity-dependence in extinction depends on equilibrium diversity: when it is low, extinction increases with diversity consistently, while when it is high, extinction is only diversity-dependent at low and high values of diversity.

Second, we described how the two parameters of the individual-based model contribute to modulate diversity-dependence. Surprisingly, we found that intense competition (higher values of σ_α) reduced the baseline rate of speciation, independently of diversity (Fig. 3.6), even when the community contains a single species ($N = 1$). That is, the level of intraspecific competition directly affects the rate of divergence of populations within species. This is a counter-intuitive result, as one could expect that intense competition would increase frequency-dependence, strengthening disruptive selection. We hypothesize that this is a consequence of a smoothening effect of σ_α on the selection gradient: large values of σ_α cause the frequency-dependent component of fitness to decrease more slowly away from individual clusters; resulting in a flatter fitness gradient, weaker disruptive selection, and eventually, slower speciation. However, the main effect of both parameters on the speciation and extinction rates is expressed through equilibrium diversity: higher values of σ_K (increasing the abundance of resources) increase the equilibrium diversity, while higher values of σ_α reduce it. More specifically, lower values of σ_K and higher values of σ_α increase the slope of the speciation rate in the second phase of decline; and advance the onset of the last accelerating phase of extinction, causing the two rates to intersect at lower value of N. An ongoing debate regarding the nature of diversity-dependence concerns whether it brings a hard limit on diversity given a finite niche space, or whether diversification is only reduced further and further as diversity rises, yet without ever stopping [38–40]. The communities emerging from the LVIBM show a clear, predictable equilibrium diversity and thus support the former. Branching does not continue ad infinitum as would happen in the deterministic version of the model [28]. An explicit expression of the equilibrium diversity as a function of both seems to exist, as evidenced by the very low variation in the equilibrium community size across replicate simulation sharing the same values of the parameters; but we were not able not identify it entirely.

While it is clear that equilibrium diversity is a linear function of σ_K, the relation between the former and σ_α has a more complex form (that is, $\hat{K} = a\,\sigma_K\,f(\sigma_\alpha)$). Our approximations for these functions are useful to anticipate the size of the community and choose the parameters of the model accordingly, but neither is satisfying from a biological perspective. Ultimately, an expression of the equilibrium diversity should be identifiable from the relation between the parameters and the equilibrium number of individuals in the community (i.e., the carrying capacity), which is easy to find: by dividing the area of the resource kernel ($K(z)$) by the area of the competition kernel ($\alpha(z)$), it follows that $N = K_{opt}\frac{\sigma_K}{\sigma_\alpha}$. This relation was verified in our simulations, although

the equilibrium number of individuals was consistently very slightly below the number predicted by this relation. At equilibrium, most species do not appear to be at a limiting population size, such that the community could in theory contain many more species, if existing populations were further divided between more species. Because the number of individuals in the community and the range of viable trait values (z such that $K(z) \geq 1$) can both be identified, the crucial next step to identify a relation between equilibrium diversity and the parameters of the model would then be to determine how individuals are distributed in clusters (species) in the trait space and through time. In particular, we note that species are separated by gaps in trait space, putting an effective limit to the number of phenotypic clusters (i.e, species) that can coexist inside the range of viable trait values. The question may then be to identify the relation between the width of these gaps and the abundance of the species adjacent to it. While we have not succeeded in characterizing this distribution here, we hope to pursue our efforts in this direction in the future.

A number of mechanistic models of diversification have been developed in the recent years [25, 31, 34, 41]. Here, we chose to base our model on a stochastic version of the coevolutionary models considered in adaptive dynamics studies. The choice of this model was motivated by its relevance and its simplicity: branching (i.e., diversification) occurs as a consequence of the Lotka-Volterra dynamics taking place at the level of individuals, which are controlled solely by the ratio $\frac{A(z)}{K(z)}$. The dynamics of branching are themselves controlled by this ecological component, along with the growth rate and the rate of mutation, both of which we fixed in this study. The core of this model rests on a Lotka-Volterra coevolutionary component, that is the ratio of the competition kernel ($\alpha(z)$) and niche (resource abundance) kernel ($K(z)$), which allows us to make connections with community- and general ecology theory. Future developments could iteratively challenge the assumptions of the model, for example switching to a sexual mode of reproduction [29], adding a spatial component [25], or explicitly modelling genetic determinism, in each case studying how each development would affect the evolutionary rates and form of diversity-dependence observed. Finally, the foundation of the model in adaptive dynamics allows us to draw predictions from existing knowledge of adaptive dynamics; for example, the equations describing the speed of evolution of the trait along a branch (and thus, the pace of divergence) are known [28], and from this we can anticipate that increasing the rate of mutation (within the limit of keeping mutations "rare", a fundamental assumption of adaptive dynamics that is a requirement for branching to occur) in the present model should accelerate evolution, and, as a result, divergence and speciation. Eventually, we hope that this work will contribute to the foundation of a mechanistic, multi-level theory of macroevolution. A call for such a theory has been made by several authors recently [3, 41, 42]. In such a view, IBMs such as the one presented here could be used to derive macroevolutionary predictions from ecological, contemporary models, and such predictions could be confronted to empirical patterns observed in the fossil record, the distribution of branches in phylogenetic trees and the range and trait distribution along the tips of phylogenetic trees. Eventually, a clearer view could emerge from iterative modifications of these initially simple models. This is nothing new of course, as studies aiming towards this goal have been (e.g., [16, 34]) and continue [33, 43] to be undertaken, but a synthetic theory has yet to emerge. Arguably, the pace

of branching events depends to some extent on the shape of the resource distribution function, $K(z)$. In the present LVIBM, the resource distribution is assumed to follow a Gaussian function, a choice that is aligned with classic ecological theory. Whether or not the Gaussian function constitutes an appropriate modelling choice is a debate that exceeds the scope of this paper, but it is interesting to note that $K(z)$ functions emerging from consumer-resource models are rarely Gaussian [28]. For example, multi-modal, or skewed resource distribution functions are not biologically unreasonable. This may certainly impact the pace of branching events: a multi-modal function may cause successive bursts-and-slowdowns as the clade expands into sections of trait space associated with different peaks; with a skewed distribution, branching will halt earlier on one side of the optimum, and continue longer on the other, stretching the sequence of speciation events on a longer time frame. Whether and how this is in turn affecting the form of diversity-dependence in the speciation rate, however, is unclear to us, as out of consistency with the birth-death models we have made the assumption that time does not affect the probability of speciation other than through diversity $N(t)$, and thus we have not studied how the time sequence of events may affect diversity-dependence. The present work constitutes, to the best of our knowledge, the second attempt after Aguilée *et al.* [33] to describe the rates of speciation and extinction, and the form of diversity-dependence that emerge from these coevolutionary models. The individual-based model by Aguilée *et al.* [33] shares the same foundation as the one we used here (namely, the fitness function is based on the ratio $\frac{A(z)}{K(z)}$), but is more complex, differing from ours in two key aspects. First, their model included a spatial component, with several sites and shifting connections between them. Second, individuals in their model reproduced sexually, and reproductive isolation was modelled explicitly. Valuable insights can be gained from a comparison of the results of our two studies. Despite of the differences between the models, we note a striking similarity between our respective results: the form of diversity-dependence reported by [33] features several phases between which the relation between diversity and the speciation and extinction rate changes. Specifically, they distinguished three phases. First, a phase of "geographic adaptive radiation", where the initial colonization of all the sites and the resulting divergence in allopatry causes speciation to be explosive and quickly decreasing, while extinction is virtually absent. Following this, diversification enters a "niche self-structuring" phase, where local (within sites) adaptation and competition result in a quick increase of extinction, followed by about constant-rate speciation and extinction. Finally, as local niches saturate, speciation slows down, while extinction blows up, precipitating equilibrium diversity. As described above, we did find the same variations in the rates of speciation and extinction with diversity, with the exception that in our results, we did not find the speciation rate to be constant, and its slowdown phase instead appears to start immediately after the initial explosive phase. It is also possible that this discrepancy is due to a different interpretation of our respective results: we note that depending on the parameter values, constant-rate speciation is not always visible in the results of Aguilée et al. (Fig S5 in [33]). Consistent with our results, Aguilée *et al.* [33] also reported an effect of $\frac{\sigma_\alpha}{\sigma_K}$ on total diversity, the speciation rate and the extinction rate (Fig. S5 in [33]). Their results also show a predictable relation between $\frac{\sigma_\alpha}{\sigma_K}$ and equilibrium diversity (Fig. S4, panel h) that is at least qualitatively consistent with our results (compare with Fig. 3.2). Taken

together, the similarities in the variations of rates between their model and ours suggest a general pattern of diversity-dependence for this class of models, and this is probably something one wants to look for as evidence for diversity-dependence. The *ad hoc* nature of this pattern we uncovered however implies it cannot be tested directly. In section 3.4.1 we discuss how well it is approximated by traditional phenomenological models of diversity-dependence.

We found that a significant proportion of extinction events concern recently diverged species through exclusion by their sister species, with a strong effect of the intensity of competition on the frequency of extinction of these short-lived species (the proportion of these events grow from 20% to 57% in settings with the largest values of σ_α). This is consistent with the concept of "ephemeral speciation" [6, 44] and Darwin's own model of macroevolution [5, 45], which Rabosky [6] described as a mechanism by which diversity-dependence takes place (that is, "Darwinian diversity-dependence"). Excluding ephemeral species from the data does reduce both the speciation rate and the extinction rate in equal measure, but does not change their qualitative variations with the values of N (Fig. 3.9). The different phases of speciation and extinction we have described above can still clearly be identified (Fig. 3.9). Therefore, while ephemeral speciation is an ubiquitous feature of the diversification process produced by the LVIBM, it does not qualitatively change the relation between the speciation or extinction rate and the number of species, so that its contribution to diversity-dependence is negligible. This finding is at odds with the results of the lineage-level mechanistic model of Aristide and Morlon [41], where an increase in the extinction of incipient lineages was largely responsible for diversity-dependence. Arguably, the frequency of ephemeral species is sensitive to the species recognition threshold we have used. Graphically, we have observed that populations diverging from one another within species (before speciation is recognized, i.e., incipient species) are equally likely to go extinct, such that there is a continuum in the distribution of length of branches going extinct before or after speciation. Ezard *et al.* [46] have shown how the choice of the criterion used to delineate species in the fossil record can affect the measured rates of speciation and extinction, including the slope of diversity-dependence. Here, justifying our species delimitation criterion is made easy by the morphological patterns produced by the LVIBM: the distribution of individuals in trait space and through time forms fairly discrete, separated clusters of individuals (Fig. 3.1). The only arbitrary choices we have made are to consider that species persist through speciation events as one of the resulting diverging lineages, and the speciation recognition threshold, which we chose to fix to $\theta(z) = 0.1$ following Pontarp *et al.* [25]. Arguably, the latter is affecting the rates of speciation and extinction we have measured: lowering the threshold would result in the recognition of incipient species as full species, thus adding many speciation and extinction events to the data. However, while changing the value of $\theta(z) = 0.1$ would certainly increase or decrease the base rates of speciation and extinction, it would not change the relation between the rates and N, and we are confident that the form of diversity-dependence we report is robust to this parameter. The ubiquity of extinction of ephemeral species was also reported by Aguilée *et al.* [33], and thus it seems to be a feature of this class of coevolutionary models.

3.4.1. EVALUATING THE SUPPORT FOR PHENOMENOLOGICAL MODELS

The description of the form of diversity-dependence that emerges from the LVIBM we have carried out above has yielded valuable insights, suggesting some signature features of this evolutionary scenario to search for in empirical data. In the absence of an explicit expression for the rates of speciation and extinction, however, it is not possible to test support for this model in empirical data directly. Phenomenological models of diversity-dependence by contrast have been routinely used to test for diversity-dependence in phylogenies and fossil diversity are valuable to assess general trends in the data, but lack strong theoretical foundation. Since the initial propositions of Sepkoski [7] and Maurer [16] for the linear and power forms of the model respectively, there has been no investigation of whether these two models indeed constitute satisfying approximations of the assumed diversification mechanism. Critically, uncertainty has persisted over which version of the model is the appropriate form to represent the effect of competition: the two models have largely been used interchangeably, and often simultaneously, with identical conclusions in case either was found to better fit the tree. At times [13], quantitative differences have been mentioned (the rate of decline of speciation declining with N in the power model), but the potential implications have seldom been explored. In the presence of perfectly complete data, our model decisively supports either the exponential version we have introduced, or the power version, depending on the choice of parameters of the LVIBM. Support appears to result from the very high speciation rate at low diversity present in the simulations, which linear diversity-dependence does not capture satisfyingly. While speciation does decline fast with the number of species, the decline of speciation with N itself does not decelerate in simulations, as would be expected in the power model, and instead speciation past the initial explosive phase is best approximated by the linear model, and to a lesser extent the exponential model. Selection of exponential diversity-dependence therefore appears to be a matter of trade-off between these two features, the exponential model producing diversity-dependence intermediate between those specified in the power and linear models. Considering that none of the three types of functions capture all features of the rates estimated for each N individually, and the discrepancy between the two phases of speciation, perhaps the most appropriate birth-death model would be one including a transition between two modes of diversity-dependence. Birth-death models featuring temporal transitions between evolutionary modes have been developed (BAMM, [47]). Although BAMM (or any other model) does not incorporate transitions along diversity rather than time, and developing such a framework is beyond the scope of this study, comparing the fit of such a model to the ones we have included here could bring interesting insights. In the meantime, among models featuring a single mode of diversity-dependence, exponential or power diversity-dependence appears to provide the best approximation. In any case, the strong signal for explosive speciation is at odds with results reported from reconstructed phylogenies where, as we discussed in the introduction, linear diversity-dependence in the speciation rate is most often found to fit the phylogeny best. This discrepancy between our results for complete trees and empirical findings can be resolved by considering that reconstructed trees are only a limited subset of the evolutionary history of the clade. Indeed, when we perform the model selection procedure again after pruning extinct lineages from the trees, we find decisive support for linear diversity-dependence on speciation. This implies that

while the signal for early explosive speciation is present, support for it is lost.

Arguably, the completeness of our assessment of phenomenological models for reconstructed trees was restricted by the two unresolved computational issues mentioned in the Results section. Below we expand a bit further on these issues, including what we suspect caused them and potential tracks to address them. First, for most trees and parameter settings, maximum likelihood estimates of the equilibrium diversity associated with exponential or power diversity-dependence on speciation are extremely high, and functionally equivalent to infinity, indicating no diversity-dependence on speciation. Paradoxically, values of parameter ϕ associated with this are also close to zero, indicating no diversity-dependence on extinction either. This apparent paradox can be resolved by considering the asymptotic behaviour of the speciation rate under these models. As shown by the values of maximum-likelihood estimates of the initial extinction rate μ_0, the signal for weak, or even absent extinction from the reconstructed trees is strong. As a result of the formulation of the models (see Section 3.2.6), low values of μ_0 are only possible if K is very high (in fact, $\mu_0 = 0$ is only possible if K is infinite). A potential solution to this would be to alter the diversity-dependent model and use parameters that are not susceptible to this behaviour. For example, one could define K as the value of N for which the speciation is a certain fraction of the initial speciation rate λ_0, thus circumventing the issue by decoupling speciation from extinction. Such a model could be helpful to quantify diversity-dependence, but unfortunately loses the biological interpretation of the equilibrium diversity.

Second, the likelihood could often not be computed for models that incorporated exponential or power diversity-dependence on extinction, and we excluded these 6 models from the initial set of candidate models. The issue appears to originate from the extinction rate growing very large under some values of the parameters explored during optimisation. High extinction requires keeping track of the probabilities of a larger set of possible states, such that the size of the system of equations grows and integration of the likelihood becomes computationally challenging. An evident solution would be to attempt to limit the size of the system of equations to a maximum value, and forego the computation of probabilities associated with high (and unlikely) values of N. Because this will inevitably bias the likelihood to some extent (as we do not calculate part of the probability density function at every step), making it difficult to apply in practice. Nevertheless, the results we do have at hand suggest that our conclusions are robust to these missing results. In the few cases where we did obtain reasonable estimates of the carrying capacity for models that incorporated exponential or power diversity-dependence on speciation, linear diversity-dependence was still largely preferred. Constant-rate extinction was largely preferred over linear diversity-dependence on extinction, such that it appears unlikely that any other form of diversity-dependence on extinction would fit the data better.

REFERENCES

[1] D. M. Raup, S. J. Gould, T. J. M. Schopf, and D. S. Simberloff, *Stochastic Models of Phylogeny and the Evolution of Diversity,* The Journal of Geology **81**, 525 (1973).

[2] D. Jablonski, *Biotic Interactions And Macroevolution: Extensions And Mismatches Across Scales And Levels,* Evolution **62**, 715 (2008).

[3] M. G. Weber, C. E. Wagner, R. J. Best, L. J. Harmon, and B. Matthews, *Evolution in a Community Context: On Integrating Ecological Interactions and Macroevolution,* Trends in Ecology & Evolution **32**, 291 (2017).

[4] L. J. Harmon, C. S. Andreazzi, F. Débarre, J. Drury, E. E. Goldberg, A. B. Martins, C. J. Melián, A. Narwani, S. L. Nuismer, M. W. Pennell, S. M. Rudman, O. Seehausen, D. Silvestro, M. Weber, and B. Matthews, *Detecting the Macroevolutionary Signal of Species Interactions,* Journal of Evolutionary Biology , 769 (2019).

[5] C. Darwin, *On the Origin of Species by Means of Natural Selection, or the Preservation of Favoured Races in the Struggle for Life.* (John Murray, London, 1859).

[6] D. L. Rabosky, *Diversity-Dependence, Ecological Speciation, and the Role of Competition in Macroevolution,* Annual Review of Ecology, Evolution, and Systematics **44**, 481 (2013).

[7] J. J. Sepkoski, *A kinetic model of Phanerozoic taxonomic diversity I. Analysis of marine orders,* Paleobiology **4**, 223 (1978).

[8] R. H. MacArthur and E. O. Wilson, *The Theory of Island Biogeography* (Princeton University Press, 1967).

[9] D. Silvestro, A. Antonelli, N. Salamin, and T. B. Quental, *The role of clade competition in the diversification of North American canids,* Proceedings of the National Academy of Sciences **112**, 8684 (2015).

[10] T. H. G. Ezard and A. Purvis, *Environmental changes define ecological limits to species richness and reveal the mode of macroevolutionary competition,* Ecology Letters **19**, 899 (2016).

[11] M. Foote, R. A. Cooper, J. S. Crampton, and P. M. Sadler, *Diversity-dependent evolutionary rates in early Palaeozoic zooplankton,* Proceedings of the Royal Society B: Biological Sciences **285**, 20180122 (2018).

[12] S. Nee, A. O. Mooers, and P. H. Harvey, *Tempo and mode of evolution revealed from molecular phylogenies,* Proceedings of the National Academy of Sciences **89**, 8322 (1992).

[13] D. L. Rabosky and I. J. Lovette, *Density-dependent diversification in North American wood warblers,* Proceedings of the Royal Society B: Biological Sciences **275**, 2363 (2008).

[14] R. S. Etienne, B. Haegeman, T. Stadler, T. Aze, P. N. Pearson, A. Purvis, and A. B. Phillimore, *Diversity-dependence brings molecular phylogenies closer to agreement with the fossil record,* Proceedings of the Royal Society B: Biological Sciences **279**, 1300 (2012).

[15] J. T. Weir and S. Mursleen, *Diversity-Dependent Cladogenesis and Trait Evolution in the Adaptive Radiation of the Auks (aves: Alcidae),* Evolution **67**, 403 (2013).

[16] B. A. Maurer, *Diversity-Dependent Species Dynamics: Incorporating the Effects of Population-Level Processes on Species Dynamics,* Paleobiology **15**, 133 (1989).

[17] A. Brayard, G. Escarguel, H. Bucher, C. Monnet, T. Brühwiler, N. Goudemand, T. Galfetti, and J. Guex, *Good Genes and Good Luck: Ammonoid Diversity and the End-Permian Mass Extinction,* Science **325**, 1118 (2009).

[18] F. L. Condamine, J. Rolland, and H. Morlon, *Assessing the causes of diversification slowdowns: Temperature-dependent and diversity-dependent models receive equivalent support,* Ecology Letters **22**, 1900 (2019).

[19] D. Moen and H. Morlon, *Why does diversification slow down?* Trends in Ecology & Evolution **29**, 190 (2014).

[20] T. Kubo and Y. Iwasa, *Inferring the Rates of Branching and Extinction from Molecular Phylogenies,* Evolution **49**, 694 (1995).

[21] S. Louca and M. W. Pennell, *Extant timetrees are consistent with a myriad of diversification histories,* Nature **580**, 502 (2020).

[22] T. Pannetier, C. Martinez, L. Bunnefeld, and R. S. Etienne, *Branching patterns in phylogenies cannot distinguish diversity-dependent diversification from time-dependent diversification,* Evolution **75**, 25 (2021).

[23] K. P. Burnham and D. R. Anderson, *Model Selection and Multimodel Inference: A Practical Information-Theoretic Approach*, 2nd ed. (Springer-Verlag, New York, 2002).

[24] H. Morlon, F. Hartig, and S. Robin, *Prior hypotheses or regularization allow inference of diversification histories from extant timetrees,* bioRxiv , doi:10.1101/2020.07.03.185074 (2020).

[25] M. Pontarp, J. Ripa, and P. Lundberg, *On the origin of phylogenetic structure in competitive metacommunities,* Evolutionary Ecology Research **14**, 269 (2012).

[26] U. Dieckmann and R. Law, *The dynamical theory of coevolution: A derivation from stochastic ecological processes,* Journal of Mathematical Biology **34**, 579 (1996).

[27] S. Geritz, É. Kisdi, G. Meszéna, and J. Metz, *Evolutionarily singular strategies and the adaptive growth and branching of the evolutionary tree,* Evolutionary Ecology **12**, 35 (1998).

[28] M. Doebeli, *Adaptive Diversification* (Princeton University Press, 2011).

[29] U. Dieckmann and M. Doebeli, *On the origin of species by sympatric speciation,* Nature **400**, 354 (1999).

[30] M. Doebeli and U. Dieckmann, *Speciation along environmental gradients,* Nature **421**, 259 (2003).

[31] F. Gascuel, R. Ferrière, R. Aguilée, and A. Lambert, *How Ecology and Landscape Dynamics Shape Phylogenetic Trees,* Systematic Biology **64**, 590 (2015).

[32] M. Doebeli and I. Ispolatov, *Diversity and Coevolutionary Dynamics in High-Dimensional Phenotype Spaces,* The American Naturalist **189**, 105 (2017).

[33] R. Aguilée, F. Gascuel, A. Lambert, and R. Ferriere, *Clade diversification dynamics and the biotic and abiotic controls of speciation and extinction rates,* Nature Communications **9**, 3013 (2018).

[34] M. A. McPeek, *The Ecological Dynamics of Clade Diversification and Community Assembly,* The American Naturalist **172**, E270 (2008).

[35] H. Morlon, *Phylogenetic approaches for studying diversification,* Ecology Letters **17**, 508 (2014).

[36] J. Alroy, *Dynamics of origination and extinction in the marine fossil record,* Proceedings of the National Academy of Sciences **105**, 11536 (2008).

[37] T. B. Quental and C. R. Marshall, *How the Red Queen Drives Terrestrial Mammals to Extinction,* Science **341**, 290 (2013).

[38] M. J. Benton, *The Red Queen and the Court Jester: Species Diversity and the Role of Biotic and Abiotic Factors Through Time,* Science **323**, 728 (2009).

[39] L. J. Harmon and S. Harrison, *Species Diversity Is Dynamic and Unbounded at Local and Continental Scales,* The American Naturalist **185**, 584 (2015).

[40] D. L. Rabosky and A. H. Hurlbert, *Species Richness at Continental Scales Is Dominated by Ecological Limits,* The American Naturalist **185**, 572 (2015).

[41] L. Aristide and H. Morlon, *Understanding the effect of competition during evolutionary radiations: An integrated model of phenotypic and species diversification,* Ecology Letters **22**, 2006 (2019).

[42] D. H. Hembry and M. G. Weber, *Ecological Interactions and Macroevolution: A New Field with Old Roots,* Annual Review of Ecology, Evolution, and Systematics **51**, null (2020).

[43] L. Xu, S. Van Doorn, H. Hildenbrandt, and R. S. Etienne, *Inferring the Effect of Species Interactions on Trait Evolution,* Systematic Biology **70**, 463 (2021).

[44] E. B. Rosenblum, B. A. J. Sarver, J. W. Brown, S. Des Roches, K. M. Hardwick, T. D. Hether, J. M. Eastman, M. W. Pennell, and L. J. Harmon, *Goldilocks Meets Santa Rosalia: An Ephemeral Speciation Model Explains Patterns of Diversification Across Time Scales,* Evolutionary Biology **39**, 255 (2012).

[45] D. N. Reznick and R. E. Ricklefs, *Darwin's bridge between microevolution and macroevolution,* Nature **457**, 837 (2009).

[46] T. H. G. Ezard, P. N. Pearson, T. Aze, and A. Purvis, *The meaning of birth and death (in macroevolutionary birth–death models)*, Biology Letters **8**, 139 (2012).

[47] D. L. Rabosky, *Automatic Detection of Key Innovations, Rate Shifts, and Diversity-Dependence on Phylogenetic Trees*, PLOS ONE **9**, e89543 (2014).

4

COMSIE – ISLAND-WIDE DIVERSIFICATION DYNAMICS EMERGING FROM AN INDIVIDUAL-BASED MODEL OF COMPETITION AND IMMIGRATION

Théo Pannetier, A. Brad Duthie, Rampal S. Etienne.

Comme-ci, comme-ça

French saying

ABSTRACT

Diversity-dependent diversification has emerged as a prime hypothesis for interpreting diversity patterns in molecular phylogenies and the fossil record, thereby offering a universal model for how competition at the ecological level may regulate evolution on geological time scales. It is often assumed that diversity-dependence operates in a clade-specific manner, with members of a clade competing exclusively with one another. This assumption is however rarely satisfied. Islands present the ideal ecological setting to explore the consequences of relaxing this assumption, with their finite set of resources and discrete, polyphyletic communities. Here, we use an individual-based evolutionary model with trait-dependent competition to simulate diversification on an island. Evolutionary branching emerges from competition, so that immigrating populations eventually form a community with multiple clades, and the island's niche space is progressively partitioned among the descendant species. We study the phylogenetic structure of the resulting communities for a range of scenarios with varying intensities of competition and immigration. First considering each clade as independent, we assess how breaking the assumption of only intra-clade competition affects the detection of diversity-dependence. Then, assuming interaction between clades, we assess how well the shared nature of diversity-dependence can be recovered. We find that inter-clade competition does not affect one's ability to detect diversity-dependence in single trees, compared to trees of similar size diversifying in isolation. Shared diversity-dependent effects are well recovered in equilibrium communities. Despite the presence of common niche space, at half the equilibrium diversity only mixed support for shared diversity-dependence is found, owing to effectively limited interactions among clades before late stages of diversification of the community.

4.1. INTRODUCTION

CLASSICAL birth-death models of diversity-dependent diversification have almost invariably assumed that diversity-dependence operates on a clade-by-clade basis [1–3]. In such models, the rates of speciation and/or extinction are a function of the number of species alive in the clade (N), such that all members of the clade, but no other species, contribute to, and suffer equally from diversity-dependent effects. That is, niche space is modelled as a property of the clade, rather than the environment, and the carrying capacity operates at the clade level (i.e., is "clade-specific" [4]).

While the assumption of diversity-dependence taking place solely within a clade may be reasonable in some cases (for example, when a lineage accesses a new, exclusive niche space through the evolution of a key innovation, [5]), it is in general incompatible with the observation that competition for resources may just as well involve distantly-related taxa [6, 7], and there is evidence for macroevolutionary outcomes from such interactions (e.g., character displacement, [8]).

A few diversity-dependent models of diversification relaxing this assumption have been considered. As a first example, Silvestro *et al.* [9] introduced a model where the diversity of putatively competing clades contribute to the carrying capacity of each other through Lotka-Volterra-like terms. The strength of each interaction is a parameter of the model and can be inferred from fossil assemblage data. Second, a model including several regimes of diversity-dependence within a single clade has been proposed. In Etienne and Haegeman [5], sub-clades may break away from the niche space of the parent clade, from this point evolving with a separate carrying capacity. Finally, Xu and Etienne [10] considered a model where lineages in a single clade shift back and forth between two habitats, each associated with its own carrying capacity. However, these models are the exception rather than the rule, which may be due to the fact that interactions between clades are typically intricate and difficult to recognise, even in present-day communities. Given the difficulty of accounting for past competition, a first valuable step would be to assess whether existing methods may be helpful in recognising diversity-dependence involving multiple clades, and how they are affected by a violation of the assumption of monophyly of competition.

We consider the scenario where an experimenter seeks to test for diversity-dependence on a clade of interest. Species in this clade present particular adaptations that allow them to exploit a specific set of resources within a limited niche space, and thus present the expected conditions for diversity-dependence to take place, with each new species contributing towards a carrying capacity (*sensu* MacArthur and Wilson [11]) defined by the niche space. Unknown to the experimenter however, other, unsampled clades have entered the same niche space via an equivalent set of adaptations and also contributed to saturation of carrying capacity, and the diversity-dependent effects experienced by the focal clade. In such a scenario, a first natural question would be whether the failure to account for competition originating from external clades would affect detection of diversity-dependence. On the one hand, it could be expected that not including all clades contributing to diversity-dependence could result in a loss of signal. On the other hand, competitive pressures from unsampled species would lead to a faster build-up of competitive effects, resulting in intensified diversity-dependence and a stronger signal than if the

clade was diversifying on its own.

We remark that the scenario described above also applies well to diversification on islands, the niche space then being defined by the island area and the set of resources available on it, while the acquisition of adaptations that allow entering the niche space are equivalent to immigration events. In an island setting, the limited and discrete area makes the assumption of a single niche space shared by the entire community (i.e, a carrying capacity, *sensu* MacArthur and Wilson [11]) reasonable. Indeed, islands have been used extensively to study the macroevolutionary consequences of ecological interactions [12]. As such, methods developed for analysis of island communities may constitute valuable tools for the study of diversity-dependence involving multiple clades.

The analysis of diversification of island communities is precisely the focus of the DAISIE (Dynamic Assembly of Island biota through Speciation Immigration and Extinction, Valente *et al.* [13]) modelling framework. DAISIE extends the classical island biogeography model of MacArthur and Wilson [11] with a macroevolutionary component, accounting for phylogenetic relations between species on the island, and thus the contribution of speciation (in addition to immigration and extinction) to diversity. The likelihood for the model is known [13] and has been used to test for hypothesized scenarios of diversification on the island, including diversity-dependence [13, 14].

However, DAISIE normally assumes diversity-dependence operates separately for each clade on the island; that is, diversity dependence is clade-specific (hereafter, CS). Island species descended from a single immigrant contribute to saturation independently for every clade, although the value of the carrying capacity is the same for every clade. In other words, each clade exploits an exclusive section of the set of resources available and competition between clades is assumed to play a limited role in the community. It has not been described how departures from this model of diversity-dependence operating separately for every clade, such as the scenario described above, affect inference of diversity-dependence or other aspects of the model, such as estimates of the rates of immigration, speciation and extinction. Yet, this may be relevant to many island systems where total area is small, or the distribution of resources is homogeneous. The model has recently been extended [4] to model a scenario where a single carrying capacity is defined for the whole island, and all clades contribute to it. That is, diversity-dependence is island-wide (IW), and its effects are shared among all clades.

This version of the model is appropriate to describe diversification in the scenario we described above, and it would thus be interesting to assess whether a comparison of both versions of DAISIE could correctly identify the shared regime of diversity-dependence; that is, if the IW version model would be preferred over the CS one. Using island community data directly simulated with the IW model, Etienne *et al.* [4] found that the generating model (IW) could be identified with a power of 72% when accepting a 5% error rate. However, no detailed analysis has been done where the inference model is not identical to the generating model, which is obviously always the case in reality.

To explore this further, here we extend a Lotka-Volterra individual-based model of trait evolution under competition [15] to consider the case of multiple clades diversifying in sympatry in a common niche space, i.e., an island in the ecological sense. By introducing immigration, we allow populations unrelated to one another to enter the shared niche space and diversify, eventually forming a polyphyletic assemblage of clades

that potentially all interact with one another. We track the growth of the community and the sequence of speciation and extinction events from the initial colonisation of the island until the saturation of the community, and build phylogenies for each clade in the simulated communities.

We then use the simulated phylogenies to answer three lines of question. First, can diversity-dependence be detected when considering each clade separately (with the R package DDD, Diversity-Dependent Diversification, [2]), ignoring the presence and contribution to diversity of other clades in the same community? Second, when accounting for the whole community as the product of a common diversification process (i.e., with DAISIE), can the shared, island-wide nature of diversity-dependence be recognised? Third, what biases are introduced when acknowledging the community as the product of a common diversification process but failing to account for a single regime of diversity-dependence? That is, what are the consequences for modelling diversity-dependence as clade-specific when the generating process is closer to an island-wide process?

4.2. METHODS

4.2.1. GENERAL APPROACH

We analyse the form of diversity-dependence observed in our simulated multi-clade island communities in two ways. First, we use the single-tree diversity-dependent model from Etienne *et al.* [2] to assess whether diversity-dependence is recovered from single clades, mimicking a scenario where an experimenter is unaware of external clades and their contribution to competitive pressures on the clade of focus. Second, using DAISIE, we test whether the island-wide nature of diversity-dependence (hereafter, IW) is correctly detected, or whether a scenario with clade-specific diversity-dependence (hereafter, CS) is instead supported more strongly.

We also examine the resulting maximum likelihood estimates for the DAISIE and DDD model parameters, with an emphasis on the equilibrium diversity parameter K. In the IW setting of DAISIE, K (hereafter, K_{IW}) is defined at the level of the island, such that species from all clades contribute to it. In the CS case, DAISIE assumes K (hereafter, K_{CS}) to be defined for every clade, but with an identical value across all clades. We assess whether each of K_{IW}, the product of K_{CS} and the number of clades, or the sum of K_{DDD} (equilibrium diversity parameter for the diversity-dependent model) across all clades in a community accurately approximates the (known) equilibrium diversity of the community.

We repeat the analyses across communities simulated with a range of equilibrium diversity values (predicted based on the parameters of the individual-based model) and rates of immigration. In each case, we repeat the analyses both for communities that have reached equilibrium diversity, and the same communities at a time where diversity has only reached half the equilibrium value.

4.2.2. INDIVIDUAL-BASED MODEL

We simulated the assemblage and evolution of island communities using a modification of the individual-based model in Pannetier *et al.* [15], which implements a classic form

of competitive interactions, where the fitness of every individual is proportional to the abundance of the value of the resource it exploits, and is penalised by a function of the density of competitors exploiting a similar resource value. Models of this form have been used widely in ecology, including for modelling the evolution of communities [16], and notably have served as the basis for the deterministic models used in adaptive dynamics [17, 18]. We summarise the model below, but refer the reader to Pannetier *et al.* [15] for more details.

1. **Reproduction** is asexual, and generations are discrete and non-overlapping. Every generation, all individuals in the community produce a number of offspring sampled from a Poisson distribution, with mean parameter $W(z)$, the fitness of the individual with trait value z. Offspring inherit the phenotype z of their parent, modified by a random mutation sampled from a normal distribution with mean 0 and a standard deviation of 0.001.

2. The **fitness function** W_z is defined as
   $W_z = e^{r\left(1-\frac{A(z)}{K(z)}\right)}$, where

3. $K(z)$ is the Gaussian **resource distribution function**, defined as
   $K(z) = K_{opt} e^{-\frac{(z-z_{opt})^2}{2\sigma_K^2}}$, with K_{opt}, z_{opt} and σ_K the height, mean and standard deviation parameters of the Gaussian function, respectively. Here, we set $K_{opt} = 1000$, $z_{opt} = 0$ and $\sigma_K = 3$.

4. $A(z)$ is the Gaussian **competition function**, defined as
   $A(z) = \sum_{i=1}^{N} \alpha(z, z_i)$, and
   $\alpha(z, z_i) = e^{-\frac{(z-z_i)^2}{2\sigma_\alpha^2}}$, where σ_α is the standard deviation parameter of the Gaussian (its height is 1).
   We consider an array of values for σ_α, which we use as a parameter of the IBM as a whole (see section 4.2.3).

5. **Speciation and extinction**: individuals each bear a species label, inherited from the mainland immigrant and passed down to all descendants, until speciation takes place. Species labels are only used to keep track of ancestry and build phylogenies, and play no role in the ecological components of the simulation. That is, all individuals with the same trait value z contribute and suffer equally from competition regardless of the species to which they belong. Diversity-dependence is thus not assumed, but can only be an emergent property.

   Branching occurs as a result of divergent selection. When a fitness optimum is reached, local density-dependence pushes a (so far monomorphic) population to split into two clusters of individuals, a well-known feature of this class of models [16, 18]. These new populations repel one another and progressively diverge. When they diverge by more than an arbitrary threshold $\theta_z = 0.1$, cladogenetic speciation happens. Unlike in Pannetier *et al.* [15], where only one of the two resulting branches was assigned to become a new species, here we assign **both** diverging populations to new species, to be consistent with how cladogenesis is modelled in

DAISIE [13]. Extinction simply happens when the last individual of a species dies without producing any offspring.

In order to create a polyphyletic community, we introduced immigration from an external, static mainland community consisting of a pool of 1000 species. Each mainland species was assigned a range of trait values defined by a Gaussian distribution representing within-species variation, with a fixed standard deviation $\sigma_z = 0.01$. The mean value of the distribution was sampled separately for each mainland species from a uniform distribution delimited by the minimum and maximum values of z that could support at least 5 individuals (that is, z and $-z$ such that $K(z) \geq 5$).

Throughout the simulation, immigration events were sampled from a geometric distribution with probability Γ, the immigration rate. At every immigration event, a single individual was sampled from the pool of mainland species, with its trait value sampled in the distribution of that species, and added to the island community. The island community was initialised with an immigration event of 10 individuals from the same species, with the same trait value, sampled as described above.

To be consistent with the set of events considered in DAISIE, we allowed island populations to undergo anagenetic speciation (i.e., formation of a new species through branching), in addition to the cladogenetic speciation described above. Anagenesis happened when the mean trait value of an island population differed from that of its mainland ancestor population by more than $\theta_z = 0.1$, upon which the island population was considered to have diverged enough from its mainland relative to be assigned to a new species. If the trait value would later become more similar to the mainland population again, the species is still assumed to be different, as it is expected to have evolved in other aspects, or that the difference in trait value has led to irreversible reproductive isolation.

We defined clades as the set of species that descended from a unique species on the mainland, including sub-clades that descended from successive immigrating populations of the same species from the mainland. The mainland species itself was included in the clade only if it was present in the island community at the end of the simulation, that is, if it had immigrated on the island and not undergone speciation.

4.2.3. SIMULATIONS

We simulated island communities with a range of predicted equilibrium diversities,

$$\hat{K} \in \{20, 30, 50, 80, 100\}$$

using the equation from Pannetier *et al.* [15]

$$\hat{K} = 0.056\,\sigma_\alpha^{-1.4} + (5.5\,\sigma_\alpha^{-0.89} - 4.1\,\sigma_\alpha^{-0.5})\,\sigma_K,$$

where parameter σ_α defines the width of the competition kernel $\alpha(z_i, z_j)$, and thus sets the intensity of competition, and parameter σ_K sets the width of the resource distribution function $K(z)$ (see Section 4.2.2). Higher values of σ_K contribute to increase the size of the community, while higher values of σ_α reduce it. We set σ_K to 3 and solved for the value of σ_α that would predict the desired value of $\hat{K}$ to the third decimal. We obtained the following values:

$$\sigma_\alpha \in \{0.369, 0.267, 0.172, 0.112, 0.091\}$$

To explore the effect of the immigration intensity and the importance of priority on the assembly of the island community, we considered increasing rates of immigration:

$$\Gamma \in \{1.1^{-4}, 5.10^{-4}, 1.10^{-3}, 1.10^{-2}\}.$$

In addition, we also ran a set of simulations with $\Gamma = 0$, where immigration thus happened only once (the initial population), to serve as a single-clade basis for comparison. The number of simulations was set to give enough time to communities to reach $\hat{K}$, based on growth of communities observed in Pannetier *et al.* [15], the number of generations ranging from 110,000 generations for $\sigma_\alpha = 0.091$ to 350,000 for $\sigma_\alpha = 0.369$.

We simulated 100 replicate communities for each of the resulting 25 combinations of σ_α and Γ. Because saving all states of the entire community was computationally unfeasible, throughout the simulations, we sampled 5% of all individuals in the community every 200 generations. To guarantee that all species present in the community at this time would be represented in the sample, we enforced that every species would be represented by at least 1 individual in the otherwise random sample.

We repeat all downstream analyses (next sections) on both communities at equilibrium, and half-equilibrium diversity, which we denote by $f = 1$ and $f = 0.5$, respectively. To obtain half-equilibrium ($f = 0.5$) diversity communities, we simply trimmed the final communities to the first time the community reached half the equilibrium diversity. For each replicate community (both at equilibrium and half-equilibrium diversity), we built the phylogenies (which may have consisted of just a single lineage, represented at a single sampling time) that descended from each immigrant sampled in the output.

4.2.4. DETECTING DIVERSITY-DEPENDENCE ON SINGLE TREES

We used the R package DDD version 5.0 [2] to fit a diversity dependent model of diversification to each tree in the simulated communities that contained at least four species at the end of simulations, using maximum likelihood. In this way we sought to explore how diversity dependence is recovered when diversity dependence is erroneously assumed to operate exclusively within a clade, such that each tree is treated as having undergone an independent evolutionary process.

DDD offers options to model multiple forms of diversity-dependence, for example as a linear or exponential function, both for speciation and extinction. Both for computational tractability, and because we are not interested in comparing between different forms of diversity dependence, we only considered linear diversity dependence in speciation and constant-rate extinction,

$$\lambda = \lambda_0\left(1 - \frac{N}{K}\right)$$

$$\mu = \mu_0$$

Along with the diversity-dependent model above, we also fitted (still using DDD) a constant-rate diversification model to each tree, with

$$\lambda = \lambda_0$$

$$\mu = \mu_0$$

The diversity-dependent model then contains three parameters, λ_0, the initial (cladogenetic) speciation rate when $N = 0$, μ_0, the rate of extinction and K (hereafter, K_{DDD}) the equilibrium diversity. We obtained the maximum likelihood for the two models and computed their likelihood ratio.

As described in Pannetier *et al.* [15] (and [19]), the appropriate test for diversity-dependence requires performing a bootstrap likelihood ratio test, involving running simulations under both models with the parameter values estimated from the tree to obtain the two distributions of the likelihood ratio under the hypotheses of presence or absence of diversity-dependence. This should be repeated for each tested tree within each replicate communities, requiring a computational time that we could not afford. While we cannot obtain a decision criterion and decisively test for diversity-dependence, the likelihood ratio nevertheless remains an indicator of strength of the signal of diversity-dependence. Arguably, clades showing a clearer signal for diversity-dependence should return a likelihood ratio with a higher (more positive) value. Thus, we compare the likelihood ratios obtained in the multiple clade case ($\Gamma > 0$) against the single clade case ($\Gamma = 0$). For this analysis, we only considered a single value of the competition kernel width $\sigma_\alpha = 0.091$, corresponding to an equilibrium diversity of about $\hat{K} = 100$ species, as for smaller communities a large proportion of the single trees tended to be too small to meaningfully fit DDD under high-immigration settings.

4.2.5. FITTING DAISIE

We fitted the DAISIE model (using the package of the same name, version 4.0.5) to the output communities to examine whether island-wide or clade-specific diversity-dependence would be inferred. Contrary to DDD, the DAISIE framework takes as input a set of phylogenies comprising all lineages currently alive on the island (phylogenies may contain a single lineage), information on the time of immigration of their ancestor (colonisation time), and endemicity status, that is, whether island populations have conspecific populations on the mainland or not. DAISIE accounts for both cladogenetic speciation (i.e, branching), which happens at rate λ^c, and anagenetic speciation, which happens at rate λ^a, whereby a non-endemic island population diverges enough from its mainland relatives to be recognised as a different species.

We fitted two versions of the DAISIE model, clade-specific (CS) and island-wide (IW), to the same sets of phylogenies produced by simulations. The two versions of DAISIE differ only in whether the variable N corresponds to the number of species in a clade (CS) or in the entire community (IW) and whether the carrying capacity K was defined at the clade (CS) or island (IW) level. As with DDD, we assumed a linear diversity-dependence on (cladogenetic) speciation and constant-rate extinction, and assumed constant-rate anagenesis:

$$\lambda^c = \lambda_0^c\left(1 - \frac{N}{K}\right)$$
$$\mu = \mu_0$$
$$\lambda^a = \lambda_0^a$$

DAISIE also allows the (per-species) immigration rate to be diversity-dependent,

$$\gamma = \gamma_0\left(1 - \frac{N}{K}\right),$$

or constant. We assumed diversity-dependence in the immigration rate, because, while immigration in the IBM was modelled with a constant factor (Γ), most of the immigration events in later stages of the simulation are expected to be unsuccessful due to species interactions, and hence unlikely to be recorded in the output. Note that the carrying capacity K parameter in γ is the same as the one used for the speciation rate λ_0^c, computed at either the clade (CS) or island (IW) level. Each version of the model thus comprises five parameters: λ_0^c and γ_0, respectively the initial cladogenesis and initial immigration rates when $N = 0$, μ_0, the rate of extinction, λ_0^a, the rate of anagenesis, and K_{IW} or K_{CS}. We obtained the maximum likelihood for each of the two models (and associated estimates of the parameters) and computed their likelihood ratio. The integration of the likelihood of DAISIE, and *a fortiori* its optimisation are computationally demanding, particularly for the IW version of the model, and this severely limited our ability to cover the breadth of the parameter space. As a result, we limited the analysis to the smallest and largest communities (that is, simulated with $\sigma_\alpha = 0.369$ and $\sigma_\alpha = 0.091$), and two values of the immigration rate, $\Gamma = 0.0001$ and $\Gamma = 0.001$.

4.3. RESULTS

4.3.1. GENERAL STRUCTURE OF SIMULATED COMMUNITIES

We first describe the general structure of the communities observed in simulations, as these may help the interpretation of downstream results. By the end of the simulation, the total number of species in the community was not growing substantially (Fig. 4.3), and we interpret this as communities being near, or at equilibrium diversity. We note that this equilibrium diversity then approaches, but always differs from the value predicted ($\hat{K}$) with the equation reported in section 4.2.3 (Fig. 4.2A). N exceeds $\hat{K}$ for all but the smallest value of σ_α (largest communities), where communities are instead smaller at equilibrium than predicted (Fig. 4.2A). These discrepancies between the predicted and observed value appear to be due to inaccuracy of our predicting function $\hat{K}$, rather than an effect of the introduction of immigration and the presence of multiple clades, which was absent from the model in Pannetier *et al.* [15]. Indeed, discrepancies persist even in settings with $\Gamma = 0$ (Fig. 4.2A), where the diversification process should thus be strictly equivalent to the model considered in Pannetier *et al.* [15]. In the next sections, we thus use the average community size at present as a proxy for equilibrium diversity. We use this value, instead of $\hat{K}$, as a reference point to extract half-equilibrium communities (see Methods) and compare it to the equilibrium diversity estimated with parameter K of the birth-death models.

The simulated island communities are largely shaped by incumbency and priority effects. The partitioning of trait space among clades and, consequently, the number and size of clades in the community are established early (Fig. 4.1). Early immigrants almost always establish successfully on the island, and the probability of successful colonisation of the island quickly drops with time (Fig. 4.5) as trait space progressively fills with clades

descended from previous immigrants (Fig. 4.1). Immigrant populations landing in an occupied section of trait space are unlikely to establish due to competitive exclusion from resident populations (Fig. 4.5). Eviction of a resident clade by an immigrant is rare, but contrary to our expectations, it does occur in simulations with high immigration (Fig. 4.1, see for example the purple- and ochre-coloured clades replacing the maroon-coloured clade near $z = -1$ in panel E, and the pink-coloured clade around $z = -0.5$ in panel O). This outcome is quite exceptional because for the vast majority of immigration events, resident populations prevent immigrant populations from establishing on the island (Fig. 4.5).

Following colonisation of the island, clades that descend from early colonist populations expand in trait space, branching and growing along the way, until reaching either the limit of viable trait space (that is, z such that $K(z) \approx 1$) or a section of trait space already occupied by another clade (Fig. 4.1), halting the clade's expansion in both cases (Fig. 4.4). From this point on, the range of trait space occupied by each clade changes only little, and slowly (Fig. 4.1). Yet, it was not as static as expected, as clades either expanded at the expense of their neighbours, or shrunk to the benefit of their neighbour (Fig. 4.1, Fig. 4.4). No apparent growth pattern is observable in this phase, and clade size appears to change in a random direction as a result of all individuals having the same competitive ability. Clades do not overlap in trait space, except on the edges of their ranges for communities with a small σ_α (Fig. 4.1), and only transiently; hence trait space is at any time clearly partitioned between the clades in the community (Fig. 4.1). As a result of these incumbency effects on colonisation and inertia in clade growth, the cladistic assemblage of the community and distribution of the number of species between clades establishes early, and tends to change little past the initial phase of filling of niche space (Fig. 4.4). Notably, the largest clades often descend from the earliest colonists (Fig. 4.4), having benefited from a longer phase of unbounded growth before their diversification is limited by neighbouring clades.

With these dynamics in mind, it is easy to interpret the effect of the individual-based model parameters, Γ (immigration rate) and σ_α (width of the competition kernel). By reducing the time between successive immigration events, increasing the immigration rate reduces the incumbency advantage of the first immigrant clades, and leads to an earlier saturation of niche space. The immigration rate thus largely controls the degree of partitioning of total niche space. Communities simulated with low values of Γ tend to be dominated by only a few, large clades, while communities simulated with high values of Γ comprise more, smaller clades, with a tendency for a more even distribution of species diversity between clades. Interestingly, more frequent immigration does appear to increase species diversity on the island, although this effect is very small (and is hardly visible in Fig. 4.2A).

Higher values of σ_α increase the intensity of competition, pushing neighbouring species further away from one another in trait space. In addition to reducing the size of communities at equilibrium, an interesting consequence of this effect was that communities simulated with larger competition width tend to comprise a larger proportion of single-species clades, or singletons, particularly when immigration is high. Such singletons may be important for the inference made with DAISIE. Indeed, because DAISIE assumes that cladogenesis always results in island-endemic species, only singleton clades

are susceptible to be present on both the mainland and the island, and to undergo anagenetic speciation (see Methods).

The same dynamics and influence of parameters holds true for half-equilibrium communities. As diversity initially grows quickly within communities, half-equilibrium diversity is reached early in the simulations, such that the phylogenetic branches are not as long relative to time as for equilibrium communities. The exception concerns singletons, which are already found in communities simulated with high σ_α, and otherwise rare in communities with a low value of σ_α. By definition, trait space is half empty in these communities, such that at this stage many clades are still expanding in trait space in one or both edges. Although some have already come in contact with competing clades some time in the past, for most clades, the timing of half-equilibrium diversity appears to correspond to a stage where contact has not yet occurred, or only recently.

4.3.2. SUPPORT FOR DIVERSITY-DEPENDENCE IN SINGLE TREES

For equilibrium communities (Fig. 4.6, $f = 1$), log-likelihood ratios suggest that the phylogenies of island clades carry a strong signal of diversity-dependent diversification. Log-likelihood ratio scores were high overall for most trees, suggesting support for the diversity-dependent model over the constant-rate model (Fig. 4.6). It is not possible here to establish what score would motivate selection of the diversity-dependent model (even when using the selection criteria of the likelihood ratio test or, equivalently, the AIC), because direct comparison of likelihoods of diversity-dependent models against diversity-independent models is biased in favour of diversity-dependence [19], even when both models predict the same expected pattern of diversification [20]. Determining a decision threshold would require simulating the distribution of likelihood ratios under both models, a computationally demanding endeavour we could not afford here. Instead, we use the threshold value found by Etienne *et al.* [19] for the *Setophaga* warbler phylogeny as a (cautious) basis for comparison. Etienne *et al.* [19] found a log-likelihood ratio above about 5 to be strong evidence for diversity-dependence, comparing the fit of the same two models we used in the present study (linear diversity-dependence on speciation and constant-rate diversification) on diversity-dependent phylogenies simulated with $K = 25$. The distribution of the log-likelihood ratio for trees of comparable size (25 species) in our simulations resembled that of trees simulated with diversity-dependence (Fig. 4.7 and Fig. 3 in Etienne *et al.* [19]), and the score almost always exceeded 10, suggesting that diversity-dependence would be recovered with confidence.

Regardless of the appropriate threshold value, more positive log-likelihood ratio scores indicate stronger support for diversity-dependence. Trees from simulations with higher immigration rates clearly show weaker log-likelihood scores, suggesting that immigration, and thus, the presence of multiple clades in the same niche space, erodes the signal of diversity-dependence in single trees. Yet, tree size appears to play a large role in log-likelihood ratio scores (Fig. 4.7), such that a higher immigration weakens the signal only through further subdivision of the niche space among more clades (Fig. 4.4), making diversity-dependence more difficult to detect when considering single (smaller) trees. When considering trees of similar size, the distribution of log-likelihood ratio scores does not differ much across values of Γ (Fig. 4.7). Thus, higher immigration makes

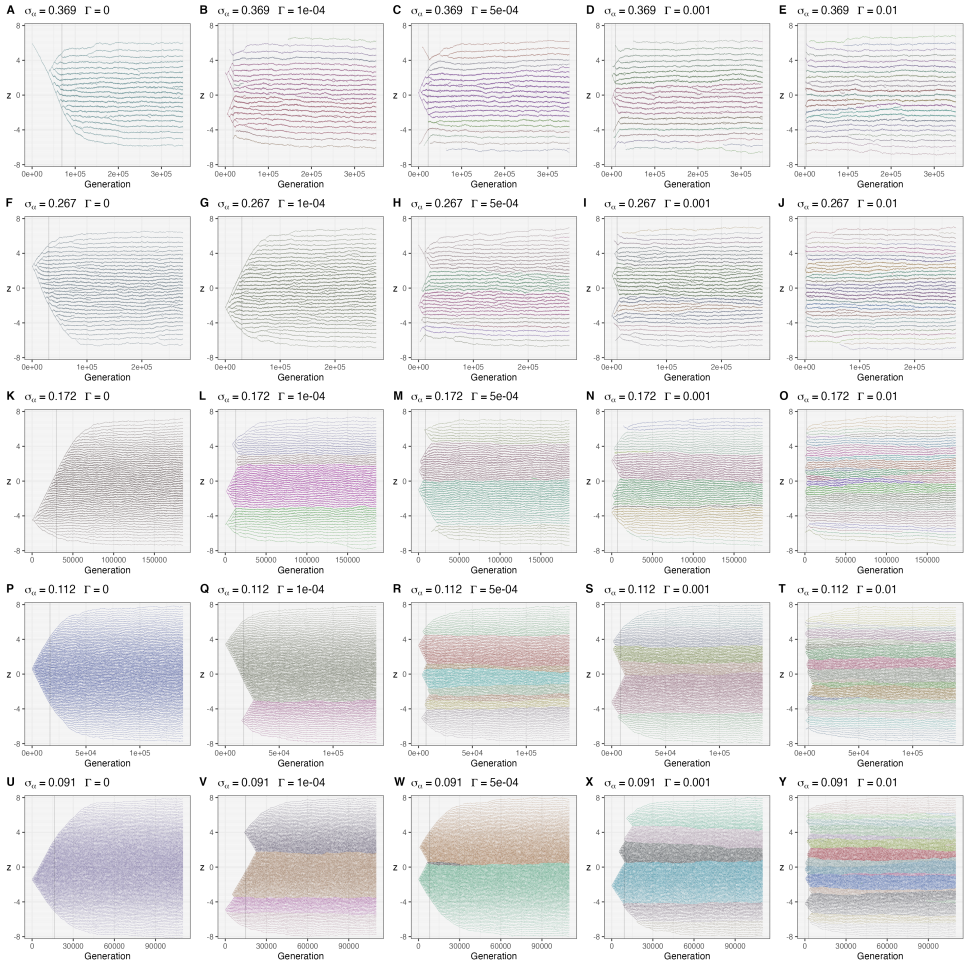

Figure 4.1 | Examples of communities generated by the individual-based model. One replicate community (out of 100) is shown for each combination of the two parameters of the IBM. Branches are coloured by clade (not by species), each descended from a single mainland species. Grey vertical lines indicate the point in time where the number of species reaches half the equilibrium diversity.

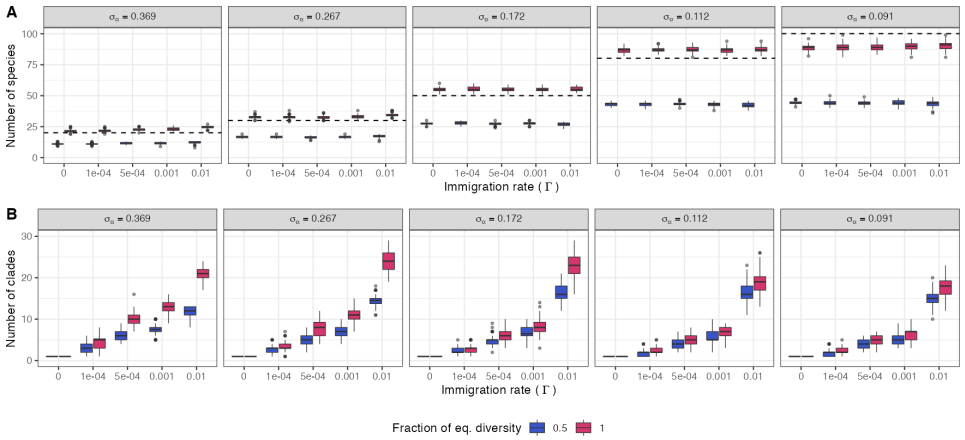

Figure 4.2 | Distribution of the number of species (A) and the number of clades (B) in each replicate community, for equilibrium ($f = 1$) and half-equilibrium ($f = 0.5$) communities. The dashed horizontal line denotes the predicted equilibrium diversity, $\hat{K}$ (see methods).

diversity-dependence more difficult to detect, when considering clades separately, by reducing the size of individual clades. Irrespective of the intensity of immigration, for large enough trees (e.g., 15 to 20 tips), log-likelihood ratios scores remain high, and we expect that diversity-dependence would still be recovered from single trees. High log-likelihood ratio scores for equilibrium communities are consistent with the strong pattern of diversification slowdown observed in the corresponding species-through-time plots (Fig. 4.4 and Fig. 4.3). As described in the previous section, most clades initially grow quickly, before reaching approximately stationary diversity early in the simulation (Fig. 4.4). This results in trees with a tendency for branches to be shorter close to the root of the tree, a pattern typical of diversity-dependent trees [5, 20] and otherwise very unlikely to be generated under constant-rate diversification.

Support for diversity-dependence is, as expected, much weaker for half-equilibrium communities (Fig. 4.6, $f = 0.5$). Except for the zero-immigration reference case (top row in Fig. 4.6), for almost all trees, log-likelihood ratio scores remain below 10, with a median score close to ($\Gamma = 0.0001$) or below 5 (all other values of Γ), falling around the grey area where stronger support for diversity-dependence may be explained by a bias alone. While the scores do suggest that diversity-dependence would be selected over the constant-rate model, the absence of a clear decision threshold implies that this is not conclusive. A higher rate of immigration does erode the signal for diversity-dependence in half-equilibrium communities too, yet here again this appears to be largely explained by tree size (Fig. 4.7). Plotting log-likelihood ratio against tree size confirms that weaker scores in half-equilibrium communities are not explained by the smaller size of trees compared to the equilibrium diversity case (Fig. 4.7). Instead, the growth curves of trees from half-equilibrium communities display a weaker pattern of slowdown of diversification, and are thus more consistent with constant-rate diversification than in the equilibrium case (Fig. 4.4).

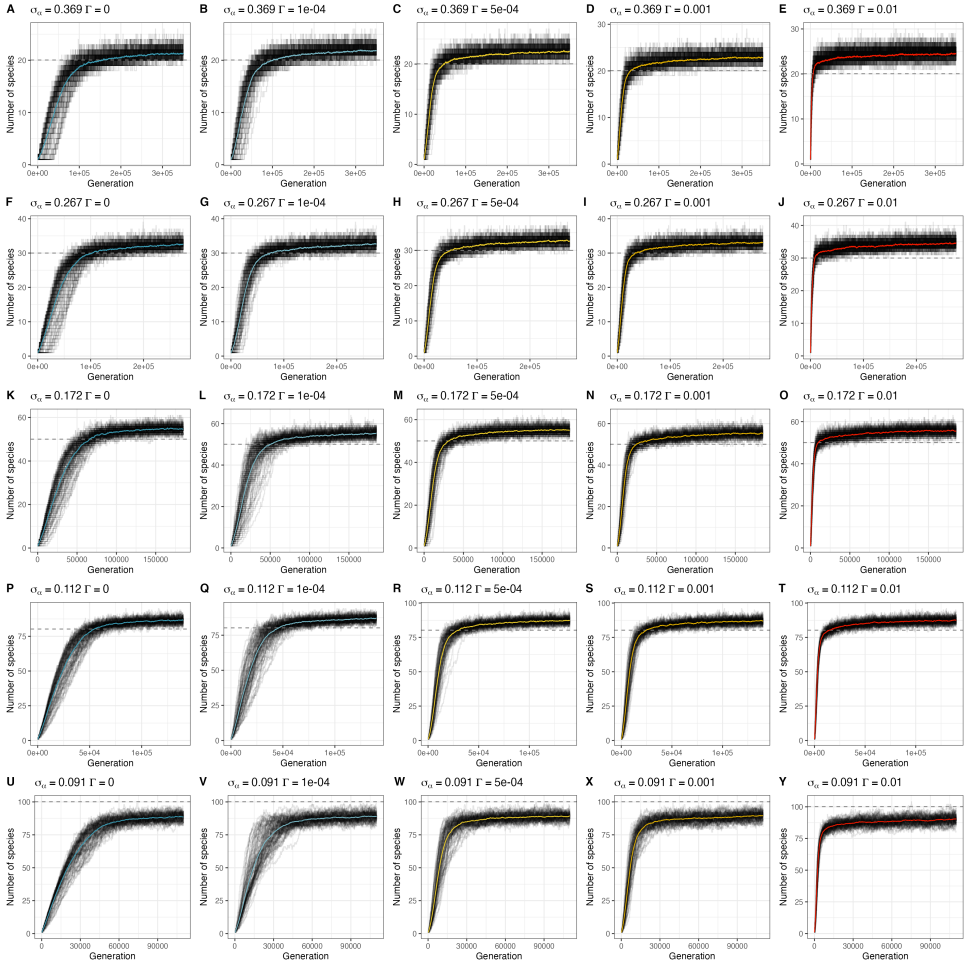

Figure 4.3 | Number of species in island communities over time. Black lines each represent a single replicate, and the coloured line is the average number of species over 100 replicates. The horizontal dashed bar denotes the predicted equilibrium diversity, $\hat{K}$, given $\sigma_K = 3$ and σ_α.

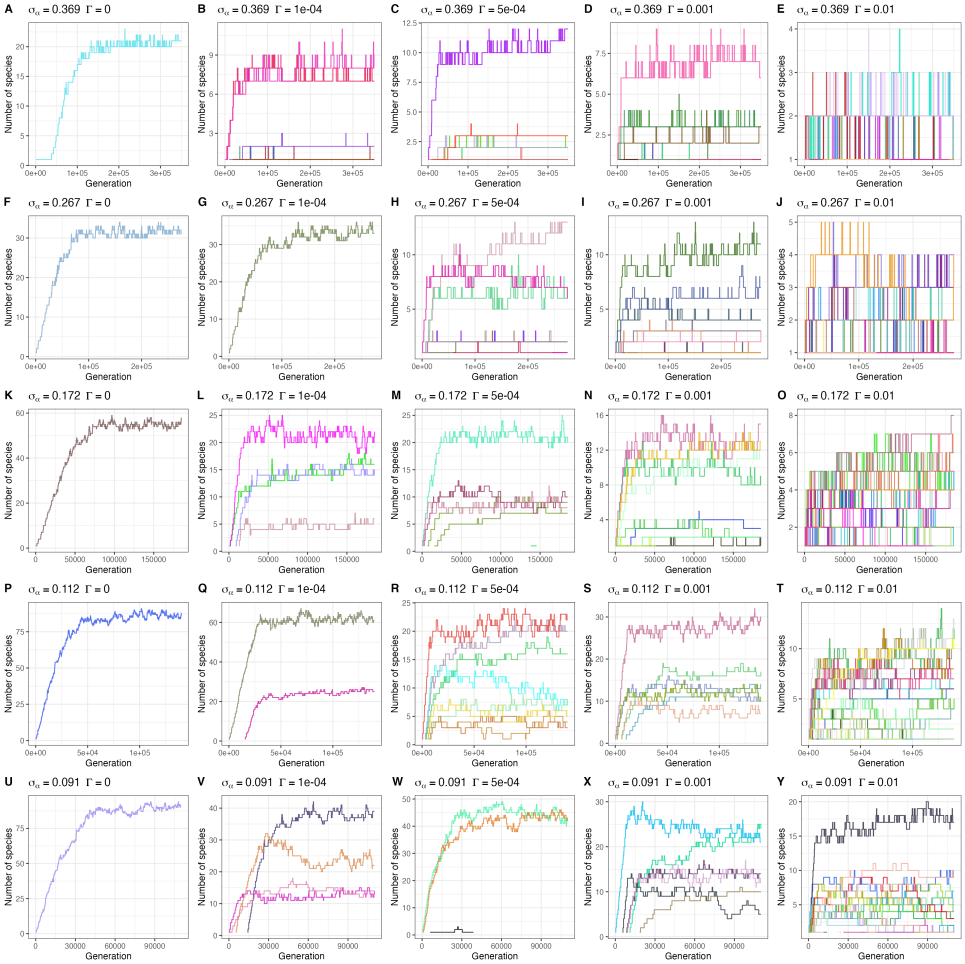

Figure 4.4 | Number of species in each clade for some example island communities. Each coloured line represents the number of species in a single clade. The communities shown as example are the same as in Fig. 4.1.

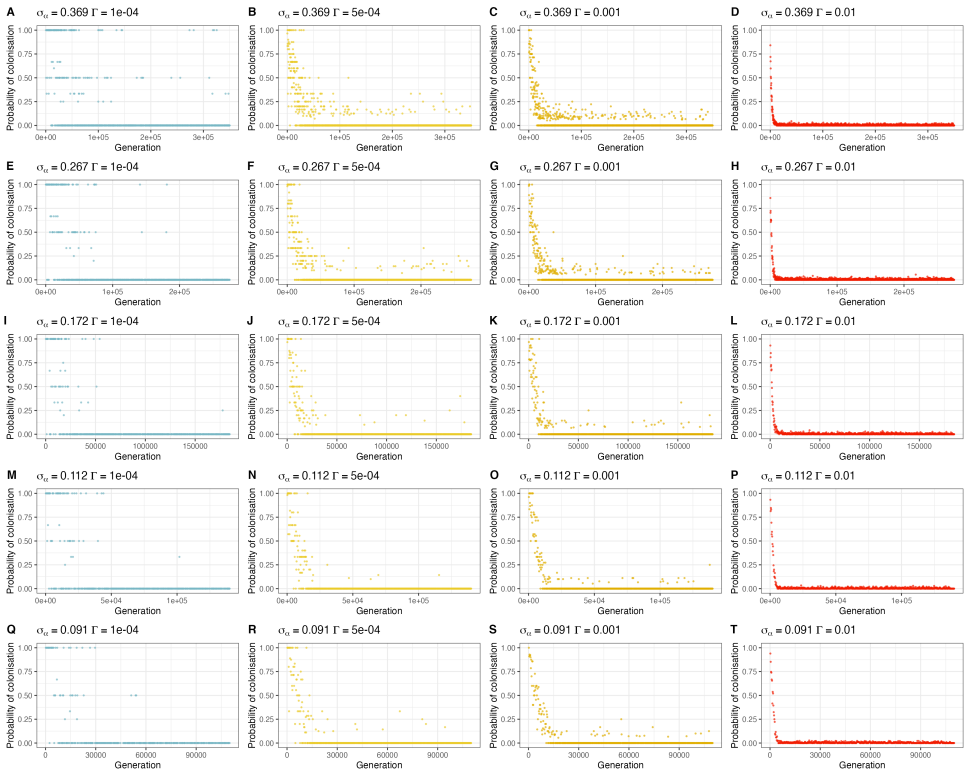

Figure 4.5 | Probabilities for an immigration event to result in successful colonisation of the island. Colonisation was considered successful if any descendant of the immigrant population was still present in the community 2,000 generations after the immigration event.

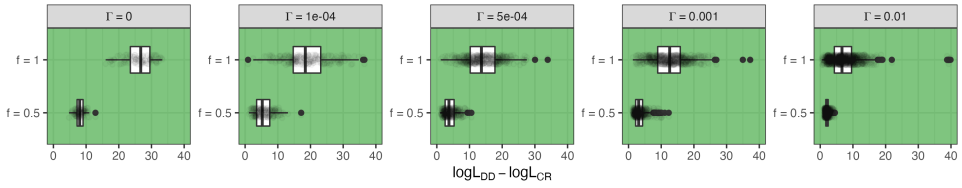

Figure 4.6 | Distribution of the log-likelihood ratio of the diversity-dependent (DD) model against constant-rate (CR) diversification, computed separately for the trees of each clade and across the 100 replicate communities. Positive scores denote stronger support for DD. All communities included in this plot were simulated with $\sigma_\alpha = 0.091$.

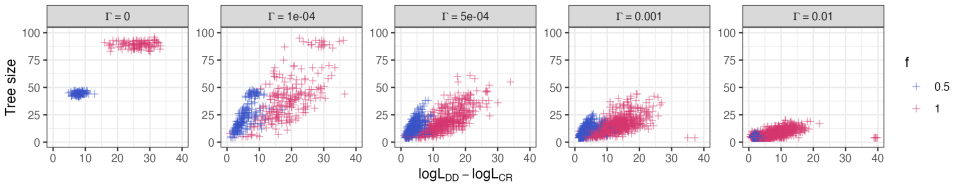

Figure 4.7 | Distribution of the log-likelihood ratio of the diversity-dependent (DD) model against constant-rate (CR) diversification computed separately for each tree and shown against the size of the corresponding tree at present.

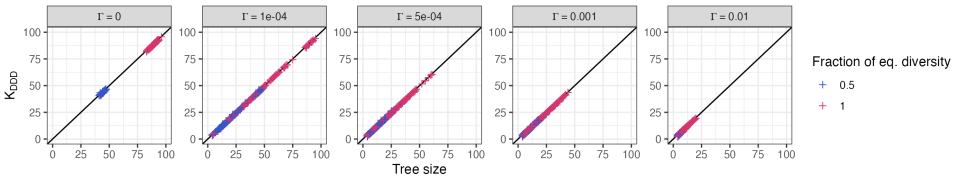

Figure 4.8 | Maximum likelihood estimates of DDD parameter K, for all trees in communities simulated with $\sigma_\alpha = 0.091$, plotted against tree size.

4.3.3. ESTIMATES OF THE EQUILIBRIUM DIVERSITY FROM SINGLE TREES

For all trees containing at least 4 species, maximum likelihood analysis from DDD always estimated K_{DDD} to be near the size of the tree at present (Fig. 4.8), both for equilibrium ($f = 1$) and half-equilibrium ($f = 0.5$) communities, implying that these trees have reached equilibrium diversity.

Because the individual-based model does not define an equilibrium diversity at the clade level, interpreting a K_{DDD} value as an intrinsic limit to the growth of the corresponding clade is bound to lead to a misunderstanding of the diversification dynamics. Yet, in the case of equilibrium communities, the inferred values of K_{DDD} correctly suggest that clade diversity has reached an equilibrium value, a conclusion that is consistent with the roughly static diversity of the these trees (Fig. 4.4). Incidentally, summing estimates of K_{DDD} across all clades in the community would yield a correct approximation of the global equilibrium diversity of the community. Taken in a community context, K_{DDD} could then inform about the proportion of niche space occupied by a clade. Interpreting K_{DDD} in the same way for half-equilibrium communities would however lead to erroneous conclusions: here too, the estimated values suggest single clades (and, when summed, communities) are close to their equilibrium diversity, whereas most of the clades can (and will) grow approximately twofold.

4.3.4. SUPPORT FOR IW VERSUS CS DIVERSITY-DEPENDENCE

The optimisation of the likelihood of DAISIE on the phylogenetic data of the communities simulated with the IBM was computationally intensive, and, in some cases, not possible to complete within the time frame set (10 days, the maximum duration allowed for a job on the high performance cluster at the University of Groningen). For communities with

low immigration ($\Gamma = 0.0001$), we obtained maximum likelihood estimates for all but one to two replicate communities for each set of parameters, both for the CS and IW models. For communities with high immigration ($\Gamma = 0.01$), we obtained results for the CS model for 91/100 ($\sigma_\alpha = 0.369$) and 83/100 ($\sigma_\alpha = 0.091$) replicates. For the IW results, however, all optimisations failed as a result of the likelihood itself being intractable. Clearly, this was a result of the large number of clades in these communities (Fig. 4.2), irrespective of the total number of species. Indeed, the size of the system of differential equations that needs to be integrated to obtain the likelihood grows quickly with the number of clades. This is because the model has to compute probabilities under both a scenario where speciation has taken place (and led to a now extinct species) and where it has not yet taken place between the colonisation time and the first branching time, thus doubling the number of equations for each colonisation event. For a community containing n single-species clades for example, the size of the system would be of the order of 2^n s, where s corresponds to the size of the system for a single clade, typically $s = 100$. For $\sigma_\alpha = 0.091$, $\Gamma = 0.01$, communities contained up to 24 clades (and 98 species), such that computing the likelihood requires integrating approximately 1.68 billion differential equations simultaneously.

Log-likelihood ratios strongly favoured IW diversity-dependence over CS diversity-dependence for the vast majority of communities at equilibrium (Fig. 4.9, $f = 1$). Only in the setting with $\sigma_\alpha = 0.369$, $\Gamma = 0.0001$ did a sizable fraction of replicate communities yield mixed support for either version (40/96 replicates have a log-likelihood ratio between -5 and 5), and strong support for CS for a few replicates (5/96 replicates with a log-likelihood ratio exceeding 5, top-left panel in Fig. 4.9). For the three remaining parameter settings, log-likelihood ratio scores are almost always (that is, for at least 93% of the replicate communities) below -10, well beyond what could be explained by a potential bias in favour of the IW model, which would result in the decisive selection of island-wide diversity-dependence under any criterion. Support for either model is much more mixed when considering communities at half their equilibrium diversity (Fig. 4.9, $f = 0.5$). The distribution of log-likelihood ratios changes primarily across widths of the competition kernel σ_α, rather than the immigration rate. For $\sigma_\alpha = 0.369$, most of the communities have negative likelihood-ratio scores (over 85%, median = -1.56 and -1.75 for $\Gamma = 0.0001$ and $\Gamma = 0.001$, respectively), suggesting stronger support for the IW model. However, support remains mixed (resp. 95% and 88% of the scores are above -5), and in the absence of theoretical or bootstrap-generated distributions for the expected scores under the IW and CS hypotheses, call for caution in interpreting these results. As such, we deem the comparison inconclusive. For $\sigma_\alpha = 0.091$, while support for either model is in general mixed (78% and 71% of scores between -5 and 5 for $\Gamma = 0.0001$ and $\Gamma = 0.001$, respectively), a large fraction (50% and 75%, respectively) of the communities support CS better than IW. In many cases (19% and 26%, respectively) log-likelihood ratio scores exceed 5 log-units of difference, suggesting that CS diversity-dependence is selected with confidence.

4.3.5. EQUILIBRIUM DIVERSITY ESTIMATES FROM FULL COMMUNITY DATA

Maximum likelihood estimates of the island-wide K (K_{IW}) are consistently similar to, or slightly under the total number of species in the community at present (Fig. 4.10A). For

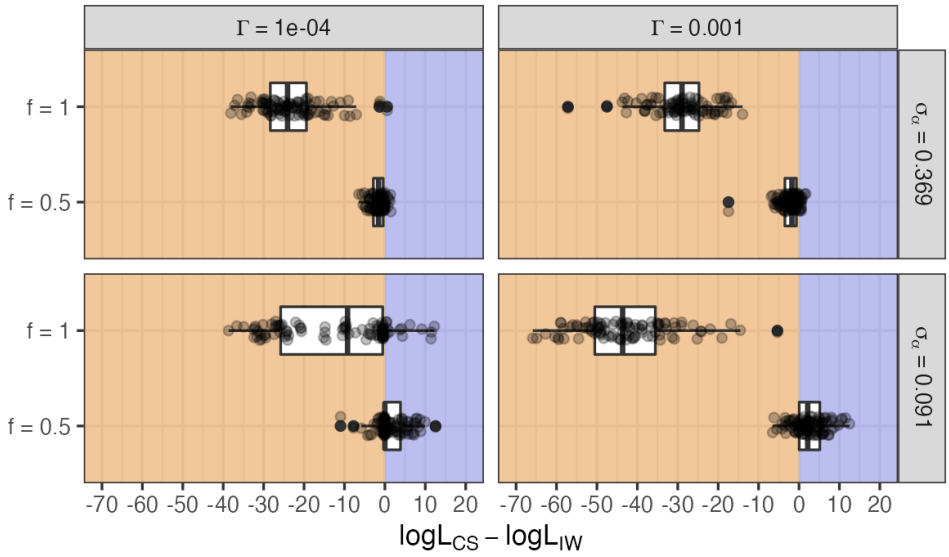

Figure 4.9 | Distribution of the log-likelihood ratio of the two versions of the DAISIE model, across replicate communities at equilibrium ($f = 1$) and half-equilibrium ($f = 0.5$) diversity. Positive scores (purple area) denote stronger support for CS diversity-dependence, while negative scores (orange area) denote stronger support for IW diversity-dependence.

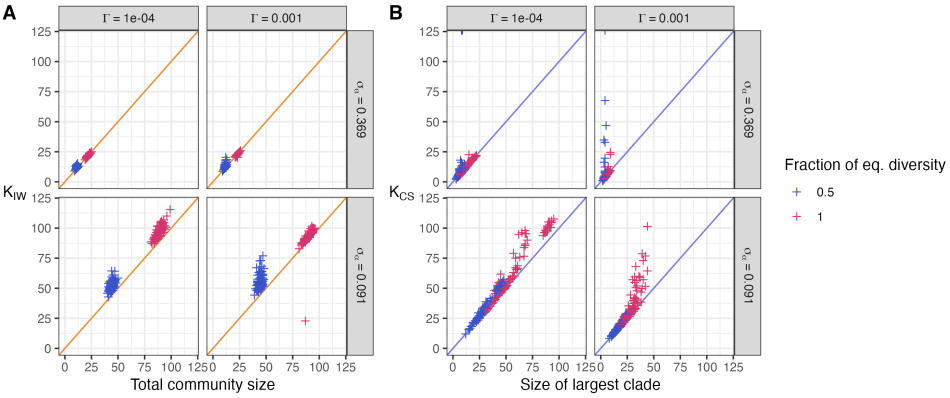

Figure 4.10 | Maximum likelihood estimates of DAISIE parameter K, (A) from the IW model (K_{IW}), plotted against the number of species in the community, (B) from the CS model (K_{CS}), plotted against the number of species in the largest clade. Estimates are shown for four combinations of the model parameters, and communities at equilibrium ($f = 1$) or half-equilibrium ($f = 0.5$).

$f = 1$ communities, this would lead to the (correct) conclusion that the community are close to their equilibrium diversity (Fig. 4.3). However, this result also extends to $f = 0.5$ communities, suggesting prematurely that communities had already reached equilibrium, while (by definition) diversity would still double before reaching equilibrium. This suggests that while DAISIE does recognise the effect of diversity-dependence on the growth of the community, it tends to interpret the presence of a slowdown of diversification as the community having reached equilibrium, regardless of the actual level of saturation. This echoes an identical conclusion already found for single trees, using DDD [19].

The corresponding estimates of a clade-specific equilibrium diversity (K_{CS}) are in fact strongly correlated with the number of species in the largest clade (Fig. 4.10B, left panels), irrespective of the total number of species in the community. This result holds both for equilibrium and half-equilibrium communities. This appears to be a result of the model recognising that diversification has slowed down as a result of diversity-dependence, and attempting to accommodate for this under the constraint of a separate equilibrium diversity for every clade. Given the smaller clades seem to have reached an equilibrium, K_{CS} must be as small as possible, yet any value significantly smaller than the largest clade size would make the latter extremely unlikely to be realised. For communities at equilibrium, this would erroneously suggest equilibrium has not been reached yet and the community would be bound to grow further, as while the largest clade would be close to equilibrium, any smaller clade could still expand before reaching this value. We also note that the issue highlighted above for the IW model also applies to the CS case: the largest clades in half-equilibrium communities are inferred as close to their (clade-specific) equilibrium value. This suggests that K_{CS} is poorly informative about the general state of the community when the diversification process departs from the assumption of an equal carrying capacity across all clades. In either case, assessing the community's total K using these estimates (by multiplying K_{CS} by the number of clades) would result in a dramatic overestimation of the community's equilibrium diversity.

4.3.6. ESTIMATES OF OTHER DAISIE PARAMETERS

INITIAL IMMIGRATION RATE

In contrast to other parameters of DAISIE, we do know the true value for the initial (i.e., before the onset of any diversity-dependent effect) immigration rate γ_0: this is simply the IBM parameter Γ divided by 1000 (that is, the number of species on the mainland, γ_0 being a per-species rate). σ_α has little effect on the estimated values of γ_0. Estimates of γ_0 from the CS model are always lower than estimates from the IW model (Fig. 4.11D, orange versus purple boxes), and estimates from half-equilibrium communities are always higher than estimates from equilibrium communities. This results in separate conclusions for both kinds of communities: in communities at equilibrium, the immigration rate is accurately estimated by the IW model, while the CS model always underestimates it (Fig. 4.11D, $f = 1$). This situation is reversed in half-equilibrium communities: γ_0 is accurately estimated with the CS model, while it is most often overestimated with the IW model (Fig. 4.11D, $f = 1$), although the bias is smaller than that for the CS model in equilibrium communities. It is possible that some estimates of γ_0 are biased upwards as a result of a discrepancy between DAISIE and the simulations: we started each simulation with an

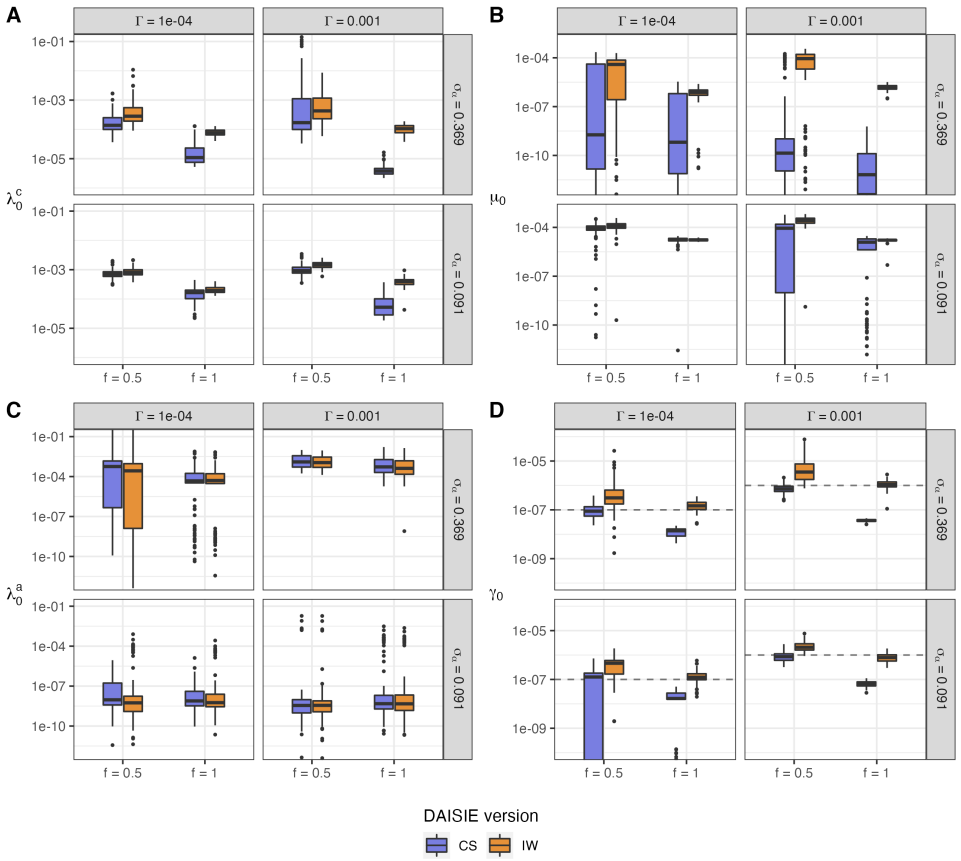

Figure 4.11 | Distribution of maximum-likelihood estimates of DAISIE parameters, across replicate communities, estimated with the CS (purple boxes) or IW (orange boxes) version of the model, for communities at equilibrium diversity ($f = 1$) or at half the equilibrium diversity ($f = 0.5$). Grids show estimates for communities simulated with four combinations of IBM parameters Γ (immigration rate) and σ_α (width of competition kernel) (A) λ_0^c, the initial cladogenetic speciation rate when $N = 0$, (B) μ_0, the extinction rate, (C) λ_0^a, the anagenetic speciation rate, and (D) γ_0 the initial immigration rate when $N = 0$. All rates are expressed per-generation and per-species.

immediate colonisation event, while DAISIE does not assume the island to be colonised immediately unless the immigration rate is very high. It is not clear to us however how this affects differences between estimates from the IW and CS models.

INITIAL CLADOGENESIS RATE

Cladogenesis constitutes the main contributor to species diversity (relative to immigration), and accordingly, estimated values of the initial cladogenesis rate λ_0^c (that is, the rate of cladogenesis when $N = 0$) are high relative to γ_0 and other parameters of the model. Estimates of λ_0^c from the CS model are consistently smaller than estimates from the IW model (Fig. 4.11A, purple versus orange boxes), although the difference is typically around an order of magnitude for equilibrium communities ($f = 1$), and even less for half-equilibrium communities ($f = 0.5$). λ_0^c is always estimated higher for half-equilibrium communities compared to equilibrium communities (Fig. 4.11A). This corresponds to a steeper slope of the diversity-dependent cladogenesis rate, and is consistent with the lower values estimated for the carrying capacity K (Fig. 4.10). There are no substantial differences in the distribution of the estimates between low and high immigration rates. Maximum-likelihood estimates of λ_0^c from communities simulated with the higher value of σ_α were generally lower than those simulated with the lower value of σ_α, by up to an order of magnitude (Fig. 4.11A, bottom row versus top row), a result consistent with the observation from Pannetier *et al.* [15] that larger competition kernels reduce the overall rate of branching irrespective of diversity-dependence.

EXTINCTION RATE

The distribution of maximum-likelihood estimates of the (constant) extinction rate μ_0 primarily changes across values of σ_α, while the rate of immigration Γ, has little effect on the distribution (Fig. 4.11B). For communities at equilibrium, narrow competition kernels ($\sigma_\alpha = 0.091$) are associated with higher estimates for extinction than for wide competition kernels ($\sigma_\alpha = 0.369$) (Fig. 4.11B, bottom row versus top row). More importantly, while for narrow competition kernels the IW and CS models yield convergent estimates of extinction, the distributions largely differ for wide competition kernels. $\sigma_\alpha = 0.369$ estimates from the CS model are very imprecise, covering a wide range of values, and are often very low, with a median below 10^{-8} (Fig. 4.11B, purple boxes in top row), suggesting extinction is a negligible process when compared to other parameters of the model. Extinction estimates in half-equilibrium communities are higher than in equilibrium communities, although this is likely a result of the higher values jointly estimated for cladogenesis (see previous section), resulting in a comparable net rate of diversification. Consistency between CS and IW estimates for $\sigma_\alpha = 0.091$ communities, and discrepancy between CS and IW for $\sigma_\alpha = 0.369$ communities are also found in half-equilibrium communities, with the extinction rate often estimated as negligible by the CS model in the latter case (Fig. 4.11B). While we do not have a "true" value for the extinction rate for comparison (as we do for the immigration rate), it is clear from the branching aspect of the communities that extinction does happen frequently in these communities, such that estimates from the IW model are in this case likely to be closer to the truth.

ANAGENESIS RATE

Anagenesis describes the transformation of an island population of a mainland species into an endemic species on the island, that is, speciation without branching. Because any subsequent cladogenesis event always result in new species, overriding the signature of anagenesis, the rate of anagenesis can only be inferred from single-species clades on the island. Maximum-likelihood estimation of the (constant) anagenesis rate, λ_0^a is, unlike other parameters, highly imprecise. The distribution of estimates always encompasses three to four orders of magnitude (Fig. 4.11C). A higher rate of anagenesis is consistently recovered for low-immigration communities compared to high-immigration communities, for half-equilibrium communities compared to equilibrium communities, and by the CS model compared to the IW model (Fig. 4.11C). In all these cases, the difference between the medians is, however, less than an order of magnitude, and these differences can be considered negligible. Instead, as for extinction, the main axis of variation is between communities simulated with different values of σ_α. In the $\sigma_\alpha = 0.091$ settings, the median estimated anagenesis rate lies around 10^{-8} (Fig. 4.11C, bottom row), such that anagenesis can be considered negligible compared to cladogenesis (10^{-4} to 10^{-3}) (Fig. 4.11A). Diversity in these communities indeed mostly originates from cladogenesis. By contrast, in $\sigma_\alpha = 0.369$ communities, where endemic singletons often constitute a large fraction of the community, median estimates are often estimated as comparable, or even higher than the initial rate of cladogenesis (10^{-4} to 10^{-3}, Fig. 4.11C, top row). The large amount of uncertainty in λ_0^a estimates may be attributable in the long branches of singletons (Fig. 4.1, panels B and D): anagenesis may have happened any time between colonisation times and the present, such that the likelihood may be rather flat with respect to the value of the rate of anagenesis.

4.4. DISCUSSION

Contributions of distantly-related clades to competition pressures is an aspect of diversity-dependence often overlooked by existing models. To represent this scenario, we simulated island communities by introducing immigration in an individual-based model where diversity-dependent diversification emerges from individual-level competition in a single, finite niche space. We used birth-death methods to analyse whether diversity-dependence in diversification could be detected from the phylogenetic data extracted from island communities, and whether its shared nature could be recognised.

The taxonomic composition of the resulting simulated communities was primarily shaped by priority of colonisation of the niche space. The intensity of immigration early in the simulations determined both the cladistic diversity of the community (Fig. 4.2), and the species diversity inside clades (Fig. 4.4), which were inversely related. The largest clades in the communities were often the first ones to have colonised the niche space (Fig. 4.4 and Fig. 4.1), as a result of having more time to grow unbounded before encountering competition, compared to clades immigrating later. Most of the niche space filled relatively early in the simulation, and colonisation of sections of niche space already occupied by resident populations was very unlikely to succeed, such that immigration did not contribute much to diversity in later stages of diversification. The cladistic composition of the community seldom changed throughout the simulation (Fig. 4.1), while the

number of species within each clade changed only slowly (Fig. 4.4). Crucially, niche space was partitioned very clearly, each clade occupying a limited and exclusive range of trait values. Once established, the portion of niche space occupied by each clade did evolve slowly, such that while diversity inside clades could change substantially throughout the simulation, it was, for many clades, almost stationary.

Results from the comparisons of maximum likelihood scores of birth-death models suggest that phylogenetic data extracted from communities that have reached equilibrium carry a strong signal to identify diversity-dependence. First, considering trees from each clade in the community separately, it is clear that a model with diversity-dependent diversification will be largely preferred over a model with constant-rate diversification, as long as the tree is reasonably large (a rough benchmark could be above 15 species, Fig. 4.7) to be used to test for evolutionary hypotheses. That is, failing to account for the contribution of unknown, competing clades to diversity-dependence does not impede the detection of diversity-dependence from a single focal clade. Second, when all trees from the same community are considered together, IW diversity-dependence is largely preferred over a CS form of diversity-dependence. That is, there is a strong signal indicating that all clades evolve and compete in a common niche space.

These conclusions are, however, challenged by the results we obtained from phylogenetic data of communities at half the equilibrium diversity. For these communities, we find only mixed support for diversity-dependence on the basis of single trees, and mixed support for CS against IW diversity-dependence on the basis of whole-community trees. The apparently contradictory results between equilibrium and half-equilibrium communities can be reconciled when considering the dynamics of the communities in trait space (Fig. 4.1, vertical bar). At the stage corresponding to half-equilibrium communities, for many parameter settings individual clades are still expanding in trait space and/or have only come in contact with competing clades recently. As a result, inter-clade competition may only play a small role in diversity-dependence relative to intra-clade competition at this stage. We interpret that mixed support for IW diversity-dependence in half-equilibrium communities may stem from an effectively low level of competition between clades at this stage of community diversification, rather than a lack of statistical power. IW diversity-dependence may be a better descriptor of the diversification process in later stages of the community (i.e., close to equilibrium), where the main limitation to clade expansion is the presence of other clades (Fig. 4.1).

While likelihood ratio scores generally point towards mixed support for both forms of diversity for half-equilibrium, for a significant proportion of communities simulated with $\sigma_\alpha = 0.091$, likelihood ratios even suggest that clade-specific diversity-dependence may in fact be a better description of the dynamics. Some differences in the maximum likelihood estimates of DAISIE parameters also point towards this interpretation. Maximum-likelihood estimates of the initial immigration rate, γ_0, were most accurate for the IW model for equilibrium communities, while for half-equilibrium communities estimates from the CS model yield less bias (Fig. 4.11D), suggesting the CS model may be more adequate in the latter case. The same pattern is found for maximum likelihood estimates of the initial cladogenetic rate λ_0^c, although in this case we lack a reference value to assess which estimates are closer to the truth (Fig. 4.11A). However, other results indicate that the CS model is inadequate to describe the data produced by the individual-based

model. Both for half-equilibrium and equilibrium communities, under high competition ($\sigma_\alpha = 0.369$) maximum likelihood estimates of the extinction rate are highly imprecise, and for a large portion of communities approach zero (Fig. 4.11B), contradicting the occurrence of extinction events observable in trait space (Fig. 4.1). More importantly, CS estimates of the equilibrium diversity K_{CS} are consistently close to the size of the largest clade in the community (Fig. 4.10B). In communities at equilibrium, interpretation of this value would suggest other clades could still grow substantially, while it is clear from diversity growth curves that communities are near saturation (Fig. 4.3). In half-equilibrium communities, these estimates are equally uninformative. This is of concern, as this model underlies the default implementation of diversity-dependence in DAISIE. Relaxing this assumption itself presents a conceptual challenge. Computational concerns aside, one could imagine implementing a version of the model where each clade possesses its own parameter for the carrying capacity (as suggested for example in Etienne *et al.* [4]), but this is likely to result in overfitting the data. As a compromise, one could instead specify an expected distribution of the carrying capacities in the community, thereby allowing for different values of the CS carrying capacities while limiting the number of parameters in the model). Upcoming developments of DAISIE are indeed proceeding in this direction (Lambert, J., personal communication), and it would be interesting to apply such a model to the communities produced by the IBM.

Unfortunately, the IW version of DAISIE, as well as the single-tree diversity-dependent model, appear to be subject to a similar tendency to suggest equilibrium prematurely. For equilibrium communities, estimates of K_{DDD} and K_{IW} correctly point towards saturation of the community. The same conclusion is however suggested when inference is performed again on communities at the stage of half-equilibrium diversity. It appears that diversity-dependent models have a tendency to suggest saturation whenever evidence for a slowdown of diversification is observed, even though diversity is still increasing. This echoes previous findings for the single-tree diversity-dependent model, which has been reported to have a tendency to estimate a ratio of saturation N/K close to 1, particularly when the level of extinction is significant [2, 19], which is the case of our simulated communities. Therefore, we reiterate these authors' warnings against direct interpretation of these estimates, as this would result in type-I errors when attempting to determine whether equilibrium has been reached, or the degree of occupancy of niche space.

Aside from the abovementioned issues with estimates of equilibrium diversity and extinction in small communities, DAISIE estimates are, overall, fairly robust to misspecification of the form of diversity-dependence. Consistent differences are found in the distribution of maximum likelihood estimates for the initial cladogenesis rate λ_0^c, constant anagenesis rate λ_0^a, and initial immigration rate γ_0 between CS and IW DAISIE, but in most cases differences in the median were small, in the worst case ($\sigma_\alpha = 0.369, \Gamma = 0.001$ equilibrium communities for λ_0^c and γ_0 estimates) spanning an order of magnitude and a half (Fig. 4.11). Estimates of constant-rate extinction for larger communities (with low competition, $\sigma_\alpha = 0.091$) converge across both versions of the model.

In this study, we explored the performance of birth-death models in recovering the presence and type of diversity-dependence using phylogenetic data from simulated communities. Such validation tests are common when developing phylogenetic comparative methods. Contrary to common practice, however, here we did not use data that were

directly generated under the model of interest (as in, for example, Etienne *et al.* [2], Maliet *et al.* [21]). Instead, we used phylogenies generated under an individual-based model of competition, where the form of competition differs somewhat from what is specified in DAISIE: competition only immediately affects the fitness of phenotypically similar individuals (and species), while in phenomenological models (DAISIE and DDD), competition affects all species equally. Still, in both cases total diversity is bounded (explicitly by parameter K in DAISIE/DDD, and by total niche space in the IBM), and new species contribute to saturating diversity, eventually limiting diversification even in phenotypically distant clades. As such, the phenomenological models represent different implementations of the same biological scenario (shared diversity-dependence across multiple clades). We have found this approach to be valuable from two perspectives. On the one hand, it is encouraging to find that the IW version of DAISIE is decisively preferred over the CS version for communities at equilibrium, indicating that the model may be used to infer shared forms of diversity-dependence. This is noteworthy, as the implementation of shared diversity-dependence differs between the simulation and the inference model, and phylogenetic birth-death models have been noted to be sensitive to departures from the evolutionary scenario described in the model [22–24]. On the other hand, the low support for island-wide diversity-dependence for half-equilibrium communities shows that DAISIE inference may be affected by the structuring of the community in (niche) space. Here, both DAISIE-IW and the IBM represent a scenario where competition for niche space between clades is bound to limit their growth, such that diversity-dependent effects are expected to take place. Yet, the models differ in the onset of those effects, as DAISIE assumes an instantaneous and homogeneous feedback of community growth on the diversification of every clade in the community. By contrast, in the IBM, the onset of diversity-dependent effects is steep and they only take place when clades come in contact in niche space, such that island-wide DAISIE appears to be inadequate to describe the communities until a late stage of diversification. Despite the evolution of half-equilibrium communities conforming to the process tested with DAISIE-IW, the results may motivate rejection of the hypothesis of island-wide diversity-dependence. Note that this is not necessarily an error: at this stage, there are indeed few IW diversity-dependent effects. This case illustrates how testing models using data that conform to the evolutionary hypothesis at hand, but otherwise depart from the precise model in other respects, may help highlighting how the model is susceptible to behave in a range of realistic scenario, and improve interpretation of its results. A related approach is using so-called robustness analyses, where the effects of processes not captured by the model (e.g., changing island are over time [25], or the presence of an unmeasured trait influencing diversification [26]) on the results of inference are iteratively measured.

Arguably, our conclusions are in part contingent on the particular community structure produced by the IBM we have used, and its assumptions. For example, our finding that the contribution of other clades to diversity-dependence may be ignored when studying single trees is largely a result of the clear partitioning of niche space into subspaces exclusively occupied by a single clade. In turn, this is a result of the unidimensional trait space, and the small mutational steps we considered. It is easy to imagine that both multidimensional trait dynamics, or occasionally larger mutational step would contribute to a disparate distribution of clades in trait space. Yet, we expect that by enabling more

interactions between species from different clades, a more heterogeneous distribution of clades in trait space would in fact strengthen the signal for IW diversity-dependence. From the single-tree perspective, we expect an intertwined distribution to facilitate the detection of diversity-dependence, by contributing to a faster deceleration of diversification (that is, a steeper slope of the diversity-dependent functions) compared to the partitioned case.

In this study of island communities, we mean islands to be considered in the broadest sense, representing island communities proper, as well as island-like systems [27], that is, any scenario where a community evolves in a discrete and isolated section of niche space. Hence this model also covers scenarios where new adaptive zones [28, 29] are made accessible to a lineage via the expression of a key innovation [5, 30, 31]. That is, modelled niche space does not necessarily correspond to spatially isolated habitats, but instead, isolated sections of phenotypic space that require specific combinations of adaptations. Whether geographically or only phenotypically isolated, such niche spaces are expected to provide ecological opportunity [32–34], and their access is expected to trigger adaptive radiations in lineages that do access them, followed by a progressive slowdown of diversification as the niche space fills with species and competition intensifies [35–37]. As such, these scenarios form the conceptual basis for the expectation of diversity-dependent diversification [1, 2, 36]. Studies of diversity-dependent diversification carried out on the phylogenies of specific groups typically assume the exclusivity of the niche space to the clade of interest, such that members of the clade only contribute to and suffer from the effects of competition with other members of the clade [9]. This assumption seems unrealistic, as island communities usually comprise taxonomically diverse assemblages [13], and independent lineages may adapt to a similar ecology, leading to competition of phylogenetically distant groups inside a common niche space [38]. This is in fact a recurrent theme in paleobiology, where inter-clade competition is often invoked to explain the simultaneous expansion and decline of ecologically similar clades [9, 39, 40].

Here, we explored how existing birth-death methods currently used to model diversity-dependent diversification can inform us when diversity-dependence is shared across multiple clades. Considering the scenario where an experimenter is interested in studying the diversification of a single, monophyletic clade (for example, when attempting to explain the main forces that have shaped the evolutionary history of a particular taxon), our results suggest that the influence of external, unknown competing clades can largely be ignored.

The main limitation to this approach is computational: optimisation of the likelihood for a single community may take up to 10 days at a time, severely limiting thorough exploration of the behaviour of the model in the parameter space. The size of the system of equations to integrate grows quickly with the number of clades, making it unfeasible in practice to obtain the maximum likelihood for settings with a high rate of immigration (or equivalently, a high rate of phenotypic transitions to the niche space). On the one hand, this is regrettable since DAISIE could allow harnessing phylogenetic data in such systems, where the high degree of partitioning is likely to result in trees too small for single-tree approaches. On the other hand, systems with high immigration may by definition depart from the isolated island systems that is the object of study. In the analogous phenotypic space system, one may question whether a high rate of transition into an isolated niche

space makes it an isolated space at all.

A significant challenge when considering isolated phenotypic niche spaces lies in the delimitation of such finite niche spaces. That is, how may one identify which clades are likely to have interacted and evolved in a common space, in the absence of the clear conditions provided by the island system proper? While the comparison of the likelihoods of DAISIE-CS and DAISIE-IW we have performed here can help confirming or contradict the coherence of a hypothesized assemblage, we do not know the sensitivity of this analysis to the erroneous inclusion or omission of some clades. It is tempting to attempt to delimitate same-niche assemblages by iteratively including and excluding taxa in the phylogenetic data and repeat the likelihood comparison of CS against IW diversity-dependence. We argue that this should be avoided, as it is likely to result in spurious positive results, by chance. Instead, DAISIE-IW can be used to test for a common regime of diversity-dependence on a cladistic assemblage *a priori* suspected to have evolved in a common niche space, and should be confronted to other lines of evidence, for example spatial distribution.

One such line of evidence that we have not exploited here is the distribution of traits across species. In biological systems where trait evolution approaches the conditions modelled in our IBM (that is, a single ecologically-relevant trait with small and frequent mutations), the distribution of traits, both inside and across clades should bear strong phylogenetic signal. The distribution of clades themselves should seldom overlap, and form a more or less contiguous occupation of trait space. Admittedly, this can only hold in ecological systems where variation in the resource acquisition traits can be measured along a single axis, as in our model (i.e., the ecological trait is unidimensional).

In this study, we have explored how two birth-death methods that assume that diversity-dependence operates on a single-clade basis, interpret phylogenetic data generated under a model that departs from this assumption, instead defining a single niche space shared between multiple clades. We have found that detection of diversity-dependence from single clades should be seldom impacted by the presence of other clades to competition, even though their contribution to diversity-dependent effects are not accounted for. This is partly due to the tendency for members of a clade to cluster together in trait space as a result of phylogenetic effects. Shared diversity-dependence is easily detected when considering the set of phylogenies from all clades in the community, but only when the community has reached equilibrium diversity, while the set of phylogenies from half-equilibrium communities seldom support shared diversity-dependence. We observe that at this stage, despite the shared resources and trait space, clade growth is hampered by intra-clade rather than inter-clade competition, the latter only becoming a prevalent factor in diversity-dependence at later stages, when available niche space saturates. This assessment of available inference methods is thus encouraging to evaluate the contribution of competition to diversification where multiple clades may interact. Our methodology provides a case for further integration of individual-based models in macroevolutionary studies. Here, the implementation of competitive interactions forming the conceptual basis for the expectation of diversity-dependence reveals a shift between the mode of diversity-dependence as niche space saturates. We expect that individual-based models may similarly help validating or refining expectations from verbal models of macroevolution.

REFERENCES

[1] D. L. Rabosky and I. J. Lovette, *Density-dependent diversification in North American wood warblers,* Proceedings of the Royal Society B: Biological Sciences **275**, 2363 (2008).

[2] R. S. Etienne, B. Haegeman, T. Stadler, T. Aze, P. N. Pearson, A. Purvis, and A. B. Phillimore, *Diversity-dependence brings molecular phylogenies closer to agreement with the fossil record,* Proceedings of the Royal Society B: Biological Sciences **279**, 1300 (2012).

[3] J. T. Weir and S. Mursleen, *Diversity-Dependent Cladogenesis and Trait Evolution in the Adaptive Radiation of the Auks (aves: Alcidae),* Evolution **67**, 403 (2013).

[4] R. S. Etienne, B. Haegeman, A. Gonzalez-Voyer, and L. Valente, *The limits to ecological limits to diversification,* in prep. , 35 (2022).

[5] R. S. Etienne and B. Haegeman, *A Conceptual and Statistical Framework for Adaptive Radiations with a Key Role for Diversity Dependence.* The American Naturalist **180**, E75 (2012).

[6] J. H. BROWN, D. W. DAVIDSON, and O. J. REICHMAN, *An Experimental Study of Competition Between Seed-eating Desert Rodents and Ants,* American Zoologist **19**, 1129 (1979).

[7] F. L. CARPENTER, *Competition Between Hummingbirds and Insects for Nectar,* American Zoologist **19**, 1105 (1979).

[8] D. Schluter, *Character displacement between distantly related taxa? Finches and bees in the Galapagos.* American Naturalist **127**, 95 (1986).

[9] D. Silvestro, A. Antonelli, N. Salamin, and T. B. Quental, *The role of clade competition in the diversification of North American canids,* Proceedings of the National Academy of Sciences **112**, 8684 (2015).

[10] L. Xu and R. S. Etienne, *Detecting local diversity-dependence in diversification,* Evolution **72**, 1294 (2018).

[11] R. H. MacArthur and E. O. Wilson, *The Theory of Island Biogeography* (Princeton University Press, 1967).

[12] M. G. Weber, C. E. Wagner, R. J. Best, L. J. Harmon, and B. Matthews, *Evolution in a Community Context: On Integrating Ecological Interactions and Macroevolution,* Trends in Ecology & Evolution **32**, 291 (2017).

[13] L. M. Valente, A. B. Phillimore, and R. S. Etienne, *Equilibrium and non-equilibrium dynamics simultaneously operate in the Galápagos islands,* Ecology Letters **18**, 844 (2015).

[14] L. Valente, A. B. Phillimore, M. Melo, B. H. Warren, S. M. Clegg, K. Havenstein, R. Tiedemann, J. C. Illera, C. Thébaud, T. Aschenbach, and R. S. Etienne, *A simple dynamic model explains the diversity of island birds worldwide,* Nature **579**, 92 (2020).

[15] T. Pannetier, A. B. Duthie, and R. S. Etienne, *On the mechanistic nature of diversity-dependent diversification,* in prep. (2022).

[16] M. Pontarp, J. Ripa, and P. Lundberg, *On the origin of phylogenetic structure in competitive metacommunities,* Evolutionary Ecology Research **14**, 269 (2012).

[17] U. Dieckmann and R. Law, *The dynamical theory of coevolution: A derivation from stochastic ecological processes,* Journal of Mathematical Biology **34**, 579 (1996).

[18] M. Doebeli, *Adaptive Diversification* (Princeton University Press, 2011).

[19] R. S. Etienne, A. L. Pigot, and A. B. Phillimore, *How reliably can we infer diversity-dependent diversification from phylogenies?* Methods in Ecology and Evolution **7**, 1092 (2016).

[20] T. Pannetier, C. Martinez, L. Bunnefeld, and R. S. Etienne, *Branching patterns in phylogenies cannot distinguish diversity-dependent diversification from time-dependent diversification,* Evolution **75**, 25 (2021).

[21] O. Maliet, F. Hartig, and H. Morlon, *A model with many small shifts for estimating species-specific diversification rates,* Nature Ecology & Evolution , 1 (2019).

[22] D. L. Rabosky and E. E. Goldberg, *FiSSE: A simple nonparametric test for the effects of a binary character on lineage diversification rates,* Evolution **71**, 1432 (2017).

[23] J. C. Uyeda, R. Zenil-Ferguson, and M. W. Pennell, *Rethinking phylogenetic comparative methods,* Systematic Biology **67**, 1091 (2018).

[24] T. Vasconcelos, B. C. O'Meara, and J. M. Beaulieu, *A Flexible Method for Estimating Tip Diversification Rates across a Range of Speciation and Extinction Scenarios*, Tech. Rep. (bioRxiv, 2022).

[25] P. S. Neves, J. W. Lambert, L. Valente, and R. S. Etienne, *The robustness of a simple dynamic model of island biodiversity to geological and eustatic change,* (2021).

[26] S. Xie, L. Valente, and R. S. Etienne, *A Simple Island Biodiversity Model Is Robust to Trait Dependence in Diversification and Colonization Rates*, Tech. Rep. (bioRxiv, 2022).

[27] Y. Itescu, *Are island-like systems biologically similar to islands? A review of the evidence,* Ecography **42**, 1298 (2019).

[28] G. G. Simpson, *The Major Features of Evolution* (Columbia University Press, 1953).

[29] S. M. Stanley, *Macroevolution: Pattern and Process.* (Johns Hopkins University Press, 1998).

[30] A. H. Miller, *Some ecologic and morphologic considerations in the evolution of higher taxonomic categories.* Ornithologie als biologische Wissenschaft , 84 (1949).

[31] S. B. Heard and D. L. Hauser, *Key evolutionary innovations and their ecological mechanisms,* Historical Biology **10**, 151 (1995).

[32] L. J. Harmon, J. Melville, A. Larson, and J. B. Losos, *The Role of Geography and Ecological Opportunity in the Diversification of Day Geckos (Phelsuma),* Systematic Biology **57**, 562 (2008).

[33] J. B. Losos, *Adaptive Radiation, Ecological Opportunity, and Evolutionary Determinism: American Society of Naturalists E. O. Wilson Award Address,* The American Naturalist **175**, 623 (2010).

[34] F. T. Burbrink and R. A. Pyron, *How Does Ecological Opportunity Influence Rates of Speciation, Extinction, and Morphological Diversification in New World Ratsnakes (tribe Lampropeltini)?* Evolution **64**, 934 (2010).

[35] S. M. Stanley, *Effects of Competition on Rates of Evolution, With Special Reference to Bivalve Mollusks and Mammals,* Systematic Zoology **22**, 486 (1973).

[36] J. J. Sepkoski, *A kinetic model of Phanerozoic taxonomic diversity I. Analysis of marine orders,* Paleobiology **4**, 223 (1978).

[37] D. Schluter, *Ecological Character Displacement in Adaptive Radiation.* The American Naturalist **156**, S4 (2000).

[38] L. H. Liow, T. Reitan, and P. G. Harnik, *Ecological interactions on macroevolutionary time scales: Clams and brachiopods are more than ships that pass in the night,* Ecology Letters **18**, 1030 (2015).

[39] J. J. Sepkoski, *Competition in macroevolution: The double wedge revisited,* in *Evolutionary Paleobiology* (University of Chicago Press, 1996).

[40] F. L. Condamine, J. Romieu, and G. Guinot, *Climate cooling and clade competition likely drove the decline of lamniform sharks,* Proceedings of the National Academy of Sciences **116**, 20584 (2019).

5

SYNTHESIS

5.1. SUMMARY OF FINDINGS

Competition has historically occupied a central position in evolutionary theory, starting with Darwin's own view that (ecological) similarity between forms prevents their survival and coexistence, promoting divergence between closely related forms. The driving role of competition remains central in the modern ecological and evolutionary paradigm [1–3], particularly at large scales where the distribution of biodiversity is interpreted through the lens of competitive exclusion [4] and its consequences perhaps most notably, character displacement [5, 6]. As a result, it is not surprising that when global compilations of fossil occurrences first became available and enabled studies of the evolution of taxonomic diversity itself, paleobiologists largely interpreted the observed taxonomic diversity curves in terms of competitive exclusion and niche partitioning [7–10]. The most prominent example of this is the diversity-dependent diversification model [8, 11], which surmises the existence of a (local or global) bounded niche space, in which the diversification of clades causes rising competition pressures, in turn impeding further diversification. With the advent of phylogenetic comparative methods [12, 13], the diversity-dependent model as a birth-death model [14, 15] has offered an unprecedented framework to explain how ecological processes may have influenced the branching patterns observed in molecular phylogenies, and by extension the distribution of species across taxonomy. Yet, it is unclear how much the model can help inference on the role competition played in past diversification, for two reasons. First, it is uncertain how much information can really be inferred about past evolutionary processes in the presence of the limited subset of evolutionary history contained in molecular phylogenies [16–18]. Second, the nature of the model itself is ambiguous, on the one hand proposing a more mechanistic interpretation to diversification relative to other models, while on the other hand remaining verbal and vague in its formulation [19]. In this thesis, I have tackled both issues, in an effort to obtain a better understanding of this unique model and its interpretation. I first compared the likelihood of a diversity-dependent model against that of a solely time-dependent model calibrated to produce the same expected number of species over time (Chapter 2). I

sought to evaluate whether the feedback of diversity on diversification introduced any identifiable signal in the branching patterns of molecular phylogenies. I found that it does not, or at least not in the information used to compute the likelihood. That is, when evaluating evidence for a role of competition in shaping the diversification of a clade, one may only rely on the expected branching pattern over time predicted by the diversity-dependent model. If there is any reason to believe that a similar branching pattern can be produced by a model that does not invoke diversity-dependence, then the two cannot be distinguished. As a result, it is crucial to obtain precise predictions for how those rates should vary over time. In turn, this requires obtaining well-identified predictions for the form of diversity-dependence that is expected if competition is indeed driving diversification. For this reason, in Chapter 3, I turned to the question of whether the power and linear functions of species diversity currently used to test for diversity-dependence in empirical phylogenies, as well as an exponential function, are consistent with the form of diversity-dependence that emerges from an individual-based model of diversification where competition does drive diversification. I found that the rates of speciation and extinction emerging from the model present features that are not captured in the simple functions. Among these, the exponential, or in the case of the larger phylogenies the power function, best approximates diversity-dependence from the IBM on the basis of the complete phylogeny, including perfect knowledge and placement of fossil taxa on the phylogeny. When fossils are not known, however, we find that linear diversity-dependence on speciation coupled with weak, constant-rate extinction fits the phylogenies without extinct species best. This paradoxical conclusion appears to be due to the loss of information about the early diversification process. Interestingly, it is entirely consistent with results frequently observed for empirical phylogenies. This suggests that the frequent selection of linear diversity-dependence in molecular phylogenies point towards an evolutionary process close to the one captured in our model, with competition indeed having played an important role in the diversification of such clades. Diversity-dependence assumes that diversification takes place in a niche space, which in many scenarios is likely to be invaded by multiple, unrelated clades. Yet, methods implementing the model, including the ones I used throughout the thesis, assume diversity-dependence operate solely within single clades. It is not known how such methods may be affected by this assumption not being satisfied, and whether a common regime of diversity-dependence across multiple clades can be identified at all. In Chapter 4, I introduced stochastic immigration in the individual-based model of the previous chapter to generalise the model to the case of multiple clades diversifiying in a common niche space, in an evolutionary scenario akin to diversification on islands. After extracting the phylogenetic trees from the community, I found that detection of diversity-dependence on the basis of single trees is not affected by the presence of other competing clades, or failure to account for their presence clades, and that immigration only reduces the signal through causing smaller tree sizes. Using methods from island biogeography to account for communities as evolutionary units, I found that shared diversity-dependence can be detected with confidence, but only in communities that have reached equilibrium diversity. Results are inconclusive for communities at half-equilibrium diversity, although this appears to be due to effectively little competition between clades at this stage, suggesting that the method is robust to false positives.

5.2. ARE DIVERSITY- AND TIME-DEPENDENT MODELS CONGRUENT?

During the course of this PhD project, an influential paper [20] was published and sparked much debate and uncertainty over the future use of birth-death models to test macroevolutionary processes. In their work, Louca and Pennell [20] provided an elegant mathematical demonstration that for any tree there are an infinite number of time-dependent birth-death models that have the same exact likelihood. This infinite set of models has in common that they produce the same expectation for the lineage-through-time curve (that is the accumulation through time of lineages that have descendants that are alive at present). Such models are called congruent. Models discussed in Louca and Pennell [20] cover all time-dependent models, that is, any birth-death model where the speciation and extinction rates can be written as functions of time ($\lambda(t)$ and $\mu(t)$, respectively). This includes the time-dependent model introduced in Chapter 2, of course, as well as the constant-rate model opposed to diversity-dependence in Chapter 4. Whether these conclusions extend to the diversity-dependent birth-death models that are the focus of this thesis is not immediately obvious, as these models cannot be written as an explicit function of time unless extinction is zero [14, 15]. While we do not provide mathematical proof, the results from Chapter 2 suggest it is indeed the case: when a time-dependent model is designed to produce the same expected number of species over time (and so, the same lineage-through-time curve, LTT), the distribution of log-likelihood ratios for the trees produced by either model almost entirely overlap. This suggests that DD models might indeed be included in the congruence classes discussed in Louca and Pennell [20], and as such, cannot be distinguished from time-dependent models producing the same expected LTT.

However, it is clear from the likelihood scores that the two classes of models are not congruent in a strict sense: the likelihood of a diversity-dependent model is not equal to, but substantially higher than the likelihood of a time-dependent model producing the same expected LTT, as we have seen in Chapter 2. While we have shown that bootstrapping likelihood ratios offers a solution around this, the issue remains unresolved. In Chapter 2, we have shown that this bias is related to the smaller variance in the distribution of LTTs produced by diversity-dependent models, causing the probability of any realisation of the diversification process to be more elevated than for an equivalent process with a wider range of possible realisations. In turn, this is due to the carrying capacity K being an attractor of N in diversity-dependent models. This suggests a link between the variance of the probability distribution of tree sizes and the likelihood of diversity-dependent models, which to the best of my knowledge has not been formally identified, i.e., described in an equation.

The variance of tree sizes does not play a part in comparisons of the likelihoods of purely time-dependent models. As Louca and Pennell [20] pointed out, the likelihood only depends on the *expected* LTT, and the probability distribution of tree sizes of congruent time-dependent models is identical (section S.1.7 in [20]). This last point further confirms that diversity-dependent models are not congruent with time-dependent models: they produce a markedly different distribution of tree sizes (Fig. 2.2 in Chapter 2), particularly in conditions that give enough time for trees to reach carrying capacity. The formulation

of time-dependent models constrained to have the same variance in tree size as a diversity-dependent model was investigated as part of preliminary work to Chapter 2 (Martinez and Etienne, unpublished results). While mathematically possible, such models are biologically unsatisfactory: either the rates are negative, or the process lacks any species turnover when diversity is expected to reach equilibrium.

If the variance in tree size in a diversity-dependent model influences its likelihood, then this should also be accounted for in comparisons between different diversity-dependent models, as it can be expected that they predict different distributions of possible tree sizes. For example, the distribution of sizes of a set of stochastic trees can be expected to be more spread around the equilibrium diversity K in the case of exponential diversity-dependence compared to linear diversity-dependence (although this will depend on the parameter values). Because the value of the speciation and extinction rates for $N > K$ typically tends towards an asymptote in the exponential case, the relative slope of the two rates is much less steep than in the linear case. As a result, diversity-dependence is weaker, in the sense that trees are more likely to reach a size above the equilibrium value than in the linear case.

Such an effect may also be playing a part in the comparison of likelihoods of diversity-dependent models that we carried out on reconstructed trees in Chapter 3. In turn, this provides an alternative explanation (compared to the already proposed explanation of a loss of information about the early diversification process) to why the likelihood of the linear model is higher for reconstructed trees, despite the power and exponential models better approximating the emergent rates of speciation and extinction when complete fossil data are available. We can also expect that biases in the comparison of the likelihoods of diversity-dependent models extend to the models considered in DAISIE, including the clade-specific and island-wide models used through Chapter 4 [21]. This is unlikely to change our conclusions, as we have been aware of the presence of such a bias and we have been conservative in the interpretation of likelihood ratio scores.

Should a link between the variance of tree sizes expected under a diversity dependent model and its likelihood be formally identified, then one could imagine using it to implement a correction for the bias in favour of more constraining diversity-dependent models, for example by adding a penalty term to the likelihood. This would make a tractable alternative to the computationally costly bootstrap procedure used in this thesis.

Unfortunately, this would not be of great help with reliably identifying the diversity-dependence against time-dependence from phylogenetic data. While diversity dependent models seem to evade the congruence issue highlighted in Louca and Pennell [20], the core of the issue discussed by these authors does apply all the same. Given an arbitrary diversity-dependent diversification model, there will always be a time-dependent model (and all models in its congruent class) that predicts the same expected lineage-through-time curve, and thus, a model that is as likely to produce any single arbitrary tree. Finding a solution to the likelihood bias will, at best, result in the likelihood of two such models being the same, as the results from Chapter 2 suggest. Thus, addressing the issue of identifying whether the slowdown of diversification observed in many trees is caused by diversity-dependence (and, *a fortiori*, by competition) requires addressing the issue of (un)identifiability in phylogenetic data.

5.3. MOVING BEYOND IDENTIFIABILITY ISSUES

Because the core of the identifiability issue highlighted by Louca and Pennell [20] will not be resolved by either the acquisition of higher quality data (larger, or better sampled trees) or further development of likelihoods methods, it is not surprising that the solution proposed by different authors consist of the reinterpretation of existing methods. In a response to Louca and Pennell [20], Morlon *et al.* [22] have remarked that the vast majority of all *possible* birth-death models existing in a given congruence class bear no tangible biological meaning, and thus can be dismissed. On this basis, Morlon *et al.* [22] argue that meaningful macroevolutionary inference using model selection on the likelihood time-variable birth-death models can still be performed, if one takes great care in the formulation of *a priori* hypotheses. That is, the set of candidate models to be compared should only contain a few models, and each should on its own represent an *a priori* credible evolutionary scenario explaining the diversification of the studied clade. The formulation of the hypotheses each model represents thus requires expert knowledge about the biology of the clade, encouraging closer collaboration between macroevolution experts and specialists of the studied group. Such collaboration indeed appears to have been a policy for many contributions to the field [23]. Given this, following likelihood optimisation and model selection, the best fitting model may indeed be congruent with an infinite set of alternative birth-death models depicting very different variations of speciation and extinction, but few to none of them would make any sense in light of natural history. This view largely echoes the case made by Burnham and Anderson [24] against automated selection procedures in the context of statistical modelling on ecological data, and their advocacy of strong emphasis on prior knowledge to build a minimum set of candidate models ahead of model selection.

I do share this view, although I feel that the use of theory-backed models in macroevolution could be pushed further. For example, Morlon *et al.* [22] illustrate their case with the use of a time-dependent model where speciation declines over time, as representing the hypothesis of adaptive radiation or (competition-driven) diversity-dependence. As we have argued in Chapter 2, such a vague decline of diversification over time is also likely to be produced by a wide range of alternative scenarios. Rather than this, I feel that an appropriate model should incorporate finer-scale variations, consistent with what would be expected from background theory. This was, in part, the motivation behind Chapter 3. There, we measured the diversity-dependent rates of speciation and extinction that emerged from an ecological scenario fitting the verbal model behind diversity-dependent diversification (described in e.g. Sepkoski [8]). The consistent direction of the effects of parameters σ_α and σ_K on the rates of speciation and extinction, the similarity of the rates we measured compared to those found by Aguilée *et al.* [25], as well as the predictability of the equilibrium diversity all suggest that the rates of speciation and extinction could be derived from the fitness function $W(z)$. A diversity-dependent model including these two rates, if they could be identified, would make a much more robust case for competition and niche saturation dynamics driving diversification if selected on the basis of the likelihood, compared to an arbitrary diversity-dependent model. Although there could always be a time-dependent model producing the same pattern, it would be hard to justify biologically.

Yet even if explicit expectations for the net rate of diversification over time can be derived from individual-based models, the *a priori* approach advocated in Morlon *et al.* [22] does not address one crucial argument made in Louca and Pennell [20]. Beyond the risk that the "true" model may be congruent with many other birth-death models representing completely different evolutionary histories, Louca and Pennell [20] warned against the much more worrisome implication that congruence may entirely bias model selection. Maximum likelihood may not necessarily select the candidate model that best approximates the “true” model, but instead the candidate model that best approximates a model congruent with the “true” model. An illustration of this is found in the common finding that rates of extinction estimated from reconstructed phylogenies are often virtually zero. Estimated zero extinction can be explained by considering that the congruent model may feature a negative extinction rate, which is biologically meaningless, but can be accommodated by the likelihood function [26]. Because the maximum likelihood of the model lies somewhere in the negative-extinction section of the likelihood landscape, constraining extinction to not be negative results in the maximum likelihood being zero-extinction. Here, we do find zero-extinction in our results from Chapter 3. This result is incoherent with the repeated occurrence of extinction events we observed in the complete trees and thus possibly the outcome of a congruence issue, as in the cases shown in Louca and Pennell [26].

It is more likely, however, that zero-extinction results from the fact that the birth-death models we used do not account for the delay between the split of populations and the completion of speciation that takes place in the IBM, i.e., protracted speciation [27]. This causes an additional apparent slowdown of diversification close to the present (as initiated, but uncompleted speciation events are not recognised yet), erasing the pull-of-the-present effect that contains information on the rate of extinction [13]. Note that these two factors are not mutually exclusive.

Alternatively, zero-extinction in our results may also result from the data not conforming to one important assumption of birth-death models (both diversity-dependent and time-dependent): that all lineages at a time are equally likely to undergo speciation or extinction. The distribution of branch lengths in trait space in our results suggest this assumption is violated in the communities produced by our IBM (Fig. 3.1, Fig. 4.1). Lineages lying on the outer sections of trait space present longer branches, and appear less likely to undergo speciation or extinction than lineages in the central section. This suggests an interesting feature to look for when trying to identify the effect of competition in real-world phylogenies. It is hard to anticipate the impact this has on the inference we performed, but model selection on birth-death model is known to be sensible to such violations [28, 29].

5.3.1. DIVERSITY-DEPENDENCE AND TAXONOMY – MAPPING NICHES ON THE TREE OF LIFE?

In order to evaluate how important the role of competition has been in generating and regulating diversity through geological time, future research will have to elucidate how to best map diversity-dependence on taxonomy. That is, how to best sample higher-order phylogenies to extract clades that constitute pertinent evolutionary units where

diversity-dependence may take place?

Simulations of diversity-dependent diversification (e.g., the three research chapters of this thesis) most often start with one (or more rarely, a few) progenitor lineage(s) with no ancestor entering a formerly pristine niche space. By contrast, empirical applications of the model are carried out on monophyletic phylogenies that are always a sampled sub-clade of a larger clade that has presumably experienced a separate mode of diversification. Typically, these clades correspond to a particular taxonomic rank. While taxonomists certainly do not delimit taxa at random, relying on morphological similarity and homogeneity of the length of branches between lineages, the sampling choice remains somewhat arbitrary with respect to evolutionary processes. Often, taxa contain organisms with disparate ecologies, and little attention has been given in tests of diversity-dependence to evaluate the chances that the taxon being studied encompasses a pertinent evolutionary unit.

On the one hand, as was the subject of Chapter 4, a monophyletic clade may fail to include lineages that are also taking part in competition with members of the taxon. This may concern lineages from a sister taxon or much more distantly related species. As we have discussed, there is little chance that this would affect one's ability to detect diversity-dependence in the focal taxon. On the other hand, a lineage in the clade may have migrated or expressed novel resource-acquisition traits, thereby switching to a new niche space and resulting in the sub-clade descended from it breaking away from the dynamics of the main clade. Depending on the timing of this decoupling, prolonged growth may hide the signature of a slowdown in diversification in the main clade, and in general lead to misinterpretation of what aspects of the ecology of the clade limits expansion. Etienne and Haegeman [30] introduced a diversity-dependent model that accounts for, and can detect such shifts in the regime of diversity-dependence undertaken by sub-clades, but the rapid growth of the number of parameters with the number of distinct regimes of diversity-dependence limits statistical power to detect more than one or two shifts for all but very large taxa [30, 31].

At a larger taxonomic scale, this method (or other methods that similarly incorporate shifts of the rate of diversification, e.g. BAMM [32]) could be applied to identify which sub-clades form cohesive diversity-dependent units, and whether or not they correspond well with lower taxonomic units. Etienne and Haegeman [30] have however cautioned that the number of parameters in the model grows fast with the number of possible shifts (and thereby, the number of possible niche spaces), such that the power to detect a large number of different regimes may be very limited. The approach of the ClaDS model [33] may offer a solution to this issue. In this model, instead of a few clade-wide rate shifts, small and incremental changes in the diversification rate occur at every node in the phylogeny, the extent and magnitude of these changes being controlled by the model's few parameters. This calls for a change in the interpretation of the results: instead of delimiting clades that experience different, discrete evolutionary modes, the output of the model provides estimates for the rate of diversification associated with each tip, which are then to be interpreted as consistent (or not) with different modes by the experimenter.

At least one rate-shift-based method has been used for this purpose. Humphreys and Barraclough [34], Barraclough and Humphreys [35] have used an extension of a species delimitation method to identify to detect a shift in the branching rate along a phylogeny

[36], in an effort to identify taxonomic ranks above species that form cohesive evolutionary units, and thus could correspond to the invasion of a new niche space. In higher clades of mammals, they [34] found that most of the evolutionary units identified corresponded to the Family or genus taxonomic rank, rather than unnamed clades. A preliminary analysis conducted on an incomplete phylogeny of land plants [35] similarly identified Families as evolutionary units, providing support for taxonomic levels corresponding to coherent evolutionary units. Two issues stand, however, in my opinion, even if these findings were found to generalise. First, the rank found to correspond to an evolutionary unit is not consistent across large clades: Family appears to be the most relevant rank in ungulates, while genus appears more relevant in lagomorphs [34], and as a result, the risk of choosing a taxonomic rank above or below the actual clade corresponding to a pertinent niche space persists. Second, the distribution of ecological and morphological traits in mammals is not consistent with the hypothesis that identified evolutionary units correspond to niche spaces, with greater variability within than between evolutionary units, with the exception of body size in ungulates [34].

The identification of clades corresponding to niche spaces within which diversity-dependence would take place may indeed require the joint examination of eco- morphological and geographical data along with the distribution of phylogenetic branches. The diversity-dependent models that have been used throughout this thesis do not incorporate evidence from, nor make any predictions for trait data. Instead, they implicitly subscribe to the view, common in community phylogenetics [37], that phylogenetic relatedness is a good proxy for trait proximity, and thus the probability or intensity of competition. Yet, it makes little sense to test for the effect of competition between lineages that occur on different landmasses, or exploit vastly different resources. A promising step towards this can be found in the model of Drury *et al.* [38], which allows testing for the effect of competition on the distribution of trait values at the tips of a phylogeny, while explicitly taking into account whether lineages are sympatric or not. Their approach however assumes no effect of competition on the diversification rate (i.e., no diversity-dependence), taking the phylogeny as static data, rather than the realisation of a stochastic process. By contrast, the SSE (state-dependent speciation and extinction) class of diversification models consider branching patterns and the distribution of traits as a joint realisation of the same stochastic evolutionary process [28, 39–41]. While rates of speciation and extinction are constant for a given trait value or area, the models could in principle be extended to incorporate diversity-dependence, with a different equilibrium diversity defined for each value of a categorical trait (e.g., diet type). Such a model would approach the process modelled in Etienne and Haegeman [30] and as a result, I expect it would similarly suffer from limited statistical power, albeit the added resolution provided by the incorporation of trait data may help mitigating this. Alternatively, separate tests for an effect of competition could be conducted on trait and branching patterns, using each as a separate line of evidence. For example, in the results of Humphreys and Barraclough [34] above, branching patterns appear to be consistent with clade diversifying in separate niche spaces, while the distribution of traits inside and between clades seems to contradict this.

The field of phylogenetic comparative methods is currently undergoing a lot of self-reevaluation, reconsidering what models can and cannot tell us about past evolutionary

processes from current biodiversity patterns [18, 20, 22, 42]. I expect that individual-based models may play an important part in future developments [43], helping to flesh out working, testable hypotheses about the macroevolutionary consequences of ecological-scale processes from intuitions and verbal models, and I hope that the studies that constitute this thesis may contribute to such developments.

REFERENCES

[1] B. Ashby, E. Watkins, J. Lourenço, S. Gupta, and K. R. Foster, *Competing species leave many potential niches unfilled,* Nature Ecology & Evolution **1**, 1495 (2017).

[2] J. Huisman and F. J. Weissing, *Biodiversity of plankton by species oscillations and chaos,* Nature **402**, 407 (1999).

[3] P. Chesson, *Mechanisms of Maintenance of Species Diversity,* Annual Review of Ecology and Systematics **31**, 343 (2000).

[4] G. F. Gause, *The Struggle for Existence* (Baltimore, The Williams & Wilkins company, 1934).

[5] D. Lack, *Darwin's Finches* (Cambridge University Press, 1947).

[6] D. Schluter, *Ecological Character Displacement in Adaptive Radiation.* The American Naturalist **156**, S4 (2000).

[7] D. M. Raup, S. J. Gould, T. J. M. Schopf, and D. S. Simberloff, *Stochastic Models of Phylogeny and the Evolution of Diversity,* The Journal of Geology **81**, 525 (1973).

[8] J. J. Sepkoski, *A kinetic model of Phanerozoic taxonomic diversity I. Analysis of marine orders,* Paleobiology **4**, 223 (1978).

[9] S. J. Gould, D. M. Raup, J. J. Sepkoski, T. J. M. Schopf, and D. S. Simberloff, *The Shape of Evolution: A Comparison of Real and Random Clades,* Paleobiology **3**, 23 (1977).

[10] S. M. Stanley, *Effects of Competition on Rates of Evolution, With Special Reference to Bivalve Mollusks and Mammals,* Systematic Zoology **22**, 486 (1973).

[11] T. D. Walker and J. W. Valentine, *Equilibrium Models of Evolutionary Species Diversity and the Number of Empty Niches,* The American Naturalist **124**, 887 (1984).

[12] J. Felsenstein, *Phylogenies and the Comparative Method,* The American Naturalist **125**, 1 (1985).

[13] S. Nee, R. M. May, and P. H. Harvey, *The reconstructed evolutionary process,* Phil. Trans. R. Soc. Lond. B **344**, 305 (1994).

[14] D. L. Rabosky and I. J. Lovette, *Density-dependent diversification in North American wood warblers,* Proceedings of the Royal Society B: Biological Sciences **275**, 2363 (2008).

[15] R. S. Etienne, B. Haegeman, T. Stadler, T. Aze, P. N. Pearson, A. Purvis, and A. B. Phillimore, *Diversity-dependence brings molecular phylogenies closer to agreement with the fossil record,* Proceedings of the Royal Society B: Biological Sciences **279**, 1300 (2012).

[16] D. L. Rabosky and I. J. Lovette, *Explosive evolutionary radiations: Decreasing speciation or increasing extinction through time?* Evolution **62**, 1866 (2008).

[17] T. B. Quental and C. R. Marshall, *Diversity dynamics: Molecular phylogenies need the fossil record,* Trends in Ecology & Evolution **25**, 434 (2010).

[18] B. O'Meara and J. Beaulieu, *Potential survival of some, but not all, diversification methods,* (2021).

[19] D. L. Rabosky, *Diversity-Dependence, Ecological Speciation, and the Role of Competition in Macroevolution,* Annual Review of Ecology, Evolution, and Systematics **44**, 481 (2013).

[20] S. Louca and M. W. Pennell, *Extant timetrees are consistent with a myriad of diversification histories,* Nature **580**, 502 (2020).

[21] R. S. Etienne, B. Haegeman, A. Gonzalez-Voyer, and L. Valente, *The limits to ecological limits to diversification,* in prep. , 35 (2022).

[22] H. Morlon, F. Hartig, and S. Robin, *Prior hypotheses or regularization allow inference of diversification histories from extant timetrees,* bioRxiv , doi:10.1101/2020.07.03.185074 (2020).

[23] J. T. Weir and S. Mursleen, *Diversity-Dependent Cladogenesis and Trait Evolution in the Adaptive Radiation of the Auks (aves: Alcidae),* Evolution **67**, 403 (2013).

[24] K. P. Burnham and D. R. Anderson, *Model Selection and Multimodel Inference: A Practical Information-Theoretic Approach*, 2nd ed. (Springer-Verlag, New York, 2002).

[25] R. Aguilée, F. Gascuel, A. Lambert, and R. Ferriere, *Clade diversification dynamics and the biotic and abiotic controls of speciation and extinction rates,* Nature Communications **9**, 3013 (2018).

[26] S. Louca and M. W. Pennell, *Why extinction estimates from extant phylogenies are so often zero,* bioRxiv , 2021.01.04.425256 (2021).

[27] J. Rosindell, S. J. Cornell, S. P. Hubbell, and R. S. Etienne, *Protracted speciation revitalizes the neutral theory of biodiversity,* Ecology Letters **13**, 716 (2010).

[28] J. M. Beaulieu and B. C. O'Meara, *Detecting Hidden Diversification Shifts in Models of Trait-Dependent Speciation and Extinction,* Systematic Biology **65**, 583 (2016).

[29] D. L. Rabosky and E. E. Goldberg, *FiSSE: A simple nonparametric test for the effects of a binary character on lineage diversification rates,* Evolution **71**, 1432 (2017).

[30] R. S. Etienne and B. Haegeman, *A Conceptual and Statistical Framework for Adaptive Radiations with a Key Role for Diversity Dependence.* The American Naturalist **180**, E75 (2012).

[31] G. Laudanno, B. Haegeman, D. L. Rabosky, and R. S. Etienne, *Detecting Lineage-Specific Shifts in Diversification: A Proper Likelihood Approach,* Systematic Biology **70**, 389 (2021).

[32] D. L. Rabosky, *Automatic Detection of Key Innovations, Rate Shifts, and Diversity-Dependence on Phylogenetic Trees,* PLOS ONE **9**, e89543 (2014).

[33] O. Maliet, F. Hartig, and H. Morlon, *A model with many small shifts for estimating species-specific diversification rates,* Nature Ecology & Evolution , 1 (2019).

[34] A. M. Humphreys and T. G. Barraclough, *The evolutionary reality of higher taxa in mammals,* Proceedings of the Royal Society of London B: Biological Sciences **281**, 20132750 (2014).

[35] T. G. Barraclough and A. M. Humphreys, *The evolutionary reality of species and higher taxa in plants: A survey of post-modern opinion and evidence,* New Phytologist **207**, 291 (2015-01-19).

[36] J. Pons, T. G. Barraclough, J. Gomez-Zurita, A. Cardoso, D. P. Duran, S. Hazell, S. Kamoun, W. D. Sumlin, and A. P. Vogler, *Sequence-Based Species Delimitation for the DNA Taxonomy of Undescribed Insects,* Systematic Biology **55**, 595 (2006).

[37] L. J. Harmon, C. S. Andreazzi, F. Débarre, J. Drury, E. E. Goldberg, A. B. Martins, C. J. Melián, A. Narwani, S. L. Nuismer, M. W. Pennell, S. M. Rudman, O. Seehausen, D. Silvestro, M. Weber, and B. Matthews, *Detecting the Macroevolutionary Signal of Species Interactions,* Journal of Evolutionary Biology , 769 (2019).

[38] J. Drury, J. Clavel, M. Manceau, and H. Morlon, *Estimating the Effect of Competition on Trait Evolution Using Maximum Likelihood Inference,* Systematic Biology **65**, 700 (2016).

[39] E. E. Goldberg, L. T. Lancaster, and R. H. Ree, *Phylogenetic Inference of Reciprocal Effects between Geographic Range Evolution and Diversification,* Systematic Biology **60**, 451 (2011).

[40] R. G. FitzJohn, *Diversitree: Comparative phylogenetic analyses of diversification in R,* Methods in Ecology and Evolution **3**, 1084 (2012).

[41] L. Herrera-Alsina, P. van Els, and R. S. Etienne, *Detecting the Dependence of Diversification on Multiple Traits from Phylogenetic Trees and Trait Data,* Systematic Biology **68**, 317 (2019).

[42] A. J. Helmstetter, S. Glemin, J. Käfer, R. Zenil-Ferguson, H. Sauquet, H. de Boer, L.-P. M. J. Dagallier, N. Mazet, E. L. Reboud, T. L. P. Couvreur, and F. L. Condamine, *Pulled Diversification Rates, Lineages-Through-Time Plots, and Modern Macroevolutionary Modeling,* Systematic Biology **71**, 758 (2022).

[43] M. Doebeli, Y. Ispolatov, and B. Simon, *Towards a mechanistic foundation of evolutionary theory,* eLife **6**, e23804 (2017).

6

SUMMARY

A puzzling feature of biodiversity is the large disparities of species richness and age between taxa. Explaining the distribution of diversity across clades is a challenging line of research, yet two facts are clear. First, global biodiversity has undergone extensive turnovers through geological time: through speciation and extinction, clades have continuously expanded and shrunk. The fossil record is rich with examples of clades that were once dominant actors of ecosystems across the globe, but are nowadays reduced to a handful of species, or have gone extinct entirely. Second, speciation and extinction do not seem to happen at random, and some groups appear to have been more likely to speciate rapidly in a short amount of time, while others have declined. These imbalances suggest the existence of overarching controls that influence the probability of species to speciate or go extinct. This was at least the stance taken by early paleobiologists, who have undertaken to uncover these processes from the diversity patterns observed in the fossil record. In an effort to reconcile macroevolution with the ecological processes known to regulate diversity in contemporary communities, paleobiologists have interpreted the growth of clades as analogous to the growth of populations. A pervasive pattern that seems to emerge across taxonomic scales was the tendency of diversity to reach plateaus, which out of consistency with island biogeography theory was interpreted as clades reaching equilibrium diversity. Under this view, the total niche space available to species in a clade is limited, and the growth of the clade results in the intensification of competitive interactions, in turn hampering further diversification. Diversity feeds back on diversification, reducing the rate of speciation and/or increasing the rate of extinction, such that diversification is diversity-dependent. Macroevolution has since expanded to include the study of diversification patterns in the distribution of branches in molecular phylogenies. Diversity-dependence remains a popular model of diversification, as it offers a straightforward and widely applicable framework for interpreting macroevolutionary patterns in term of ecological processes.

Diversity-dependent diversification has been invoked to explain why an important fraction of the molecular phylogenies of living taxa exhibit longer branches closer to the present, opposite to the pattern expected if diversification happened at a constant-rate.

Diversity-dependence is consistent with this, because diversification would slow down over time as species accumulate, but so would any other mechanism predicting a slowdown of diversification over time without reference to species diversity. Because these two competing hypotheses would then predict a similar pattern, it is not obvious whether one would be able to distinguish phylogenies that experienced diversity-dependent diversification from those that did not. In Chapter 2, we introduce a time-dependent, but diversity-independent model calibrated to produce the same expected diversification pattern. We simulate phylogenetic trees according to either this model or the diversity-dependent model it is based on and use maximum-likelihood based model selection to study whether this method could correctly identify the model that produced the tree. We find that a strong bias exists in favour of diversity dependence, as the diversity-dependent model was selected for almost all trees, regardless of the generating model, such that model selection of diversity-dependent models based on the likelihood ratio (or the Akaike Information Criterion derived from it) should be avoided. The existence of this bias was known for comparisons of diversity-dependence against constant-rate diversification, and here we show that it extends to any comparison between diversity dependent and diversity-independent models. To circumvent this, we used the results from simulated trees to generate the distributions of the log-likelihood ratio scores expected under either model, and assess whether a given score would be more consistent with diversity-dependence or time-dependence. We found that the distributions nearly always almost entirely overlap, such that it is not possible to tell apart slowdowns that result from diversity-dependence from an equivalent decline of diversification over time.

The issue originates in part from the absence of precise predictions for the diversification patterns expected under diversity-dependence, other than a general decline toward the present. The models used by researchers for testing for a role of competition in shaping phylogenies typically assume a linear or power-like relation between diversification and the number of species. Yet, it is not known whether these functions are indeed consistent with competition playing a driving role in diversification. In Chapter 3, we measure the form of diversity-dependence in evolutionary rates that emerges from an individual-based model (IBM) where competitive interactions play a key role in both speciation and extinction. Reconstruction of the rates, when estimated point-by-point (as opposed to assuming a model) point out to more complex relations than linear or power functions, suggesting several phases of diversity-dependence where the slope of the relation between diversification and diversity changes at several points as diversity builds up in the clade. Because the obtained rates cannot be used directly for inference in empirical phylogenies, we then turn to the question of which diversity-dependent function best approximates it. In an ideal setting where complete information about extinct lineages is available, the form of diversity-dependence produced by the IBM is best approximated by an exponential function of the number of species, both for speciation and extinction. By contrast, after phylogenies are pruned of extinct lineages, model selection suggests linear diversity-dependence in the speciation rate, a result that is consistent with what is commonly inferred in empirical phylogenies. This suggests that the support for diversity-dependence often found in molecular phylogenies is in fact consistent with competition of the form implemented in our IBM driving speciation and extinction. Alternatively, this may stem from phylogenies of extant species not preserving information about the

early diversification process, where the linear and exponential models differ the most. In either case, diversity-dependence in the extinction rate is never recovered in phylogenies without fossils.

In Chapter 4, we studied the consequences of an assumption often made when testing for diversity-dependence in the phylogeny of living taxa: that competition takes place solely between members of the clade of interest. It is clear, from both present and fossil communities, that competition often involves distantly related species. The opposite scenario, where multiple unrelated clades contribute to a shared regime of diversity-dependence as a result of competing inside a common niche space, corresponds to the evolution of communities on islands. We introduced immigration to the individual-based model considered in Chapter 3 and assessed how the shared regime of diversity-dependence affected the inference of diversity-dependence in the resulting phylogenetic trees. Likelihood methods considering diversification in single trees (i.e., DDD, as used in Chapter 2 and 3) suggest that phylogenies retain a strong signal of diversity-dependence, even when it is incorrectly assumed to operate on a single-clade basis. Using likelihood methods developed for the analysis of diversification of island communities (DAISIE), we find that the shared nature of diversity-dependence is well detected when communities have reached equilibrium diversity. Shared diversity-dependence is not detected in an earlier phase of diversification, but the distribution of individuals in trait space suggest that inter-clade competition is only of secondary importance at this stage. This study and its conclusions illustrate how individual-based models can provide insights into the behaviour of a verbal model, and what phenomenological, inference-oriented models derived from it are able to recover.

7

SAMENVATTING

Een raadselachtig kenmerk van biodiversiteit is het grote verschil in soortenrijkdom en leeftijd tussen taxa. Het verklaren van de verdeling van diversiteit over clades is een uitdagende onderzoekslijn. Twee feiten zijn duidelijk. Ten eerste heeft de biodiversiteit wereldwijd in de loop van de geologische tijd grote veranderingen ondergaan: door soortvorming en uitsterven zijn clades voortdurend uitgebreid en geslonken.

Fossielen laten voorbeelden zien van clades die ooit een dominante rol speelden in ecosystemen over de hele wereld, maar die nu gereduceerd zijn tot een handvol soorten, of geheel uitgestorven zijn. Verder lijken soortvorming en uitsterven niet willekeurig te gebeuren, en sommige groepen lijken meer kans te hebben gehad om in korte tijd snel nieuwe soorten te vormen, terwijl andere juist achteruit zijn gegaan. Deze disbalans in soortendiversiteit suggereert het bestaan van overkoepelende sturingsmechanismen die van invloed zijn op de waarschijnlijkheid dat soorten worden gevormd of uitsterven. Dit was althans het standpunt van vroege paleobiologen, die deze processen trachtten af te leiden uit de diversiteitspatronen die in het fossielenbestand zijn waargenomen. In een poging om macro-evolutie in verband te brengen met de ecologische processen waarvan bekend is dat zij de diversiteit in hedendaagse gemeenschappen reguleren, hebben paleobiologen de groei van clades geïnterpreteerd als analoog aan de groei van populaties .Een alomtegenwoordig patroon dat zich op alle taxonomische schalen openbaart, is dat diversiteit naar een plateau toe gaat. Net als in eiland-biogeografietheorie werd dit geïnterpreteerd als dat clades een evenwichtsdiversiteit bereiken. Volgens deze hypothese is de totale niche-ruimte die beschikbaar is voor soorten in een clade beperkt, en de groei van de clade resulteert in een intensivering van competitieve interacties, hetgeen weer verdere diversificatie belemmertm omdat de snelheid van soortvorming afneemt en/of de snelheid van uitsterven toeneemt. Kortom de snelheid van diversificatie is afhankelijk van diversiteit. Macro-evolutie heeft zich sindsdien uitgebreid tot de studie van diversificatiepatronen in de verdeling van takken in moleculaire fylogenieën. Diversiteitsafhankelijkheid blijft een populair model voor diversificatie, omdat het een eenvoudig en breed toepasbaar kader biedt voor de interpretatie van macro-evolutionaire patronen in termen van ecologische processen.

Diversiteitsafhankelijke diversificatie is aangevoerd om te verklaren waarom een belangrijk deel van de moleculaire fylogenieën van levende taxa langere takken vertonen dicht bij het heden, in tegengestelling tot het patroon dat verwacht zou worden als diversificatie met een constante snelheid zou plaatsvinden. Diversiteitsafhankelijkheid is hiermee in overeenkomst, omdat diversificatie zou vertragen als soortendiversiteit groeit, maar dat zou ook gelden voor elke ander mechanisme dat een vertraging van diversificatie in de loop van de tijd veroorkzaakt zonder invloed van soortendiversiteit. Omdat deze twee concurrerende hypothesen dan een vergelijkbaar patroon zouden voorspellen, ligt het voor de hand on te onderzoeken of het mogelijk is om fylogenieën te onderscheiden die diversificatie-afhankelijkheid hebben ondergaan en fylogenieën die dat niet hebben ondergaan. In Hoofdstuk 2 introduceren we een tijds-afhankelijk, maar diversiteitsonafhankelijk model dat gecalibreerd is om hetzelfde verwachte diversificatiepatroon te produceren. Wij simuleren fylogenetische bomen volgens dit tijds-afhankelijke model of volgens het diversiteits-afhankelijke model waarop het gebaseerd is, en gebruiken op maximum-likelihood gebaseerde modelselectie om te bestuderen of deze methode het model dat de boom gegenereerd heeft correct kan identificeren. Wij stellen vast dat er een sterke bias bestaat ten gunste van diversiteits-afhankelijkheid, aangezien het diversiteits-afhankelijke model voor bijna alle bomen wordt geselecteerd, ongeacht het genererende model, zodat modelselectie van diversiteits-afhankelijke modellen op basis van de likelihood ratio (of het Akaike Informatie Criterium) moet worden vermeden. Het bestaan van deze bias was bekend voor vergelijkingen van diversiteitsafhankelijkheid met diversificatie met constante snelheid, en hier tonen wij aan dat het ook van toepassing is op elke vergelijking tussen diversiteitsafhankelijke en diversiteitsonafhankelijke modellen. Om dit te omzeilen gebruiken wij de resultaten van gesimuleerde bomen om de verdelingen van de log-likelihood ratio scores te genereren die verwacht worden onder beide modellen, en te beoordelen of een gegeven score meer consistent zou zijn met diversiteit-afhankelijkheid of tijds-afhankelijkheid. We vinden dat de verdelingen elkaar altijd bijna volledig overlappen, zodat het niet mogelijk is om vertragingen die het gevolg zijn van diversiteits-afhankelijkheid te onderscheiden van een equivalente afname van diversificatie in de tijd. Het probleem komt gedeeltelijk voort uit het ontbreken van precieze voorspellingen voor de diversificatiepatronen die verwacht worden onder diversiteitsafhankelijkheid, anders dan een algemene afname naar het heden toe. De modellen die door onderzoekers worden gebruikt voor het testen van een rol van competitie in het vormen van fylogenieën, nemen gewoonlijk een lineaire of machtsrelatie aan tussen diversificatie en het aantal soorten. Het is echter niet bekend of deze functies inderdaad consistent zijn met het feit dat competitie een stuwende rol speelt in diversificatie. In Hoofdstuk 3 meten we de vorm van diversiteits-afhankelijkheid in evolutionaire snelheden die naar voren komt uit een individu-gebaseerd model (IBM) waar competitieve interacties een sleutelrol spelen in zowel soortvorming als extinctie. Reconstructie van de snelheden, wanneer punt-voor-punt geschat (in tegenstelling tot het aannemen van een model) wijzen op complexere relaties dan lineaire of machtsfuncties, die meerdere fasen van diversiteits-afhankelijkheid suggereren, waarbij de helling van de relatie tussen diversificatie en diversiteit op verschillende punten verandert als de soortendiversiteit in de clade toeneemt. Omdat de verkregen snelheden niet rechtstreeks kunnen worden gebruikt voor inferenties in empirische fylogenieën, bekijken wij

vervolgens welke diversiteit-afhankelijke functie deze het best benadert. In een ideale setting waar volledige informatie over uitgestorven lineages beschikbaar is, wordt de vorm van diversiteits-afhankelijkheid die door de IBM wordt geproduceerd het best benaderd door een exponentiële functie van het aantal soorten, zowel voor soortvorming als voor uitsterven. Daarentegen, als de uitgestorven takken uit de fylogenieën weggehaald zijn, suggereert modelselectie een lineaire diversiteits-afhankelijkheid in de snelheid van soortvorming, een resultaat dat consistent is met wat gewoonlijk wordt afgeleid uit empirische fylogenieën. Dit suggereert dat het bewijs voor diversiteits-afhankelijkheid die vaak wordt gevonden in moleculaire fylogenieën consistent is met competitie (in de vorm zoals geïmplementeerd in onze IBM), als stuwende kracht in soortvorming en uitsterven, althans niet. Een andere mogelijkheid is dat dit wordt veroorzaakt doordat fylogenieën van bestaande soorten geen informatie bevatten over het vroege diversificatieproces, waarin de lineaire en exponentiële modellen het meest van elkaar verschillen. In beide gevallen wordt de diversiteit afhankelijkheid in de snelheid van uitsterven nooit hersteld in fylogenieën zonder fossielen.

In hoofdstuk 4 bestuderen we de gevolgen van een aanname die vaak wordt gemaakt bij het testen op diversiteits-afhankelijkheid in de fylogenie van levende taxa: dat competitie alleen plaatsvindt tussen leden van de betrokken clade.

Het is duidelijk, zowel voor de huidige als voor de fossiele gemeenschappen, dat concurrentie vaak verwante soorten betreft.

Het tegenovergestelde scenario, waarbij meerdere niet-verwante clades bijdragen aan een gedeeld regime van diversiteit-afhankelijkheid als gevolg van competitie binnen een gemeenschappelijke niche-ruimte, komt overeen met de evolutie van gemeenschappen op eilanden.

Wij introduceren immigratie in het op individuen gebaseerde model dat in Hoofdstuk 3 werd beschouwd, en beoordelen hoe het gedeelde regime van diversiteits-afhankelijkheid de gevolgtrekking van diversiteits-afhankelijkheid in de resulterende fylogenetische bomen beïnvloedt.

Waarschijnlijkheidsmethoden die diversificatie in afzonderlijke bomen in aanmerking nemen (d.w.z. DDD, zoals gebruikt in Hoofdstuk 2 en 3) suggereren dat fylogenieën een sterk signaal van diversiteits-afhankelijkheid behouden, zelfs wanneer ten onrechte wordt verondersteld dat dit op een single-clade basis werkt.

Met behulp van waarschijnlijkheidsmethoden die zijn ontwikkeld voor de analyse van diversificatie van eilandgemeenschappen (DAISIE), vinden wij dat het gedeelde karakter van diversiteits-afhankelijkheid goed wordt gedetecteerd wanneer gemeenschappen een evenwichtsdiversiteit hebben bereikt. Gedeelde diversiteit-afhankelijkheid wordt niet gedetecteerd in een eerdere fase van diversificatie, maar de verdeling van individuen in de eigenschappenruimte suggereert dat inter-clade competitie in dit stadium slechts van secundair belang is. Deze studie en haar conclusies illustreren hoe op individuen-gebaseerde modellen inzicht kunnen verschaffen in het gedrag van een verbaal model, en wat fenomenologische, op inferentie gerichte modellen die daarvan zijn afgeleid, kunnen herstellen.

CURRICULUM VITÆ

Théo PANNETIER

18-04-1995	Born in Pithiviers, France.

EDUCATION

2012–2015	B.Sc. in Life Sciences
	Université d'Orléans, France (2012–2015)
	National University of Ireland Galway (2015)
2015–2017	M.Sc. Evolutionary Biology
	Université de Tours, France (2015–2016)
	Université de Montpellier, France (2016–2017)
2017–2022	PhD. Theoretical Biology
	Rijksuniversiteit Groningen, The Netherlands
	University of Stirling, United Kingdom
	Thesis: Diversity-dependence and the role of competition in clade diversification
	Promotor: Prof. dr. R.S.Etienne
	Copromotor: Dr. A.B. Duthie

LIST OF PUBLICATIONS

2. **Pannetier, T.**, C. Martinez, L. Bunnefeld, R. S. Etienne, 2020. Branching patterns in molecular phylogenies cannot distinguish diversity-dependent diversification from time dependent diversification. *Evolution* 75-1: 25–38 DOI: 10.1111/evo.14124

1. Sentis, A., R., Bertram, N., Dardenne, F., Ramon-Portugal, G., Espinasse, I., Louit, L., Negri, E., Haeler, T., Ashkar, **T. Pannetier**, J. L., Cunningham, C., Grunau, G. Le Trionnaire, J.-C., Simon, A., Magro, B., Pujol, J.-L., Hemptinne, E., Danchin. 2018. Evolution without standing genetic variation: change in transgenerational plastic response under persistent predation pressure. *Heredity*. DOI: 10.1038/s41437-018-0108-8

ACKNOWLEDGEMENTS

. . . And someday, we are done!

(A wise man once said)

Rampal, like many starting PhD students I guess, I used to be terrified to talk science with you, but your habit of starting meetings with jokes and casual chat helped a lot in bringing this barrier down. I have conflicted feelings about your style of supervision. On the one hand, and as others before me have stated, the level of freedom you trust your students with has definitely been empowering, and has allowed me to explore my own ideas, make mistakes and mature as a scientist. On the other hand, I believe I would have benefited from more framing – we both know how easily I tended to get sidetracked and focus on very minute aspects of the results! We did set up deadlines, which helped a little but I do feel were a tad ineffective – there was after all no follow-up to crossing them. Still! It is in great part thanks to your continued guidance and advices that I have finally managed to overcome perfectionism and move forward in the late stages of the PhD. You also taught me the invaluable skill of taking the shortest road to expedite administrative tasks. Thank you for supporting me through these years and helping me grow as a scientist.

Lynsey, you were the first person I met on the first day, in Stirling. I was feeling terribly awkward then, and you helped me feel comfortable and settle in this new academic environment. Your support through the first half of the PhD was instrumental to my eventual success. Your encouraging feedback during both my times in Groningen and Stirling helped me dealing with the bouts of impostor syndrome that I experienced until late in the PhD. It also seems that you were the only one among us three to have a realistic perception of passing time, and I have enjoyed that you reframed our plans when Rampal and I were scheduling overambitious targets. It is thanks to this that I have managed to finish in those quasi-five years – instead of, say, seven? Thank you again for being a committed supervisor, and for having ensured to make a smooth transition in supervision when you eventually took the decision of leaving academia.

Brad, you're one of the most brilliant and kind scientists I have been given to meet, and the best supervisor I could possibly hope for to take over after Lynsey left academia. Despite not being familiar with the main subject of the thesis, you've arranged to meet and chat whenever I needed to give sound advice on all my statistics-, maths- or academy-related questions (not the least!), or simply listen, in times where I needed to vent on whatever was the struggle of the day. All of this have been of tremendous help.

I am grateful to the many friends I have met in Groningen, and who contributed to make a good time of these few years I have spent in the city. Thank you all for bringing your ray of sun to brighten its cloudy sky. When asking their favourite word in the dutch

language to a dutch speaker, learner or a search engine, the top pick is often "gezelligheid". I happily side with the majority on this question. You would all deserve a dedicated paragraph, but I am running out of time to get the thesis in print and, admittedly, my own brain running out of ink. I regret I'll have to be briefer than I would have liked to.

First, I would like to thank my friends and colleagues in the TECE research group through the years. **Pedro** and **Raph**, my fellow cohort fledglings, for tagging along from day 1 through the many adventures and misfortunes of the PhD journey. **Shu**, for always bringing good moods to the lab, and for organising dinners to die for. **Giovanni** and **Liang**, for happily helping with the many maths questions I could bring to them (Giovanni, you are forgiven for jumping on my bed). **Karen**, thanks for lending me your flat during the first two months of my time in Groningen. This helped me getting settled tremendously. **Josh**, you loyal, you smart. I appreciate that. Working with you on DAISIEprep was a major key. **Tianjian** and **Yang**, for sharing a fun trip to London and the burning English lands. Yang, thanks for a great hat. I know I was born cool, I'll make sure to stay pretty. **Lucas**, thanks for your kindness, and for your enthusiasm to my modest canid drawings. **Thijs** for maintaining and sharing clean code practices. **Cyrus**, thanks for sharing spicy pieces of wisdom, along with maxims I don't think I'd be allowed to transcribe here. **Ornela**, **Carol** and **Vicente**, for bringing life back into a lab that had been devastated by depopulation.

There many others I would like to thank generally for the great work environment we had in TRÊS and/or for the fun moments we shared. Many thanks to **Annie**, **Boris**, **Inès**, **Jakob**, **Jan**, **Jana**, **Kevin**, **Leonel**, **Loz** and **Shay**, **Megan**, **Miguel**, **Mirjam**, **Omer**, **Pancho**, and **Xiaoyan**. Special thanks to **Ingeborg** for patiently answering all our administrative questions, and to Sinterklaas for never forgetting TRÊS during his yearly national tour.

Richèl, for teaching me solid programming practices, for challenging my relationship to work, and keeping Giacomonday/Keivrijdag alive through a pandemic. **Albertas**, thanks for the many political coffee breaks, and for polish beer. **Hylke**, I owe to you about 95% of my very limited knowledge of dutch. Thank you as well for always emphasising the priority on wellbeing over work! **Timo**, thanks for taking me to the quarry to meet the quarrymen. **Basti**, thanks for the gluten-free tips and the Pokémon nerdry. **Elisa**, thank you for sharing my drag race enthusiasm, for your fantastic baked goods, and for all the hugs. **Stefano**, thanks for initiating our regular game nights, and for ruthlessly keeping nicotine away from me. **Christoph**, **Claire**, and Raph again of course, many thanks for all the amazing parties thrown at El Camino Real / the Mondriaanboot! **Pratik**, thanks for sharing the tidyverse gospel, and for being a caring friend and academic. Sorry for that disastrous sofa episode! **Apu**, thanks for joining me in our shut-up-and-write sessions, I hope they were as useful to you as they were to me!

Marina and **Andrea**, thanks for all the fun times at Hereweg, for tolerating my moodiness during times of high pressure, and overall for being fantastic housemates and friends. Bilbo and Sauron, thanks for ruining my clothes, lacerating my legs, stealing my food, interrupting important meetings, and for being the adorable little monsters you are.

I must also thank all the members of Donar, the Stabbing club: **Gijs**, **Sophia**, **Jeffrey**, **Alexa**, **Martijn**, **Arnoud**, **Krysztof**, **Meine**, **Michiel**, **Nathan**, **Lara**, **Ioana**, **Slavyana**, **Max**, **Jorn**, **Cecilia**, **Lisette**, **Peter**, **Jesse**, **Arthur**, and everyone else I had the pleasure to fence with over the years! Special thanks to our two amazing coaches **Jan Jurjen** and **Rink**, for their dedication to making us better fencers.

Although my time there was shortened by the pandemic, I would like to express my gratitude to everyone at the Biological and Environmental Sciences for the pleasant time I had in Stirling: many thanks to **Robin**, **Mia**, **Paulo**, **David**, **Sara**, **Matt Nuttall**, **John**, **Lucy**, **Lidia**, **Alan**, **Emmanuel**, **Rosie**, **Luc**, **Matt Tinsley**, **Stu**, **Nigel**, **Izzy** and **Nils** for contributing to making a welcoming and academically fulfilling work environment there.

Because starting the PhD would have been out of reach without your mentorship and teachings, I would like to thank my former Master's supervisors, **Arnaud** and **Fabien**. Fabien, I am forever in your debt for that all-nighter you happily pulled to help your students write up our theses at the last possible minute.

I would also like to thank Jenny Brian, Jim Hester, Yihui Xie, Hadley Wickham, Thomas Lin Pedersen and all of the former Rstudio team, for building an ecosystem that makes R a bearable, and even pleasant (!) language to work with.

Thanks to Tim Haines, Jasper James, Ben Bartlett and the many paleontologists who contributed to *Walking with Dinosaurs*, for sparking an interest for macroevolution in my younger self.

Because most of the results presented in this thesis could certainly not have been obtained without access to a high performance cluster, praise is due to the Center of Information Technology at the University of Groningen, and in particular to Fokke Dijkstra and his team for keeping the Peregrine High Performance Cluster flying and for providing essential resources and training for its use.

Un grand merci à **Yohan**, **Allan**, **Océane** et **Alrick** pour avoir partagé mes nombreux moments de doutes et m'avoir aidé à pondérer mes perspectives et mes choix de vie.

Enfin, je dois évidemment remercier ma famille pour avoir été mon plus grand soutien pendant toutes ces années. **Élioz**, merci d'être un frère formidable et pour ton soutien moral au cours de ces années. **Papa**, **Maman**, merci infiniement d'avoir pris à votre charge l'integralité de la charge financière de mes longues études avant la thèse. Merci pour vos encouragements, et votre foi indéfectible dans ma réussite. Je vous dois tout.

Look on my works, ye Mighty, and despair!